Dynamic behavior of stress laminated timber bridges

by

Matthew Richard Johnson

A Thesis Submitted to the
Graduate Faculty in Partial Fulfillment of the
Requirements for the degree of
MASTER OF SCIENCE

Department: Civil and Construction Engineering
Major: Civil Engineering (Structural Engineering)

Iowa State University
Ames, Iowa

1993

TABLE OF CONTENTS

1. INTRODUCTION

1.1 General

The use of timber as a bridge material is rarely considered by many designers. Not only is timber a renewable and readily available resource, it also provides good performance with little maintenance. Timber bridges can be constructed with relatively low skilled labor and can have life spans of over 50 years.

As part of an effort to promote the use of wood for bridge construction, the United States passed the Timber Bridge Initiative in 1988. This program, headed by the United States Department of Agriculture (USDA) Forest Service, aides local governments in the construction of demonstration timber bridges. These bridges are then evaluated and monitored by the Forest Products Laboratory (FPL) through a series of periodical field tests. Information obtained from these tests provides insight into changes that can be made to improve the performance, design, and cost effectiveness of timber bridges.

One type of bridge currently being monitored by FPL is the stress laminated timber bridge. Although static deflections due to heavy vehicle loads are recorded as part

of the monitoring process, no data has been collected pertaining to the bridge performance under dynamic loads. Application of dynamic loads can significantly increase the deflections, moments, and stresses over that of static loading. Therefore, information is needed on the dynamic behavior of the stress laminated bridge system.

1.2 Objective and Scope

The objective of this study was to evaluate the dynamic behavior of stress laminated timber bridges. This objective was broken into two investigations, experimental and analytical.

The experimental investigation involved the field testing of a stress laminated timber bridge crossing the Teal River near Hayward, Wisconsin. Deflections of the bridge, hereafter referred to as the Teal River bridge, were recorded at several locations every five thousandths of a second during the passage of a heavy vehicle over the bridge. The dynamic response of the bridge was evaluated for several different vehicle velocities. In addition, the affect of changing the approach roughness was investigated by placing an artificial bump at the bridge entrance. As a way of quantifying the behavior, a dynamic load factor was calculated for each test performed. The dynamic load factor

(DLF) is defined as the factor by which the maximum dynamic response exceeds the maximum static response at a particular point. That is, the maximum dynamic deflection divided by the maximum static deflection at the same point. Through the series of tests, a single upper bound value of the DLF was determined for the bridge.

The second phase involved the development of an analytical model to predict the dynamic response of stress laminated timber bridges. A finite element model of the bridge was used to produce time-history curves of deflection to define the bridge response. The vehicle loading was modeled as a rolling mass at each axle location. Again, the response was quantified using a DLF for each run. In addition, comparisons were made between the analytical and experimental results to verify the use of the model.

1.3 Stress Laminated Timber Bridges

1.3.1 Background

Stress laminated timber bridges use steel prestressing rods to compress individual longitudinal laminates. During construction, threaded prestressing rods are placed transversely at even intervals along the length of the bridge (see Fig. 1). These rods are pulled in tension, anchored, and released producing a compressive stress between the

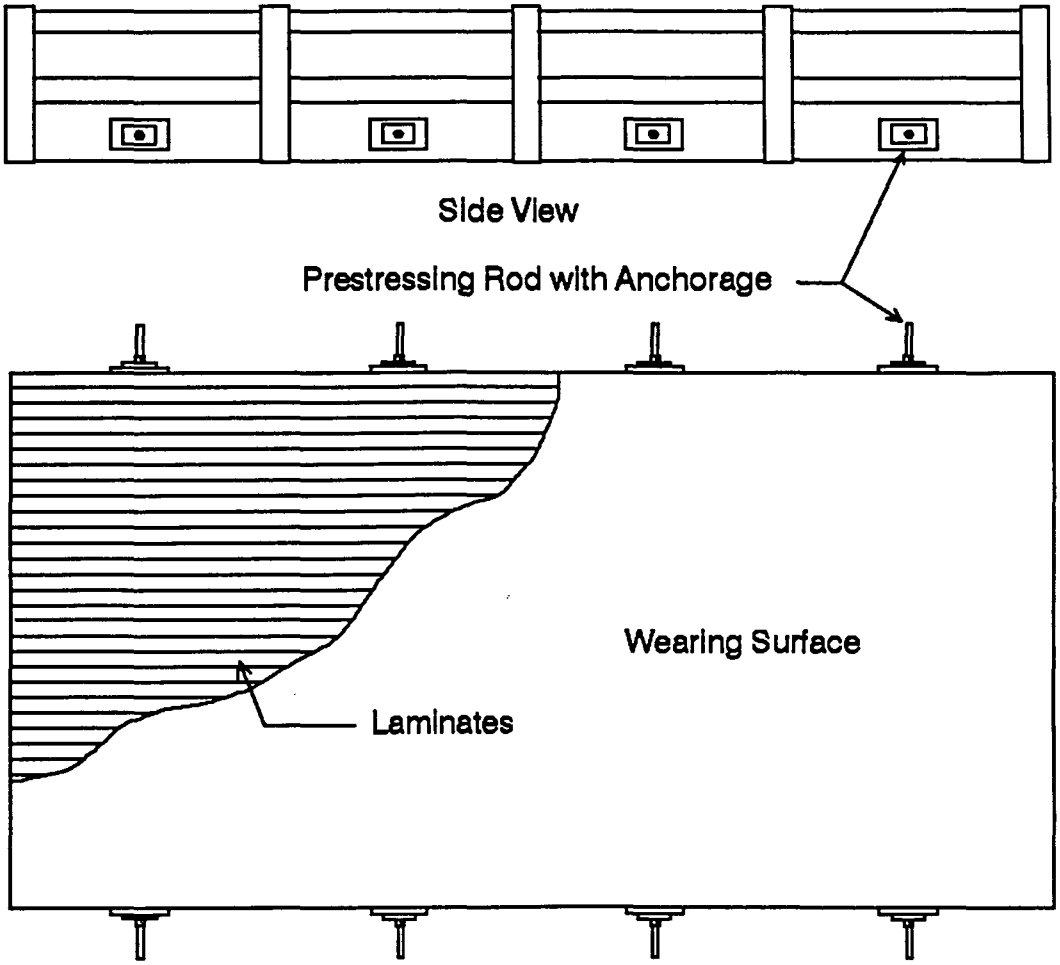

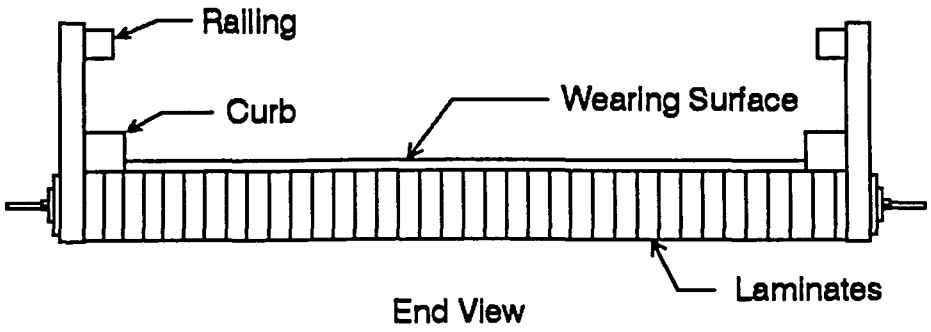

Fig. 1. Stress laminated timber bridge system

individual laminates. Once compressed, the friction force between laminates allows the transfer of vertical shear and thus distributes any applied loading. The stressed deck then acts as a uniform slab without any discontinuities at laminate interfaces.

The idea of using prestressing rods to compress longitudinal laminates originated in Ontario, Canada, as a means of strengthening existing nail laminated bridges. It was noticed that asphalt wearing surfaces were cracking and breaking up due to differential movement between individual laminates. The repetitive loading of vehicle traffic over the bridge caused the nails to crush the wood thus decreasing their effectiveness. The individual laminates were able to slip and move independently causing the wearing surface damage and a decrease in load carrying capacity. Rather than replacing the entire bridge, prestressing rods were used to compress the deck and eliminate the differential laminate movement.

This method of strengthening was first tried on the Herbert Creek Bridge in 1976. The stressing of the deck greatly increased the load carrying capacity of the bridge and it was decided to further research the method as both a strengthening technique as well as a procedure for new construction. The research was conducted by the Ontario Ministry of Transportation (MTO) and Queen's University.

Design procedures and specifications were developed and included in the 1979 Ontario Highway Bridge Design Code (OHBDC).

In the United States, research and development was carried out by the USDA Forest Service FPL in cooperation with the University of Wisconsin, Madison. The American Association of State Highway and Transportation Officials (AASHTO), provides design provisions for stress laminated timber bridges in a sperate publication from their Standard Specifications for Highway Bridges. This publication, Guide Specifications for the design of Stress Laminated Wood Decks [1], became available in 1991.

1.3.2 Construction and Behavior

Ritter [13] describes the general construction and design procedures used in stress laminated timber bridges. Newly constructed bridges are generally made of 2 to 4 in. thick laminates. The depth of the members are generally controlled deflection limitations rather than stresses. It is important that the laminates have a uniform thickness to ensure contact with adjacent laminates thus allowing proper transfer of the loading. A limited number of butt joints are allowed since adjacent laminates can receive the load, carry it past the butt joint, and transfer it back to the discontinuous member. This allows the use of shorter, more

available, and less expensive members. However, butt joints do reduce the longitudinal stiffness and must be accounted for in the design. All timber must be treated with an oil-type preservative to inhibit decay and control fluctuations in moisture content.

The steel prestressing rods are identical to those used in prestressed concrete. They have, at minimum, an ultimate tensile stress of 150,000 psi and are available in diameters ranging from 5/8 to 1 3/8 inches. Some type of corrosion protection must also be provided. Most commonly the rods are galvanized, but epoxy coating has also been used with success. Any damage to the rod coating during construction must be patched in the field.

Two types of anchorage systems are currently used in new construction. Figure 2 illustrates the two methods. The OHBCD requires the use of a channel bulkhead. The channel serves three purposes. First, if provides additional stiffness to the bridge, second, it distributes the load from the rods to the decking material, and third, it provides a clean edge visible to the public.

Research in the United States, however, found that the channels contributed little to the overall performance of the bridge and a second anchorage system was developed. This system uses rectangular bearing plates at each rod location. Using this system, the compressive stress is evenly

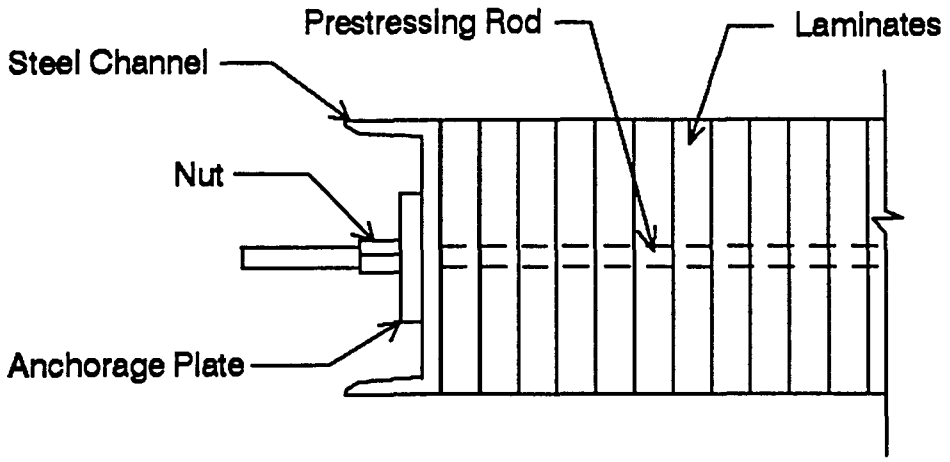

Channel Bulkhead

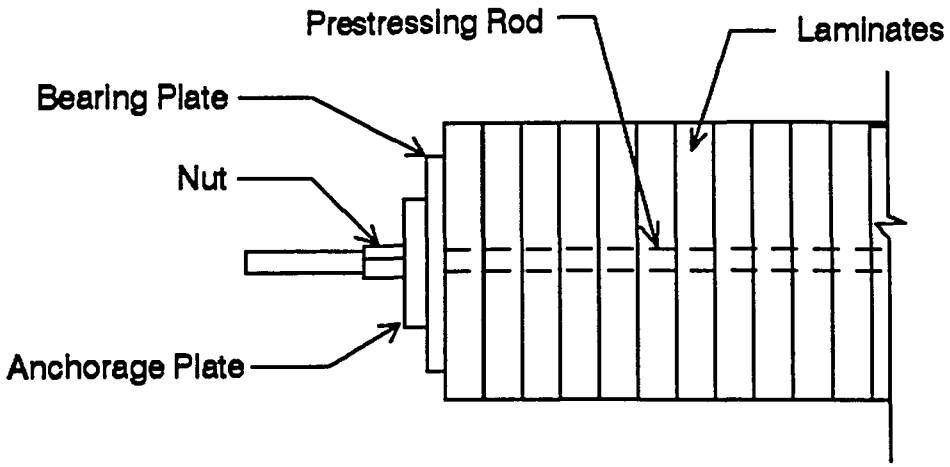

Bearing Plate

Fig. 2. Prestressing anchorage systems

distributed on interior laminates even though the stress is more localized on a few exterior laminations.

The bridges are constructed by placing the individual laminates on the substructure, inserting the prestressing rods into prebored holes, and applying the force in the rods. The tensile force is applied by pulling on the rod against the bearing plate or channel using a hydraulic jack. Forces of approximately 80 to 100 kips are applied. The nut is then tightened on the rod and the jack is removed thus compressing the laminates together. A minimum 24 psi compression stress between laminates is needed in order for the deck to perform effectively. Initial stresses of 100 psi or more are applied at construction to account for losses due to creep and moisture content changes in the timber. Losses of up to 60 percent of the initial stress are expected during the life of the structure, leaving 40 percent to maintain the needed friction force between laminates. The deck is stressed three times to account for and minimize stress losses due to creep. The designed initial stress is applied at the time of construction, reapplied one week later, and reapplied for the final time 5 to 7 weeks after construction.

The stressed deck behaves as an orthotropic plate. That is, different properties exist parallel and transverse to the laminates. The longitudinal stiffness is affected by the modulus of elasticity as well as the depth of the laminates.

The transverse modulus of elasticity (E_{TS}) and transverse shear modulus (G_{TS}) are a small fraction of the longitudinal modulus. It should be noted that the transverse modulus of elasticity and shear modulus are function of the stressed system, that is, they depend on the timber species used as well as the stress applied and are not solely properties of the individual laminates. The values of E_{TS} and G_{TS} are experimentally determined using the various species of wood and the minimum stress level required for acceptable performance. The values have been determined for Douglas Fir-Larch, Hem-Fir, Red Pine, and Eastern White Pine and are defined by equations 1-1 and 1-2.

$$E_{TS}=0.013E' \tag{1-1}$$

$$G_{TS}=0.03E' \tag{1-2}$$

$E'=E(C_M)$
E'= Allowable modulus of elasticity
E = Modulus of elasticity
C_M = Moisture content factor

C_M values can be found in Ref [13] or other timber manuals.

1.4 Literature Review of Bridge Dynamic Behavior

The dynamic behavior of bridges has been studied by many researchers both analytically and experimentally. Overall,

the problem is very complex, being influenced by many parameters. The response is affected by the bridge characteristics, vehicle characteristics, number of vehicles, vehicle velocity and path, road surface roughness, and initial bridge and vehicle conditions. All of these parameters combine to define the dynamic response of the bridge.

Models used to predict bridge behavior have varied in complexity. The bridge has been modeled as a single beam, grillage system of longitudinal and transverse members, plate elements, and a combination of plate and beam elements. The vehicle has been represented, in simplest form, as a constant force transversing the bridge. While models having twelve degrees of freedom and incorporating springs and dash pots to represent the suspension system have also been used. However, Humar and Kashif [7] point out that in most cases, sophisticated analytical techniques still fail to determine the parameters that influence dynamic behavior. Design procedures can be developed and parameter studies performed more effectively with a simplified model.

Gupta [6] modeled a bridge as both a beam and an orthotropic plate to study the influence of surface irregularities and vehicle braking on dynamic response. A half sine wave bump was placed at various approach locations to model surface irregularities. The largest impact was

obtained when the bump was placed directly at the bridge entrance. He also determined that vehicle braking while on the bridge span appreciably increases the response.

Gupta also comments on the bridge models. For the two dimensional plate model, eccentric vehicle loading was found to increase the dynamic response depending on the distance between the bridge center line and vehicle position. Between the two different bridge models, the one dimensional beam model predicted higher impacts than the two dimensional plate model. Humar and Kashif also cite this difference between models.

An analytical study performed by Hwang and Nowak [8] included surface roughness on a bridge modeled as a prismatic beam. The road roughness was incorporated using a power spectral density function to produce a random road profile. The vehicle was modeled as a distributed mass supported by axles with springs representing the tires and nonlinear, energy dissipating devices representing the vehicle leaf spring system. For each solution, the vehicle was run over twenty different road profiles with the final response being the average of the twenty runs. It was found that the amplitude of dynamic oscillation remained almost constant for different vehicle weights. The static deflection increases with vehicle weight resulting in a reduction in dynamic load factor with increasing vehicle weight.

The use of a power spectral density function to represent road surface roughness was also used by Wang, Huang, and Shahawy [20]. Road profiles for very good, good, average, and poor road conditions were produced. They modeled the bridge as a grillage system and used a complex vehicle model with twelve degrees of freedom to represent a standard AASHTO HS20-44 loading. Masses representing the tractor and semitrailer were assigned three degrees of freedom each corresponding to vertical displacement, rotation about a transverse axis (pitch), and rotation about a longitudinal axis (roll). Each of the three axles had two degrees of freedom; one for vertical motion, and one for roll. Results from their analyses found only slight variances in the dynamic load factor with increasing vehicle velocities for good and very good road profiles, but large changes using a poor road profile.

The effects of initial bridge and vehicle motion were studied by Wen and Veletsos [21]. Their model used a simply supported beam that was reduced to a single degree of freedom by assuming the deflected shape at any time is proportional to that of the static deflection produced by the vehicle and bridge weights. The vehicle was represented by a rigid sprung mass (chassis and payload mass) with vertical and pitching degrees of freedom, and two unsprung masses (axle and tire mass) assumed always to remain in contact with the

bridge. The effects of initial vehicle motion were investigated for both initial pitching and vertical motion. The effects of initial pitching were found to be less severe than initial bouncing. The increases in impact due to initial oscillations were nearly linear with the amplitude of the oscillation.

If the bridge is in a state of motion prior to the vehicle entrance, the dynamic response depends on the timing of vehicle entrance. An additive effect can result if load application is in phase with the initial bridge motion, or a canceling effect can result from out of phase interaction.

Wen and Veletsos also noticed an increase in the dynamic response when the time between axle entrance was equal to an integer factor of the bridge period. Further studies on the effect of multiple axle loads on a bridge were done by Looney [10]. He noted that field test data had shown an accumulation of oscillations at some velocities and an interference at others. Analytically, he found that the oscillations caused by two axles crossing a point on the bridge in a time equal to one or two times the natural period of the bridge were much larger than those crossing a point in 1.5 times the natural period. This phenomenon was verified experimentally by a field test conducted by Foster and Oehler [5]. The above is true if the frequency of the loaded bridge is close to the loaded frequency.

Looney also did studies to evaluate the affect of vehicle mass. Using live load to dead load ratios of 0.4, 0.5, 0.7, and 1.2 comparisons were made between modeling the loading as a constant force or a rolling mass. Results show that a moving force analysis is not adequate to define the total bridge response. Moving force theory is useful in a qualitative sense in describing the response, but is inadequate in computing the oscillations.

Biggs and Suer [3] conducted a series of field tests on five simple span bridges. From the tests they concluded that one of the most important factors influencing bridge response is the dynamic characteristics of the vehicle. Another important factor is the condition of the roadway. They noted that field test data show amplitudes of dynamic oscillation being 18 to 40 percent of the maximum static deflection. These are much higher than would be produced by a theoretical smoothly running load. It was also found that the frequency of vibration while the vehicle is on the span was not the natural frequency of the bridge. This suggests the response is a forced vibration caused by the oscillation of the vehicle on its suspension system. The best indication of the bridge natural frequency was in the free vibration occurring after the vehicle left the span. This frequency was found to be dominated by first mode vibration. Also noted was that no apparent correlation existed between the characteristics of

vibration and the speed of the vehicle, but the range of speeds was limited and it is expected that higher speeds would have caused larger impacts.

Bakht and Pinjarkar [2] summarize the results of dynamic studies and develop a testing procedure for determining a single impact value or dynamic load factor for a bridge. Using a single vehicle is not representative of the loads a bridge will encounter in its life. A single vehicle can only provide insight into the problem of dynamic loading and should not be used to determine a single value of impact. The only way a representative value can be determined is to collect data under normal traffic over long periods of time. From the data collected, a statistical procedure using the mean and variance of the impact values, and a safety index for highway bridges can be employed to obtain a single value.

From previous research it was found that the impact decreases with vehicle weight, therefore light vehicles, whose loading is insignificant compared to design loads, will tend to incorrectly shift the value of impact to the high side. To avoid this, data from light vehicles should not be used in the calculation of an impact factor. Also, dynamic load factors at points away from the load can be larger than those directly under the load. Deflections at points away from the load are smaller and of less importance than those under the loading, therefore, data should only be considered

at points where large deflections are occurring. Bakht and Pinjarkar suggest using only that data at the reference point where the maximum static deflection occurs at the monitored cross-section.

The use of an artificial bump placed on the road surface to account for riding surface irregularities is common. Bakht and Pinjarkar note that this practice may produce overly conservative results on bridges where the road is well maintained. Placement of a bump should only be done if the bridge is not expected to be paved for long periods of time, or if unevenness at the bridge entrance or expansion joints is expected.

Bakht and Pinjarkar additionally point out that there is little uniformity in how the impact factor is calculated. Eight equations are listed, all giving a slightly different value for a given situation. In the paper it is suggested that the following equation be used to calculate the impact factor:

$$I=\frac{\delta_{dyn}-\delta_{stat}}{\delta_{stat}} \qquad (1\text{-}3)$$

I=Impact factor
δ_{dyn}=Maximum dynamic deflection
δ_{stat}=Maximum median dynamic deflection

The median dynamic deflection is the dynamic deflection after filtering out the oscillations. The value of the maximum

median dynamic deflection is normally very close to the maximum static deflection. The static deflection is not used in equation 1-3 because its use would require static data from every vehicle that crosses the bridge. This is obviously not possible when collecting data under normal traffic.

2. EXPERIMENTAL INVESTIGATION

2.1 Bridge Description

In order to evaluate the dynamic performance, field tests were conducted on a stress laminated timber bridge located in northwestern Wisconsin. The bridge crosses the Teal River on County Highway S, approximately 20 miles east of Hayward, Wisconsin (see Fig. 3). County Highway S is a two-lane paved road located within the Chequamegon National Forest transportation network. The bridge is used by approximately 100 vehicles per day with much of its heavy loading coming from logging traffic.

The stress laminated timber bridge was constructed in 1989 to replace an existing steel stringer, concrete deck bridge. Partial funding for the project was provided by the USDA Forest Service as part of the Timber Bridge Initiative. The bridge is one of the many being periodically monitored by FPL.

Initial designs for the bridge used Wisconsin grown Red Oak lumber for the laminates. Further design concluded that lumber of the required dimensions was not readily available and a different alternative would be necessary. After further consideration, it was decided to use horizontally

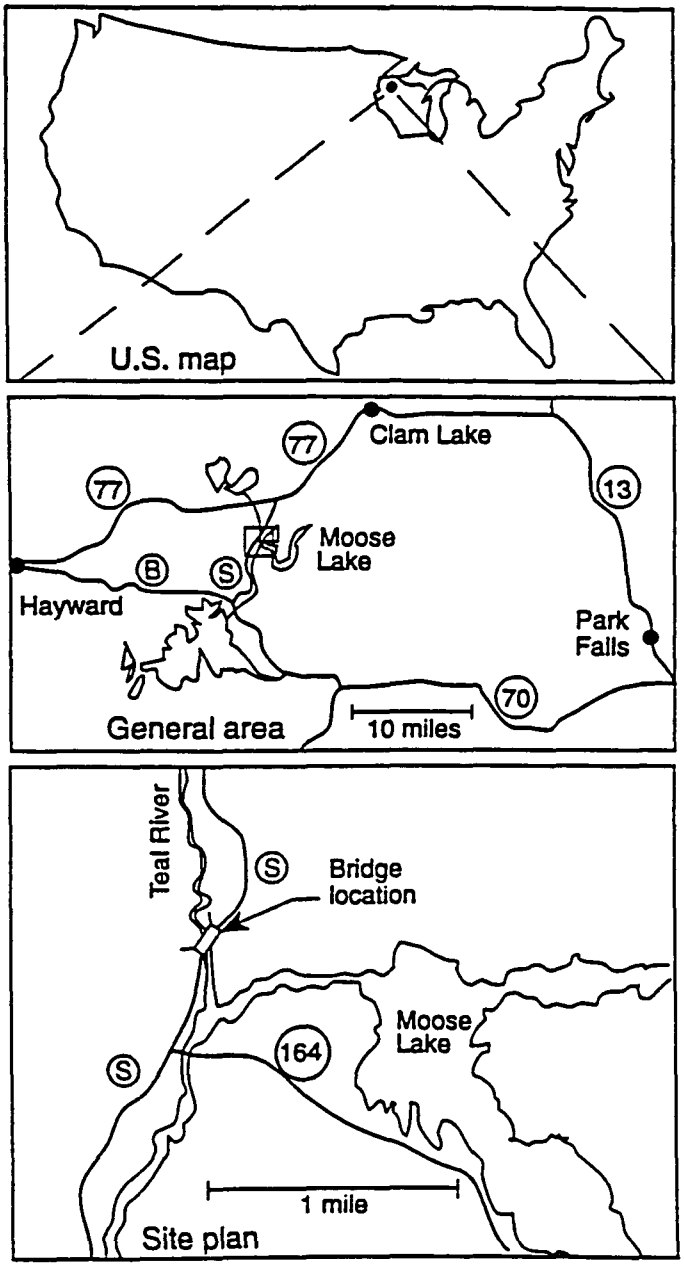

Fig. 3. Teal River bridge location

glue laminated members made of Wisconsin grown Red Pine along with Southern Pine. These glulam members would then make up the laminates used in the stress laminated decking. Southern Pine laminates were used in the exterior portions of the glulam members to provide additional stiffness over that which could be obtained using only Red Pine. In addition, two glulam members were made entirely of Red Oak. These hard wood members were used on each side of the bridge to prevent the prestressing bearing plates from crushing the timber. Each glulam member was designed to be 13 3/4 in. deep, 3 1/8 in. wide, and 32 1/2 ft long. Since each glulam member could be constructed to the full length of the bridge, no butt joints were needed and thus no adjustments to the longitudinal bridge stiffness were needed for design or analytical calculations.

Nine one inch prestressing rods were placed at 44 in. on center to provide a design stress of 100 psi between laminates. The design stress was achieved by applying a design force of 60,500 lb to each prestressing bar. Bearing and anchorage plate dimensions are given in Fig. 4 along with the overall bridge dimensions. An approximately 2 inch thick asphalt wearing surface was applied in June 1990.

The modulus of elasticity of the glulam members was determined by several tests conducted at the manufacturing plant, FPL, and in the field prior to the bridge

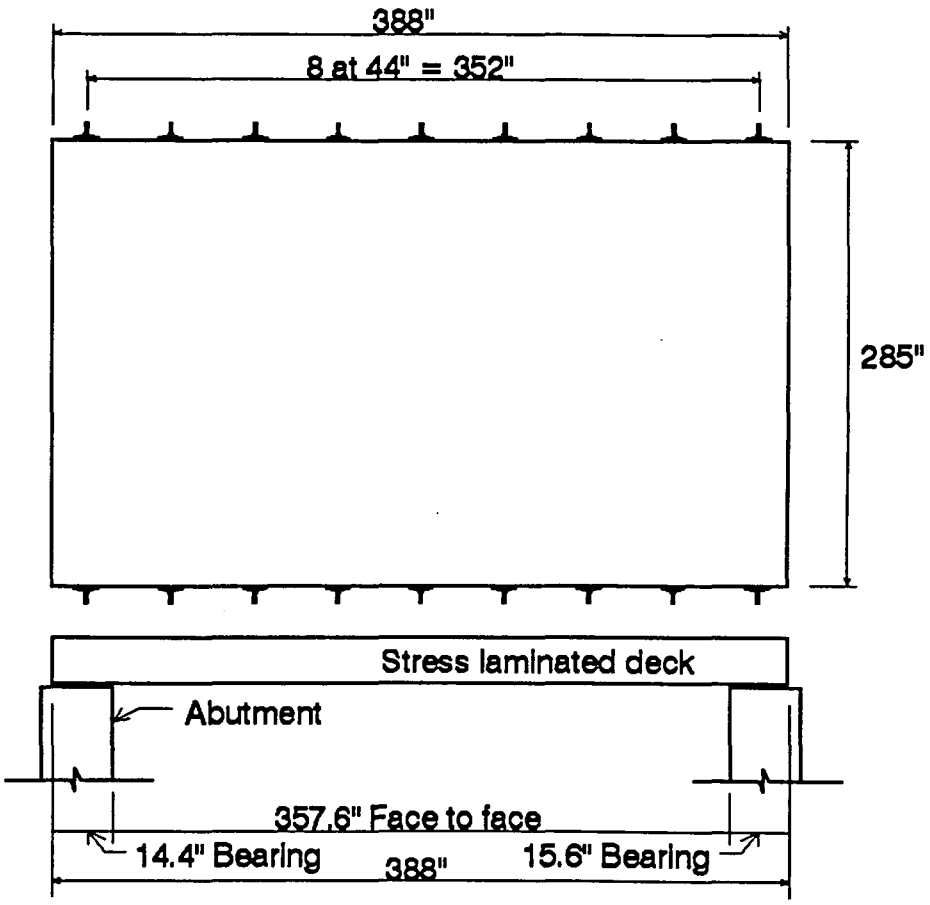

Bridge dimensions

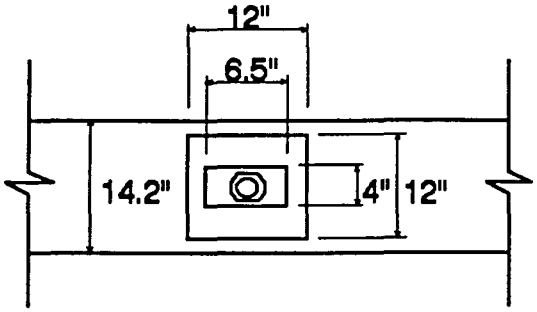

Anchorage system dimensions

Fig. 4. Teal River bridge dimensions

construction. Based on these tests [19], an allowable modulus of elasticity of 1,780,000 psi was used for analytical calculations of deflections and dynamic response.

2.2 Field Test

Field testing of the Teal River stress laminated timber bridge was performed on June 2nd and 3rd, 1993. The testing instrumentation, data acquisition program, and procedure will be described in this section.

2.2.1 Instrumentation

Vertical displacements were recorded at both mid and quarter span locations during passage of a three axle dump truck traveling at various velocities (truck characteristics and traveling speeds are discussed in Section 2.2.3). Additionally, deflections were monitored at four abutment locations to ensure no movement occurred during loading application. Figure 5 illustrates the measurement locations and numbering system.

At midspan, displacements were measured at mostly two foot intervals transversely across the entire bridge width. At each quarter span, measurements were taken at four locations all in the upstream lane of the bridge. The centerline, upstream edge, and two intermediate measurements

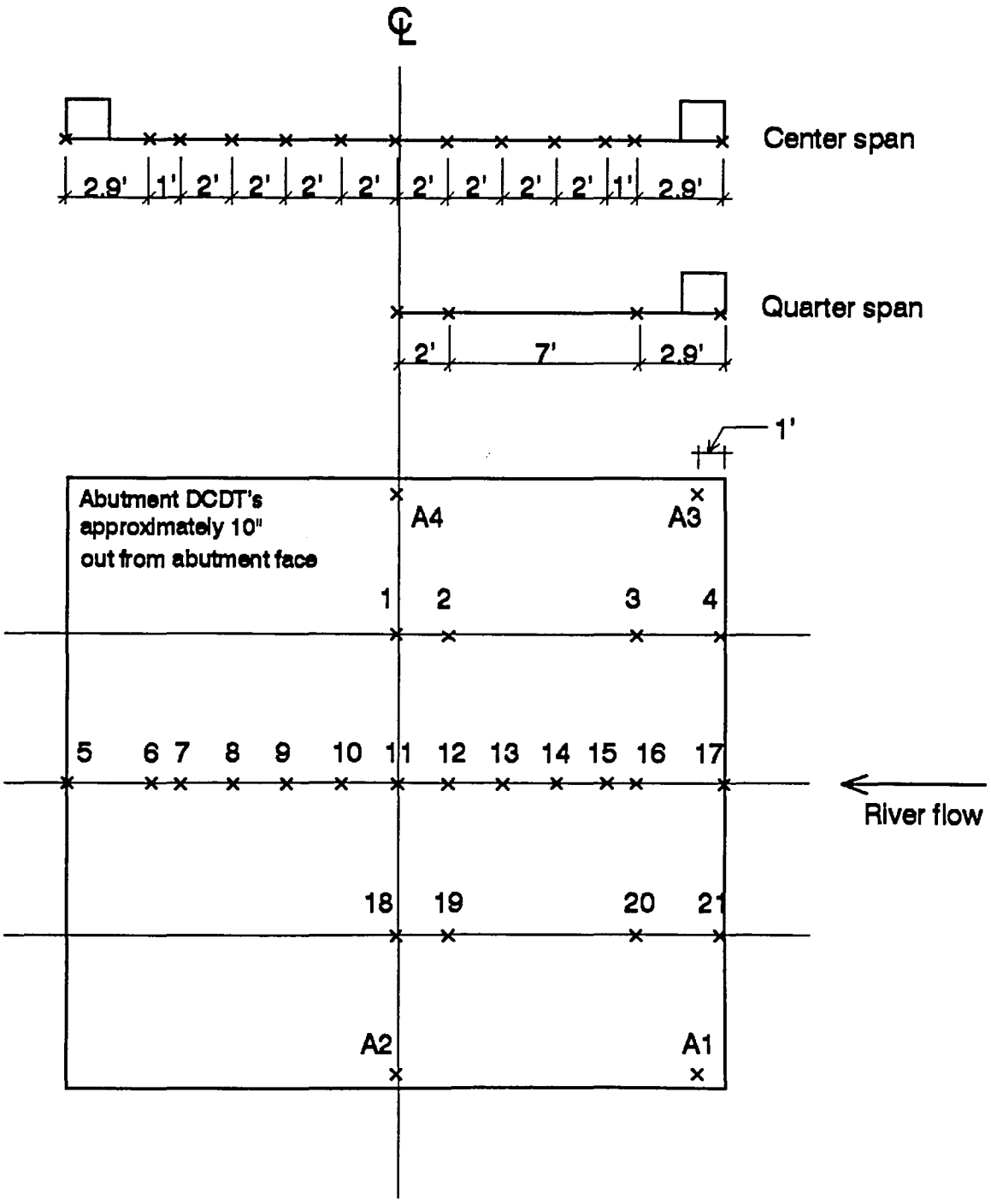

Fig. 5. Field measurement locations and numbering system

were taken. Movement of the abutments were monitored by taking measurements on the underside of the deck as close to the abutment as possible. Again, only the upstream lane was instrumented.

In addition to displacements, the position and velocity of the vehicle were monitored using two tape switches. Each tape switch consisted of two current carrying wires that when compressed, such as by the passage of a vehicle tire, short the circuit. The change in voltage caused by the short could be detected by the data acquisition system and used to start data collection or monitor vehicle location. The first tape switch was placed 5 ft before the bridge entrance and used to trigger the data collection. The second was placed at the bridge exit.

The displacements were measured using Celesco string type direct current differential transducers (DCDT's). Each DCDT had a 20 in. stroke allowing measurements of plus or minus 10 inches. As the DCDT string is pulled or retracted, an internal potentiometer changes the output voltage which is read by the data acquisition system. The change in voltage is calibrated to a corresponding displacement allowing deflections to be determined any time the output voltage is recorded. Two by eight inch lumber were spanned across tripods and cabled securely to the ground to act as stands onto which the DCDT's could be mounted. The stands were tied

down at several locations such that no movement could occur. This ensures that the measured deflections were that of the bridge itself and did not include movement of the stand. A plum-bob was used to locate the position of the DCDT's directly beneath the measurement locations, and wood screws used to secure them to the stand.

The data was collected using a Hewlett-Packered (HP) 3852A data acquisition/control system (DAS). The DAS was equipped with two HP 44711, 24 channel, FET multiplexers and an HP 44702, 13 bit high speed voltmeter. The DAS was controlled and the data post-processed and stored in a portable 486DX-33 PC running IBASIC for WINDOWS. The program used for controlling the DAS is described in the next section.

2.2.2 Data Acquisition Program

In order to obtain a good representation of the dynamic response of the bridge, data needed to be collected often enough such that peaks in the dynamic oscillations were not missed. This requires the collection of large amounts of data and a means of putting it together in an understandable form. The data acquisition program was used for this purpose. The program was written in BASIC language using the software HP instrument BASIC for WINDOWS. A general flow chart of the program is given in Fig. 6 and a copy of the

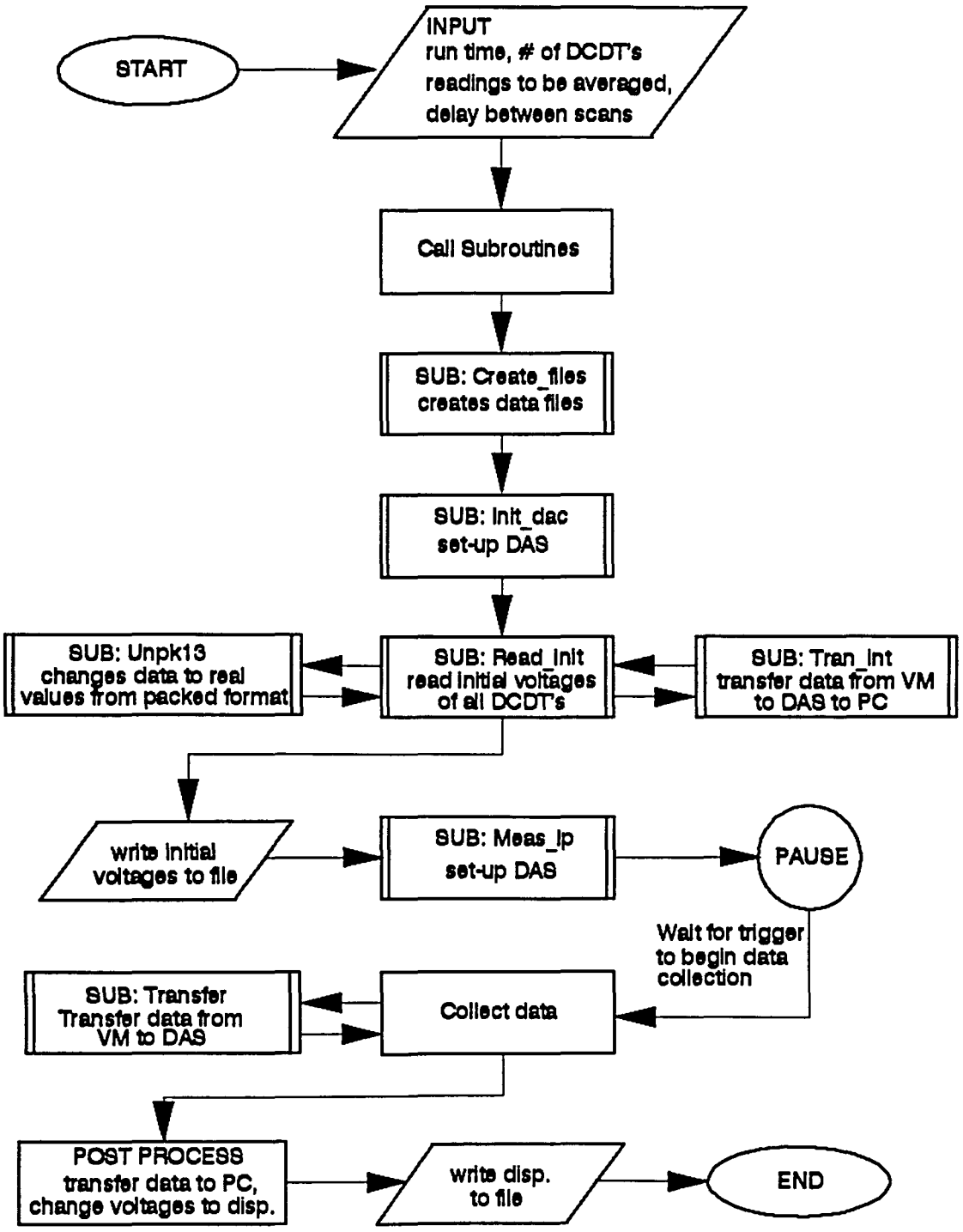

Fig. 6. DAS program flowchart

entire program is printed in Appendix A.

The program allows the user to input the parameters used in defining the data collection process. The length of time data will be collected is input and is based on the time required for the vehicle to cross the bridge. The reading of all channels is referred to as a scan, and the scan delay, which is user input, is the time between scan readings. That is, the scan delay is the time between voltage readings of all DCDT's and monitored tape switches. The time between voltage readings of the individual channels is not input, but is set at the fastest possible, 10 microseconds. The time required to read the individual channels in a single scan is considered to be instantaneous and neglected in interpreting the data. Also input is the number of channels to be read which is the number of DCDT's plus the number of monitored tape switches. For this bridge, 26 channels were monitored; 25 DCDT's along with one tape switch.

Once the above parameters have been input, the program sets up the DAS to collect the initial output voltages. The initial voltages are then recorded by reading one scan of the channel list with the bridge in an unloaded condition. The voltages are read by the high speed voltmeter (VM) and transferred to DAS and then to the PC where they are converted into a real format and stored.

The DAS is reset and set-up once again, this time to

collect the voltages during application of the dynamic loading. The program pauses waiting for a trigger to start the data collection. The trigger comes from the first tape switch located before the bridge entrance. Once triggered, voltages are collected and stored within the DAS according to the input scan delay and length of time. After all data has been collected, the voltages are converted to real format and transferred to the PC were they are held in a two dimensional array awaiting post processing.

The post processing converts the collected voltages to displacements. Every reading for each DCDT is subtracted from its initial voltage to obtain the change in output voltage caused by the bridge deflection. The change in voltage is converted to a displacement by multiplying by the corresponding calibration factor for the DCDT. The displacements are then written to a file for storage and analysis at a later time. The program is rerun for each additional test.

2.2.3 Testing Procedure

The dynamic load testing of the Teal River stress laminated timber bridge was completed in cooperation with FPL. In order to minimize the time at the bridge, normal static load monitoring procedures were conducted for FPL along with the dynamic testing. Deflections due to six

static load cases were recorded as part of the monitoring process. Static test procedures were carried out under the supervision of Michael Ritter of FPL. The results of these tests are not the focus of this study and are therefore not discussed.

The dynamic load behavior of the bridge was evaluated for several vehicle velocities under smooth and rough approach conditions. The test vehicle was a three axle dump truck loaded with sand. The gross weight of the vehicle was 70,040 lb with 22,180 lb being distributed to the front axle and the remaining 47,860 lb assumed divided evenly between the rear two axles. Axle spacings were 14.6 ft between the front two axles and 4.7 ft seperating the rear two axles (see Fig. 7a). The axle track width was 6 feet.

All tests were conducted for two different vehicle positions. The first was with the left wheel line two feet right of centerline in the upstream lane. For the second position, the truck straddled the centerline of the bridge. That is, one wheel line 3 ft on either side of centerline (see Fig. 7b). String lines were fastened to the bridge deck to act as a guide for the driver to follow while crossing the bridge.

In order to obtain a basis by which the dynamic load effects could be compared, crawl tests were performed for each loading position. During crawl tests the vehicle

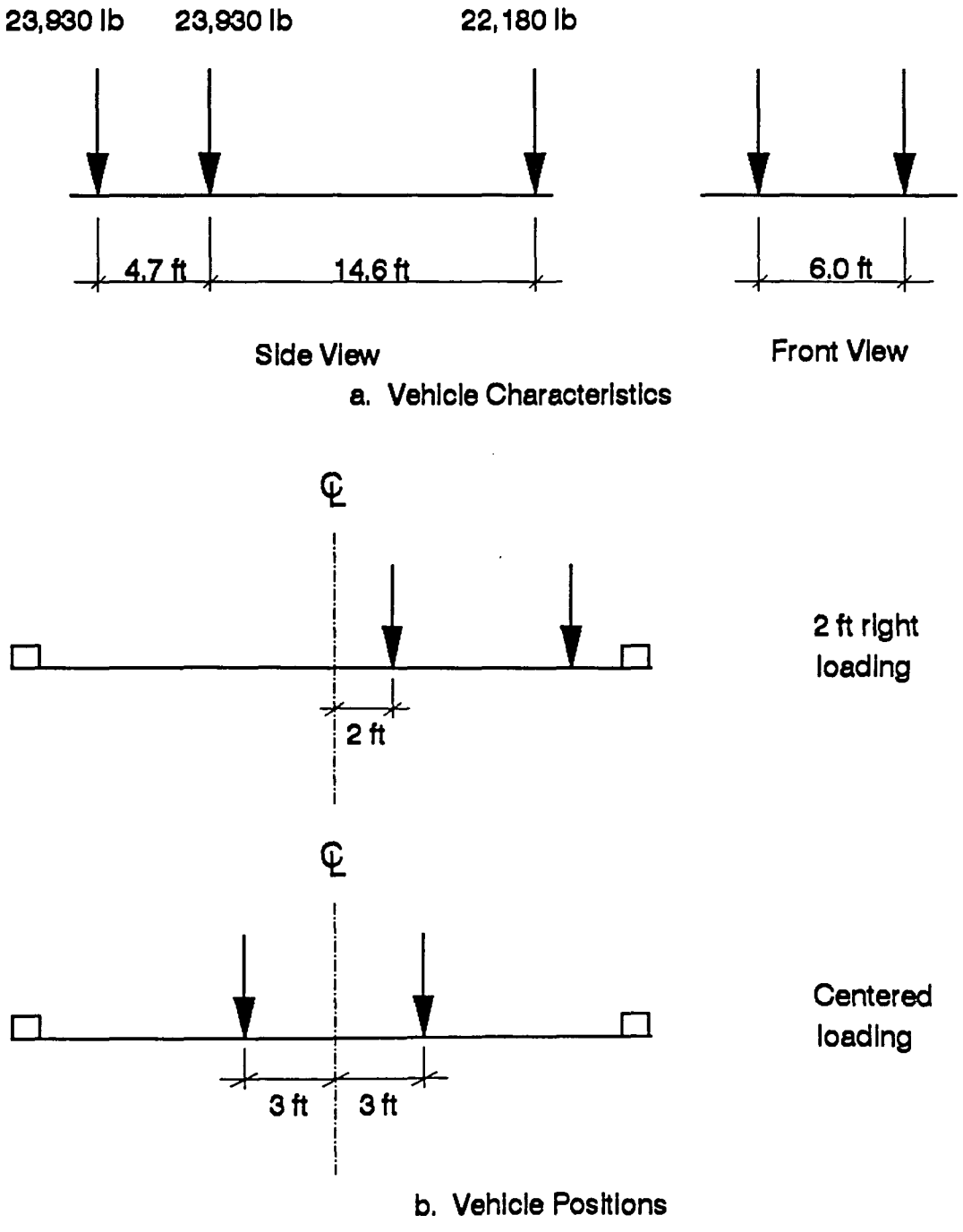

Fig. 7. Vehicle characteristics and lane positions

crossed the bridge at a low velocity (approximately 5 m.p.h.) producing deflections very near that of static application of the load. It is assumed that during crawl speed loading there is no dynamic contribution to the deflection. Deflections caused by higher velocity loadings can then be compared to that of crawl speed to evaluate the dynamic performance of the bridge.

Load tests were then conducted at several velocities at each vehicle position. A sharp curve in the road only a few hundred feet past the bridge restricted the truck velocities to approximately 40 miles per hour. Using this as an upper limit, velocities of 20, 25, 30, and 40 m.p.h. were chosen for the tests. As mentioned in the literature review (Section 1.4), increases in the dynamic response can occur if the time between application of consecutive axles across a point on the bridge is equal to the natural period of the bridge. However, this is only true if the frequency of the bridge is not effected much by the mass of the vehicle. For this short span timber bridge, the ratio of live load to dead load masses is 1.5. With the live load being such a large portion of the total loaded mass, the loaded frequency of the bridge will change significantly from the unloaded frequency. Therefore, the increase in dynamic response would not be realized, and additional velocities were not necessary.

Knowing the minimum velocity and bridge and truck

lengths, the maximum amount of time needed for the truck to cross the bridge at speeds other than crawl was 1.8 seconds. Based on this, a test duration of 5 sec was chosen for data collection. A test duration of 20 sec was used for the crawl speed loadings.

Preliminary analysis (see Section 3.3) predicted the natural period of the bridge being about 0.14 seconds. Taking readings every 0.005 seconds would allow more than 25 data points on a period of vibration, therefore well defining the bridge response. Using a scan delay of 0.005 sec and a test duration of 5 sec, 1000 readings were taken on each DCDT for every non-crawl speed test. A scan delay of 0.01 sec was used on the crawl speed tests resulting in 2000 readings on each DCDT. A larger delay between scan readings could be used on the crawl tests because no dynamic effects were expected.

Unevenness at the joint between bridge entrance and approach roadway or the presence of ruts and potholes due to low maintenance of the road surface can increase the impact caused by dynamic vehicle loading. As the truck runs over irregularities in the road surface, the mass supported by the vehicle suspension system begins to vibrate. If the vehicle enters the bridge span with initial displacements and accelerations of the suspended mass, the bridge may see an increase in response depending on the vehicle characteristics

and initial conditions. Even with the road surface in good condition, the bridge response may still be influenced by initial vehicle oscillations. Small irregularities in the roadway or even the shifting of gears will cause some vibrations, however, these are considered small when the approach roadway is in good condition.

The effects of altering the approach roughness were evaluated by placing an artificial bump at the bridge entrance to simulate a rough condition. The bump was made by securing a 2 x 4 in. board to the wearing surface using lag screws. The dynamic load tests were repeated with the bump in place for three velocities in each vehicle position.

2.3 Test Results

2.3.1 Dynamic Response

In order to evaluate the dynamic performance of the Teal River bridge, it was first necessary to determine at which reference points the response would be most critical. As discussed in Section 1.4, Bakht and Pinjarkar recommend using only those points where the maximum static deflections occur. The crawl speed tests were used to determine those locations.

For each scan during the crawl speed tests, a transverse profile of the midspan deflections could be plotted using the data from DCDT's 5 through 17 (the midspan DCDT's). Each of

these plots represents the static midspan deflections of the bridge corresponding to a vehicle position at the time the scan was taken. The maximum midspan profile was selected out of all the scans and was found to occur when the rear axles of the truck were approximately centered about the bridge midspan. The maximum midspan deflections for each vehicle position and are plotted in Fig. 8.

For the 2 ft right of centerline crawl speed test, the maximum transverse deflection profile occurred at the same vehicle position as one of the static tests conducted for FPL. Assuming there is no dynamic contribution to the deflections in the crawl speed test, the two midspan deflection profiles should be the same. The static profile is superimposed on the maximum crawl speed profile in Fig. 8. As can be seen from this plot, the two profiles are very well matched. Although there was no static load case to compare with the second vehicle position (straddling the centerline), it was concluded from the first that the crawl speed deflections had little dynamic contribution and could be used to accurately represent the static deflections.

The crawl speed transverse profiles were then used to determine the reference points at which the maximum static response occurred. These points would be used to evaluate the dynamic performance of the bridge as suggested by Bakht and Pinjarkar. From Fig. 8, the maximum crawl speed response

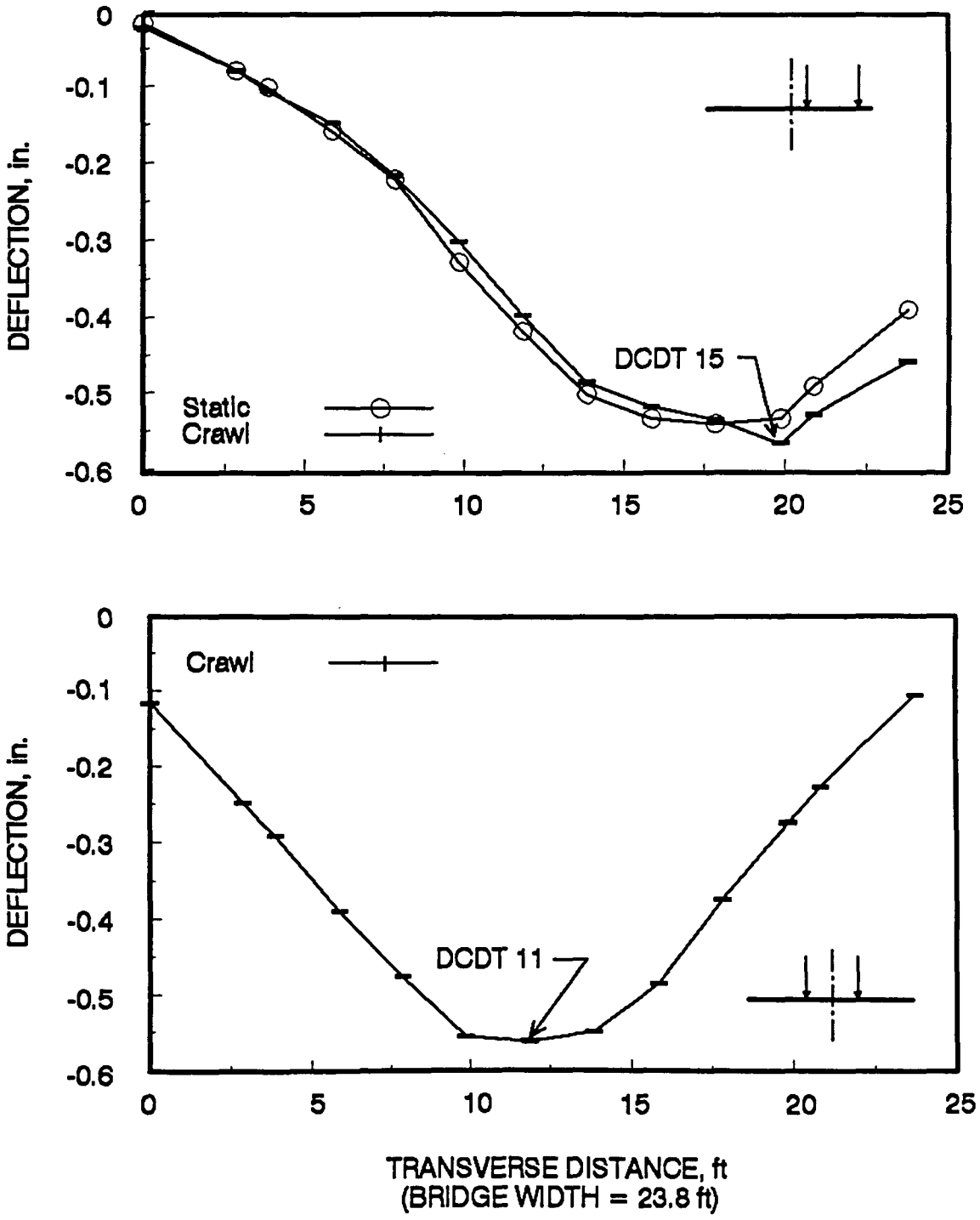

Fig. 8. Maximum transverse deflection profiles

occurred under DCDT 15 for the 2 ft right loading, and under DCDT 11 for the centered loading. Although the maximum static response occurred under DCDT 14 (2 ft to the left) for the 2 ft right loading, the dynamic data consistently showed the maximum deflection occurring under DCDT 15. Therefore, it was chosen as the reference point. The reference points are located under the right wheel line and at centerline for the 2 ft right and centered loadings respectively.

All plots presented in this section are done with respect to the reference points unless otherwise noted. Many of them show the vertical deflection of the reference point versus position of the front axle. The position of the front axle was used to provide a common reference against which the deflections could be plotted for any vehicle speed. That is, a plot of a 20 m.p.h. test can superimposed on a 30 m.p.h. test using the same x-axis. A position key noting the bridge layout and location of the center of the rear axles in terms of the front axle position is provided in Fig. 9 for cross reference.

The majority of the plots are superimposed over the crawl speed response to allow a comparison between the dynamic and static behaviors. Although dynamic effects in the crawl speed tests were minimal, a curve was fit through the data to eliminate any small irregularities. The curves fit the data very well and made the plots visually more

Bridge layout

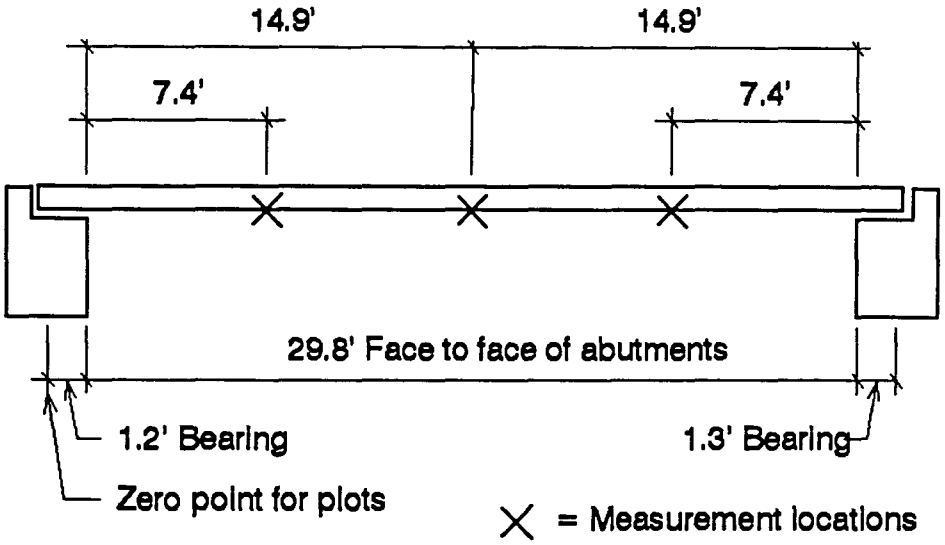

Position key

Position of front axle (feet)	Location of center of rear axles (feet)	Description
14.6	-2.4	Just prior to rear axle entrance
17.0	0	Rear axles centered over zero point
25.6	8.6	Rear axles centered over quarter span
33.1	16.1	Rear axles centered over midspan
40.6	22.4	Rear axles centered over three quarter span
51.6	34.6	All axles off bridge

Fig. 9. Plot position key

presentable.

As previously mentioned, velocities of 20, 25, 30, and 40 m.p.h. were chosen as target velocities to be used in the field tests. The driver was instructed to maintain a truck velocity as close as possible to the target velocity while crossing the bridge. The actual average velocities during the tests were calculated using the data from the monitored tape switch. A spike in the tape switch data occurs as the front axle exits the bridge and shorts the signal. Knowing how many scans had occurred since the front axle triggered the data collection, the rate of scan readings, and the distance between the two tape switches, the actual average truck velocity could be calculated. The actual velocities and target velocities for all tests are compared in Table 1.

Table 1. Target and actual velocities (m.p.h.)

2′ Right Loading		2′ Right Bump		Centered Loading		Centered Bump	
Target	Actual	Target	Actual	Target	Actual	Target	Actual
5	4.1	25	28.3	5	3.8	25	25.5
20	22.4	30	33.5	20	17.4	30	32.2
25	22.8	40	43.4	25	23.0	40	43.0
30	29.8			30	23.5		
40	41.3			40	42.0		
40	41.3						

As listed in Table 1, two tests were run at a target velocity of 40 m.p.h. for the 2 ft right of centerline loading position. This was done because it was observed during the first test that the truck was 1 ft left of the proper position. The effect of the vehicle being off line is discussed later in Section 2.3.5.

Plots of the bridge deflections for the 2 ft right loading are given in Fig. 10. These plots show the bridge response at the reference point (DCDT 15) versus front axle location for velocities of 22, 30, and 41 miles per hour. Although target velocities of 20 and 25 m.p.h. were used in the field test, the actual average velocities for the two tests were 22.4 and 22.8 m.p.h. respectively. With these velocities being nearly the same, only the 22.4 m.p.h. response was plotted. The 41 m.p.h. plot is that of the second 40 m.p.h. target velocity test where the vehicle path was not off line.

Similarly, plots are presented for the centered loading in Fig. 11. These plots show the response at 17, 24, and 42 m.p.h. at the centered loading reference point (DCDT 11). For this loading position, target velocity tests of 25 and 30 m.p.h. resulted in actual average velocities of 23.0 and 23.5 miles per hour. Only the 23.5 m.p.h. response is plotted.

All the plots show relatively little dynamic response caused by the front axle alone. The amplitude of the dynamic

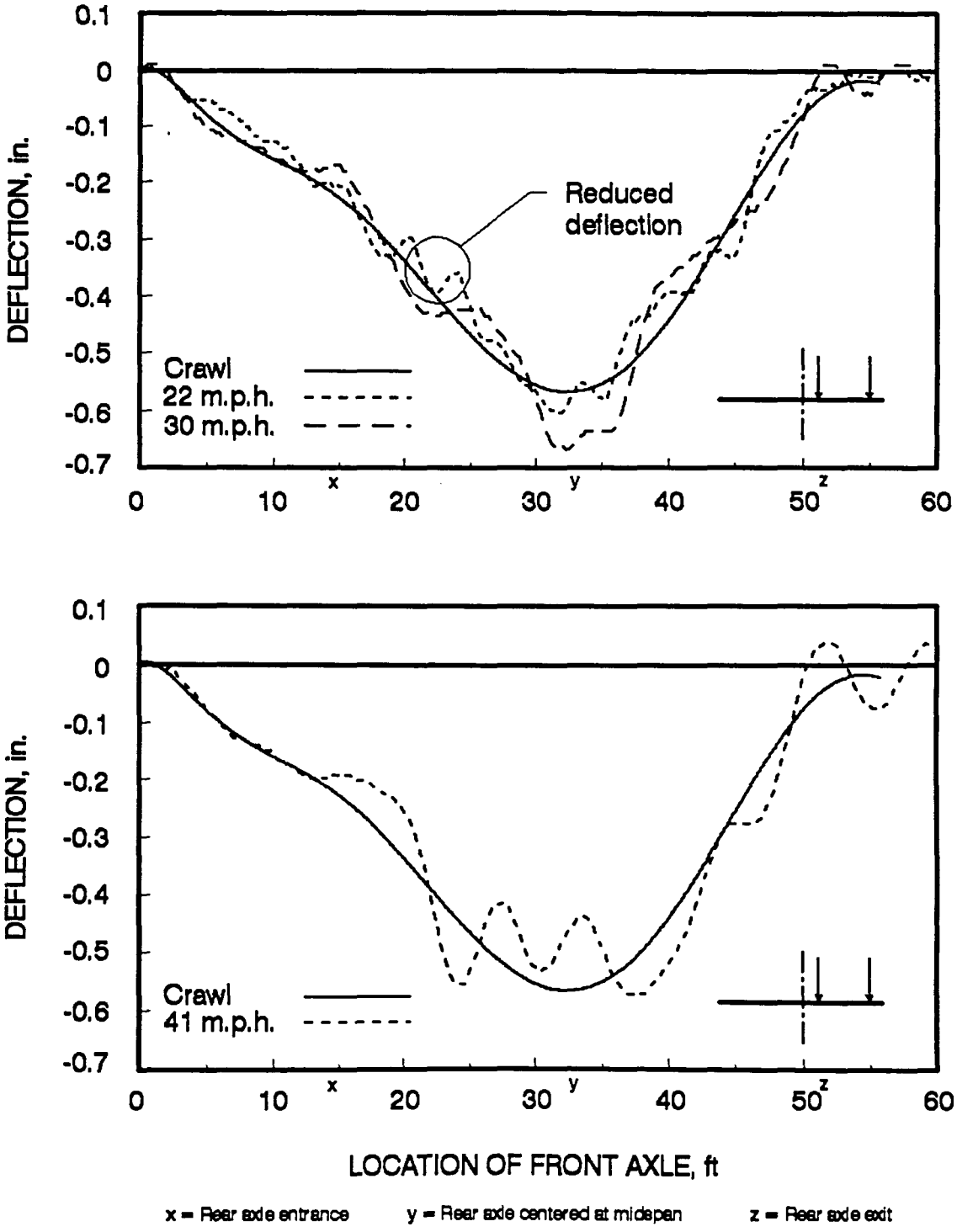

Fig. 10. Bridge response for 2 ft right loading

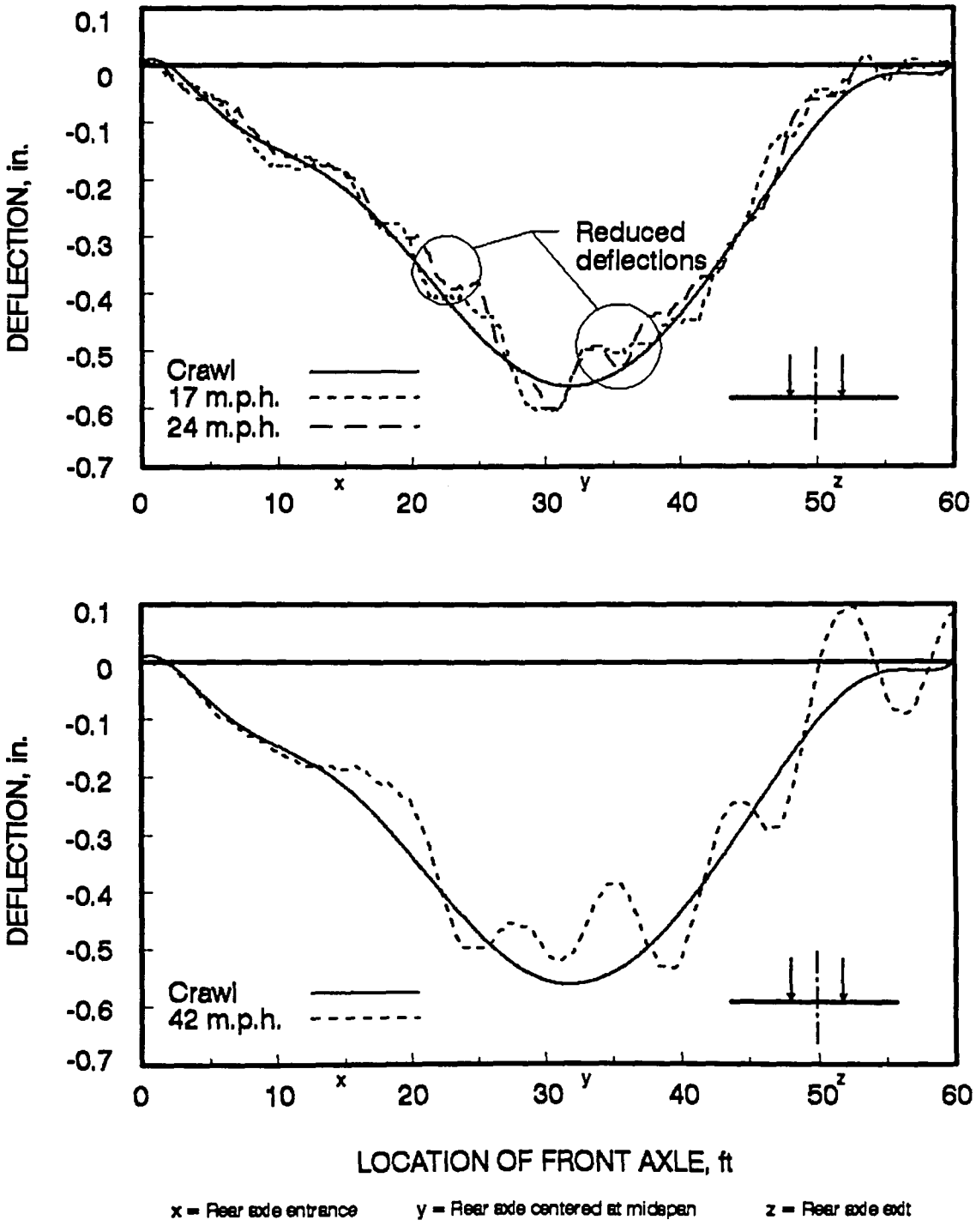

Fig. 11. Bridge response for centered loading

oscillations occurring while only the front axle is on the bridge are small, resulting in a response near that of crawl speed. The amplitude of the oscillations increases when the closely spaced, heavier rear axles enter the bridge. This suggests that the response is mainly influenced by the rear axles.

Figures 10 and 11 show the number of oscillations decreasing with an increase in velocity. However, this does not mean the bridge is vibrating slower at higher velocities. The amount of time the vehicle is on the bridge decreases as the vehicle speed increases, resulting in fewer oscillations occurring while the vehicle crosses the bridge. Therefore, as a consequence of plotting with respect to the vehicle location, fewer oscillations show up at higher velocities.

It is also noted from the plots that the amplitude of the dynamic oscillations tended to increase as the vehicle velocities increased. As a slowly moving vehicle crosses the bridge, forces applied by the vehicle are applied slowly resulting in small bridge accelerations and small amplitudes of dynamic oscillations. In contrast, as a truck moving at high speed crosses the bridge, the forces are applied quickly causing larger bridge accelerations and as a result, larger dynamic oscillations. It would seem logical then that the overall maximum deflections of the bridge would increase as the vehicle velocity increased. However, this was not the

case.

Table 2 summarizes the maximum deflections occurring under each test plotted in Fig. 10 and 11. The maximum deflections seemed to be increasing for the 2 ft right of centerline loading at 22 and 30 m.p.h., but then dropped at 41 m.p.h. to a deflection equaling only that of the maximum crawl speed deflection. For the centered loading, the maximums were equal at 17 and 24 m.p.h. and slightly larger than the maximum crawl speed deflection. However, the maximum at 42 m.p.h. did not even reach that of crawl speed.

Table 2. Maximum crawl and dynamic deflections

2′ Right Loading		Centered Loading	
Velocity (mph)	Max Defl. (in)	Velocity (mph)	Max Defl. (in)
crawl	0.57	crawl	0.56
22	0.60	17	0.60
30	0.67	24	0.60
41	0.57	42	0.54

The decrease in deflection at the higher velocities is believed to be caused by the interaction of the vehicle dynamics with the bridge vibration. The vehicle has its own dynamic characteristics with the mass of the body and axles and the stiffness of the suspension system. This system will interact with and influence the bridge response. If the

suspended mass is accelerating upward while the bridge is deflecting downward, the force applied by the vehicle will be small and the resulting deflection may not even reach the static displacement.

The dynamic response of the vehicle, and thus the interaction with the bridge, will change with different velocities. Therefore, the reduction in dynamic response may not occur for all velocities or may occur when the truck is at a different position. Further observation of Fig. 10 and 11 reveals a similar effect happening for the other velocities but in different locations (see noted reduced deflections).

Results of the bridge response at the quarter spans are compared to the midspan response in Fig. 12. For these plots, the deflections of three in-line DCDT's are compared for each loading position; DCDT's 3, 16, and 20 (all 9 ft right of centerline) for the 2 ft right loading, and DCDT's 1, 11, and 18 (all on the bridge centerline) for the centered loading. The deflection histories for the quarter spans demonstrate the same behavior with lesser magnitude. The dynamic oscillations occurring at the quarter spans closely match those occurring at midspan. As would be expected, the magnitude of the 1/4 span response is slightly larger than that of the 3/4 span response while the rear axles are crossing the first half of the bridge. Once across midspan,

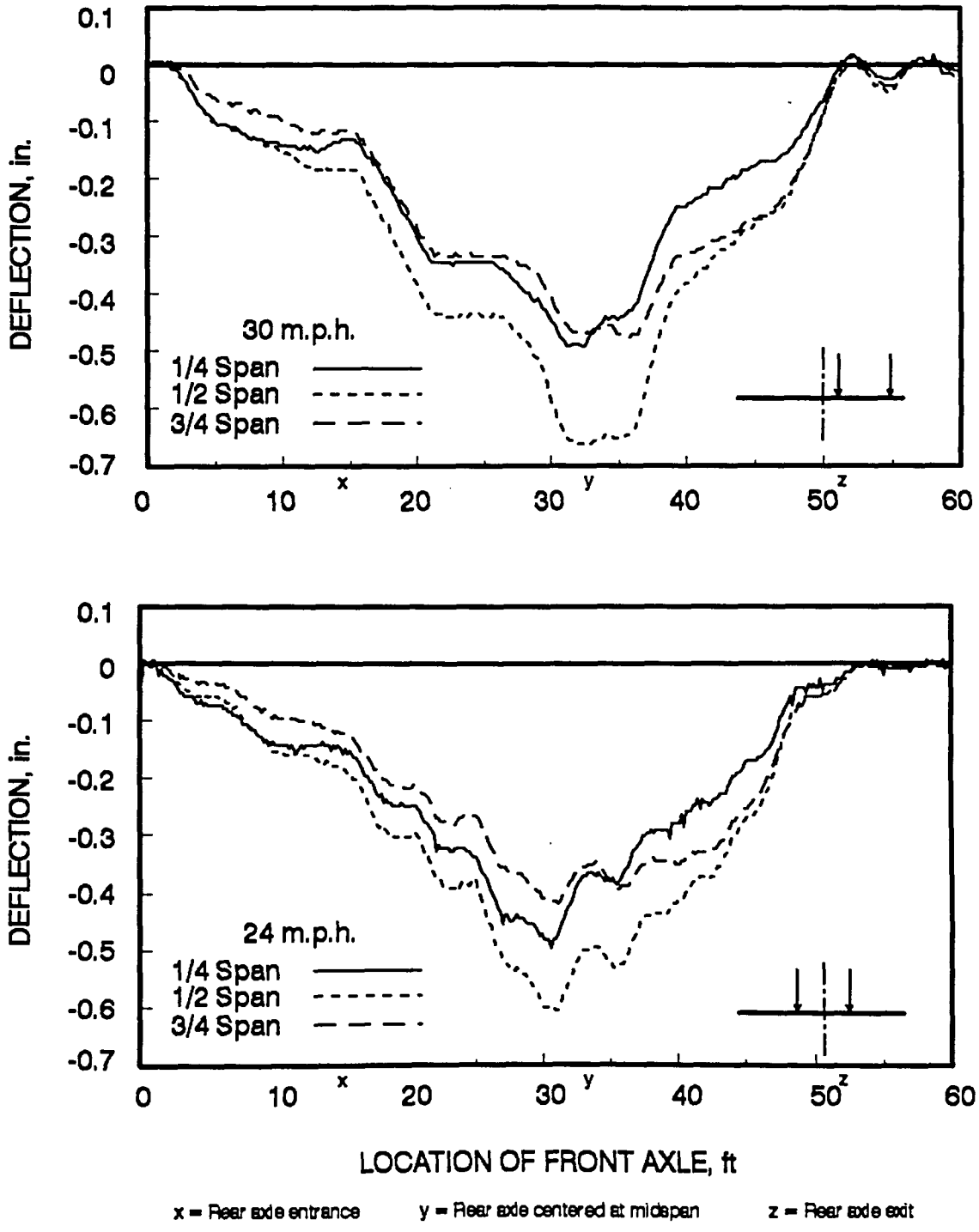

Fig. 12. Quarter span response

the 3/4 span deflections become slightly larger. The quarter span plots presented in Fig. 12 are for the velocities which produced the maximum dynamic deflections for each vehicle position, however, the results were similar for the other velocities tested.

The behavior at points away from the vehicle loading was also observed. Figure 13 illustrates the results. Along with the response of reference point DCDT number 15, the responses of DCDT's 7 (8 ft left of centerline) and 11 (centerline) are plotted for the 2 ft right loading. Similarly, DCDT's 5 (left edge of the bridge), 7, 11 (reference point), and 15 are plotted for the centered loading. The further away from the loading location, the less the behavior resembles that of a point beneath the load. This is evident in Fig. 13, especially as the rear axles are past midspan and exiting the bridge, where the response at points away from the load exhibit well defined oscillations that are not found at points under the load. This would suggest that the response under the loading is a forced vibration, being affected by the vehicle characteristics and vibrations, whereas points away from the load are allowed to vibrate more freely. Again, plots are only presented for the velocities producing the maximum dynamic response, but results were similar at other velocities.

As discussed in Section 2.2.1, movement of the abutments

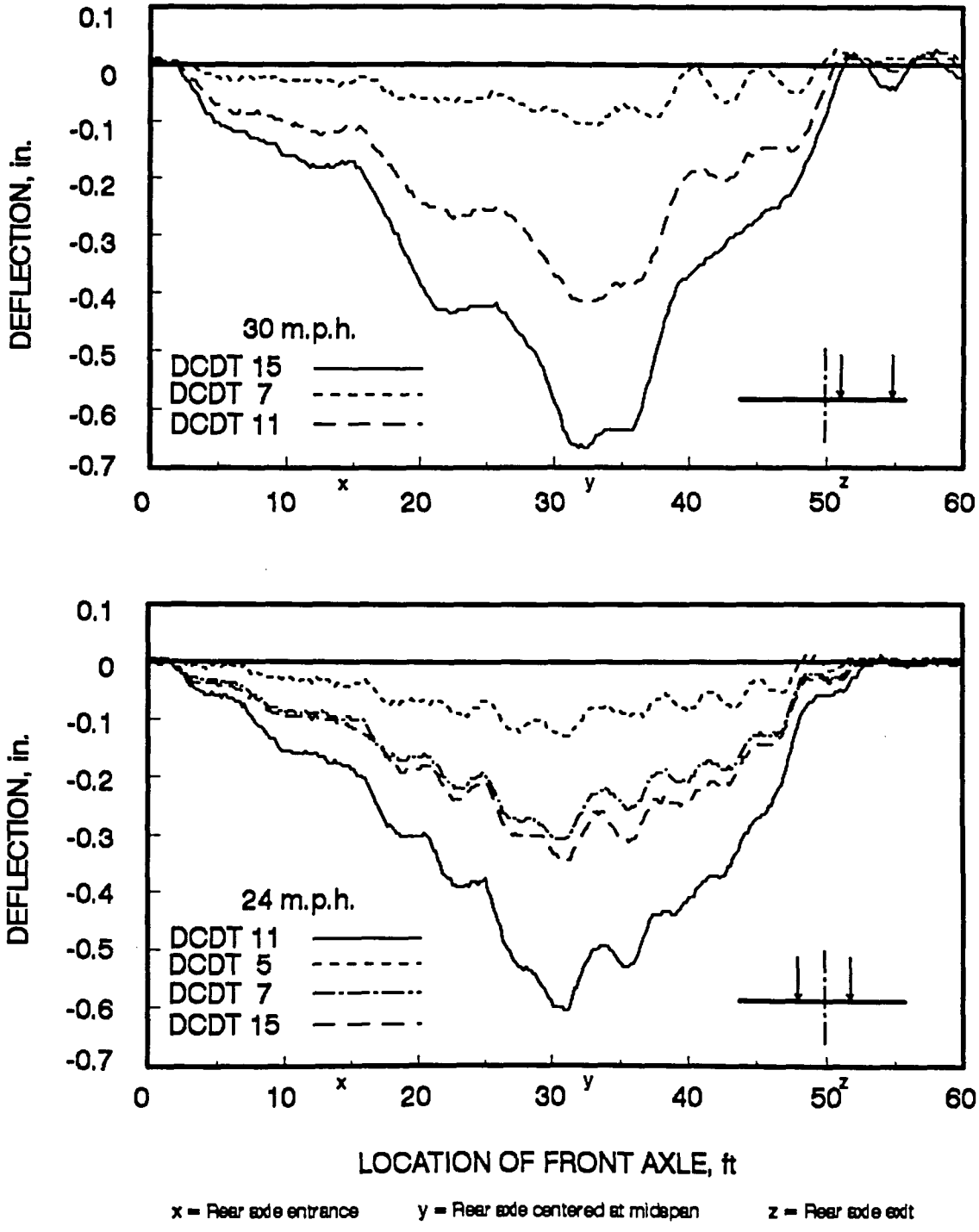

Fig. 13. Response at points away from loading

was monitored by taking measurements on the deck itself, but as close as possible to the abutments. Plots of deflections recorded at those locations (DCDT's A1 through A4) are printed in Fig. 14. The abutment surface provided for bearing was approximately 1.2 feet. However, the actual point at which the deck beared on the abutment varied across the width of the bridge. Accessibility limited how close to the abutment measurements could be taken to 0.9 ft from the abutment face. Assuming the actual bearing of the deck was at the midpoint of the bearing surface, measurements were actually being recorded at 1.5 ft from the actual bearing point. Therefore, even though deflections of up to 0.15 in. were realized, they are believe to be that of the bridge deck itself and do not represent abutment movements.

Changing the road approach roughness significantly increased the maximum dynamic deflections. By placing the bump at the bridge entrance to simulate a rough approach roughness, the vehicle entered the span with initial vertical and rotational motion. The resulting dynamic responses are plotted in Fig. 15 and 16.

No two velocities matched between tests with and without the bump. In order to compare behaviors, the bridge responses with the bump are superimposed on the test most nearly matching in velocity. All tests with the simulated rough approach condition resulted in an increased overall

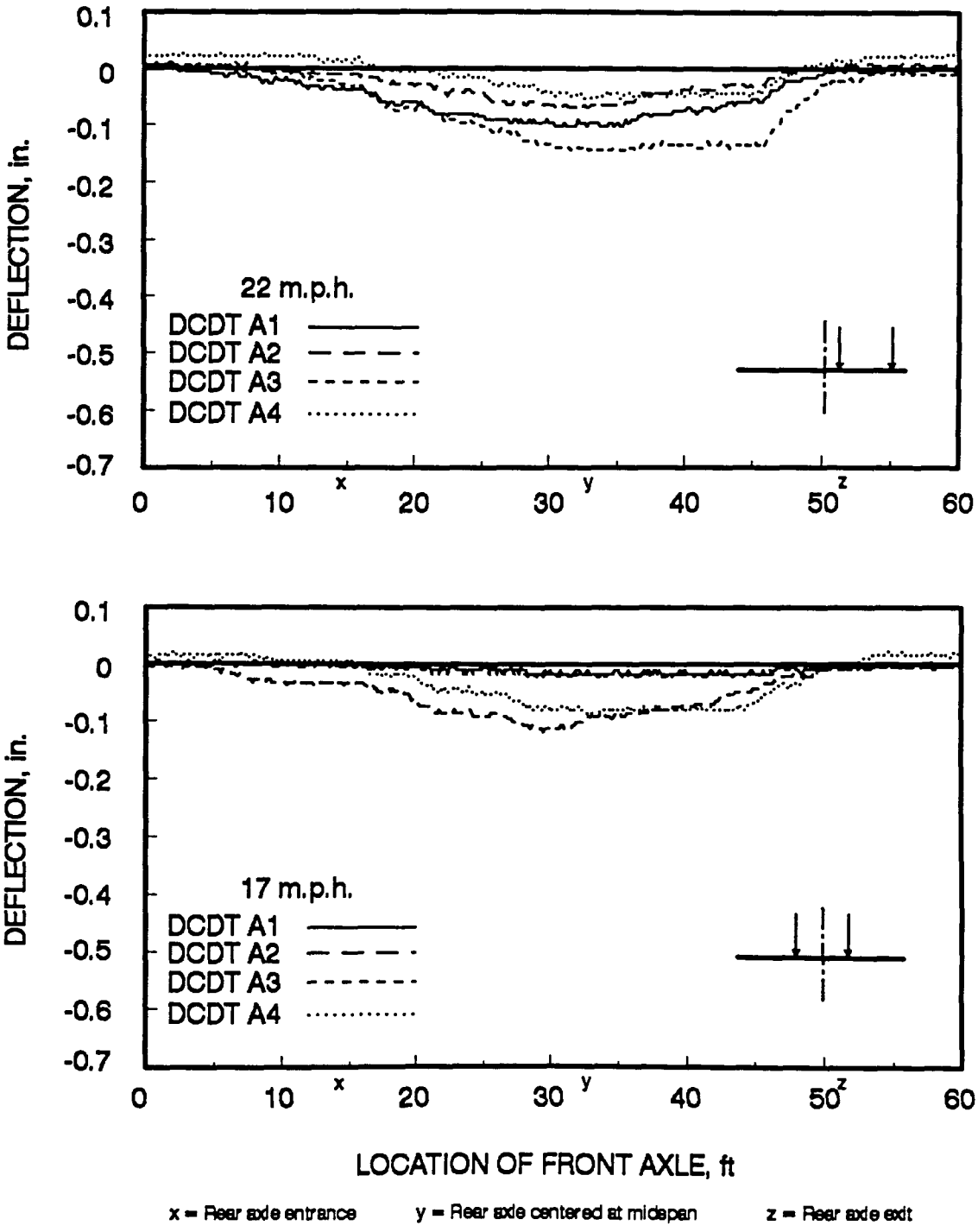

Fig. 14. Abutment DCDT responses

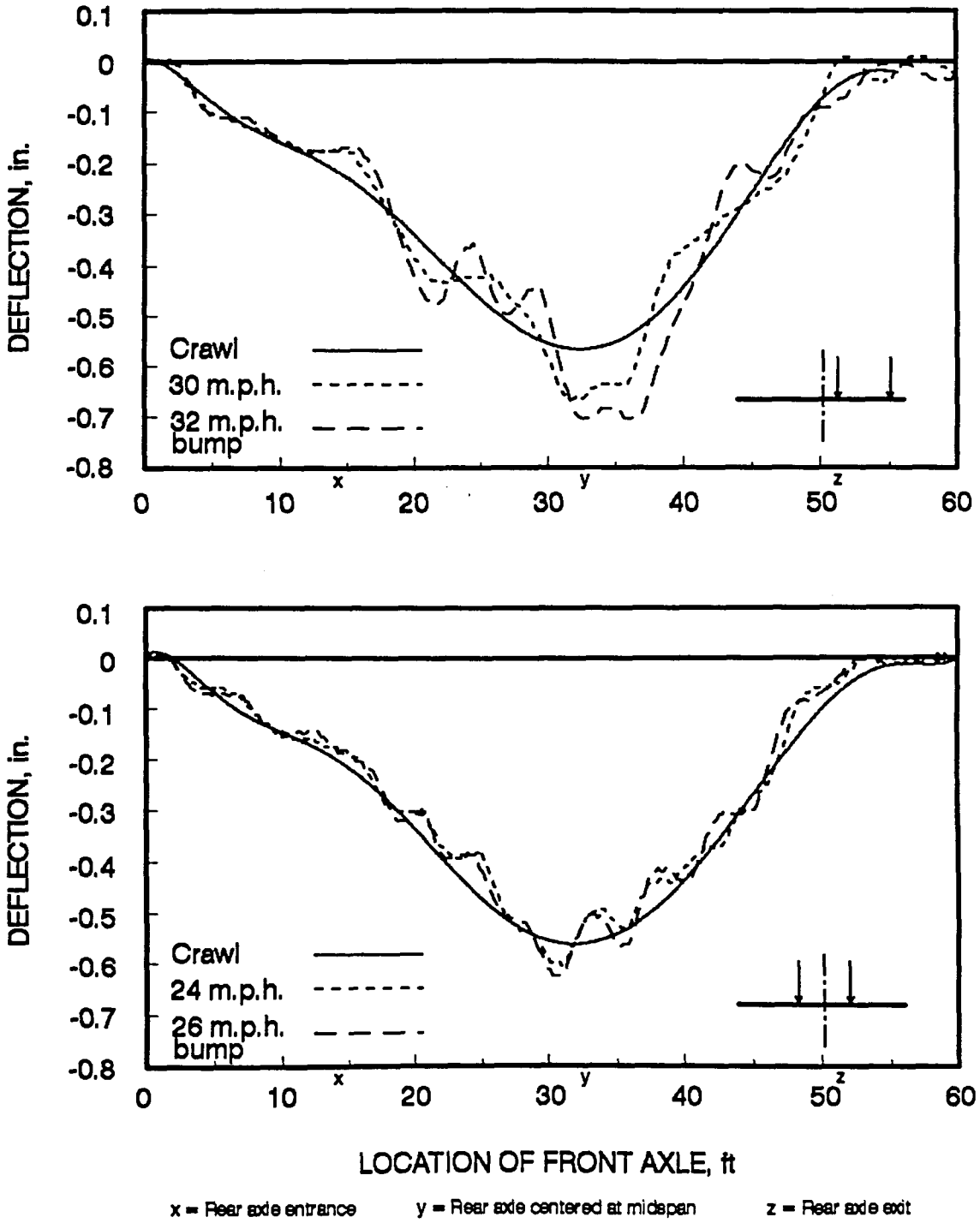

Fig. 15. Response with rough approach roughness

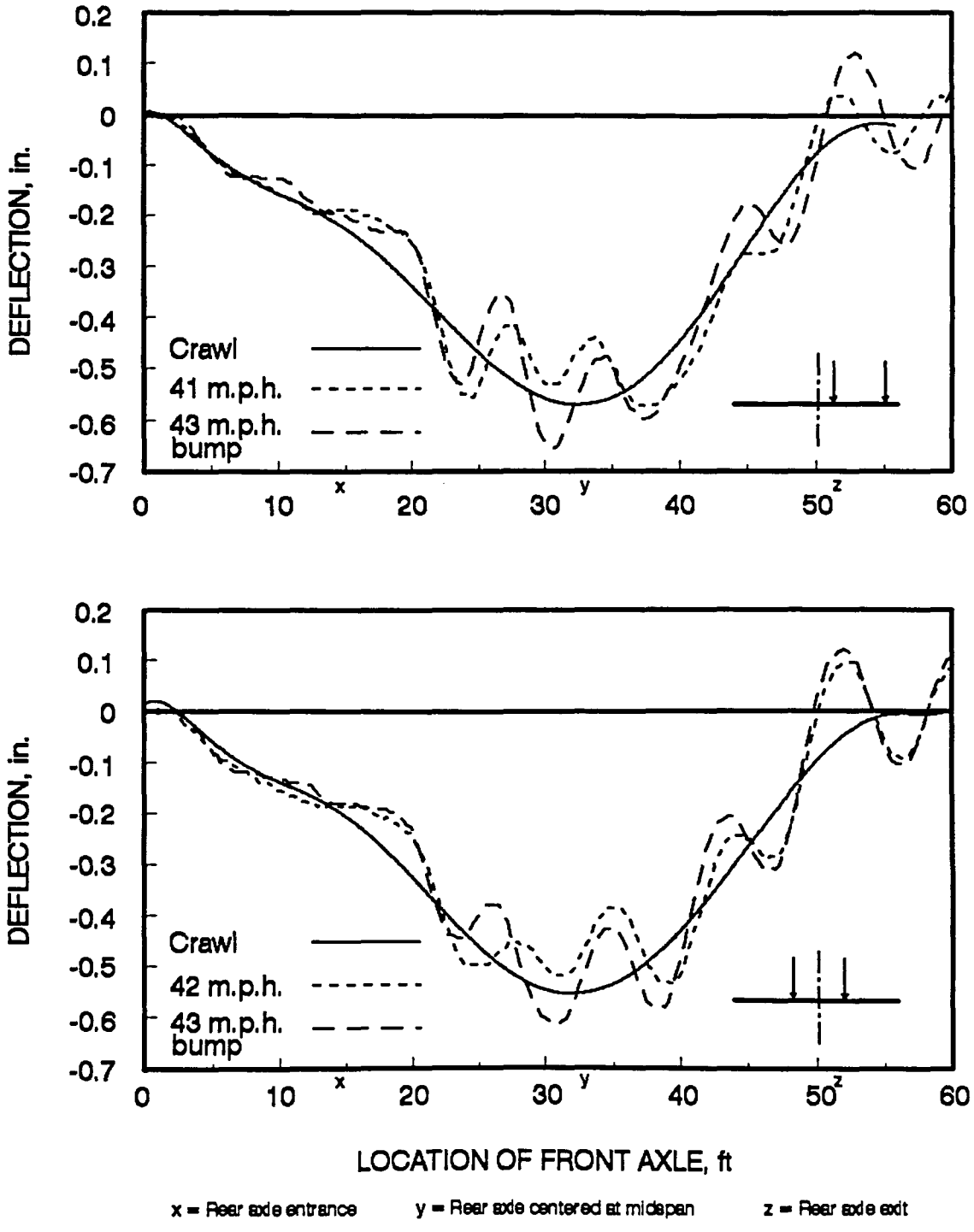

Fig. 16. Response with rough approach roughness 40 m.p.h.

maximum dynamic deflection as well as an increased amplitude of the dynamic oscillation. The maximum dynamic deflections are summarize in Table 3.

Once again, the maximum deflections increase with velocity up to the last test. At the highest velocity, the maximum deflection is reduced, but is now greater than the maximum crawl speed deflection.

Table 3. Maximum dynamic deflections with bump

2′ Right Loading		Centered Loading	
Velocity (mph)	Max Defl. (in)	Velocity (mph)	Max Defl. (in)
28	0.66	26	0.63
33	0.70	32	0.65
43	0.66	43	0.62

2.3.2 Dynamic Load Factors

The calculation of a dynamic load factor (DLF) for each load test was done to quantify the results from all tests conducted. As suggested by Bakht and Pinjarkar and discussed in the literature review (Section 1.4), the impact factor can be calculated using equation 1-3. This equation includes δ_{stat} which is defined as the maximum median dynamic deflection. The median value was used so that static tests were not needed for each vehicle crossing the bridge. This would be necessary if data were being collected under normal traffic,

but this test involved only one vehicle in two defined positions. Therefore, static tests were performed and δ_{stat} could be replaced with the actual maximum static deflection, δ_{st}. The resulting equation after rearranging to solve for the maximum dynamic deflection, δ_{dyn}, is written as equation 2-1.

$$\delta_{dyn}=\delta_{st}(I+1) \tag{2-1}$$

The quantity (I+1) is the dynamic load factor. Thus, the following equation was used to quantify the test results.

$$DLF=\frac{\delta_{dyn}}{\delta_{st}} \tag{2-2}$$

The DLF's were calculated for all tests and are summarized in Fig. 17 and 18 and Table 4.

The general trend of the bridge response from the data collected shows the DLF increasing between 20 m.p.h. and approximately 30 m.p.h. and then decreasing at 40 miles per hour. More data would need to be collected between 30 and 40 m.p.h. to conclude that the maximum response is occurring at 30 miles per hour. In plots where not enough data was collected to follow the mentioned trend, data points were marked but not connected.

In Fig. 17 the DLF's are compared for the two different

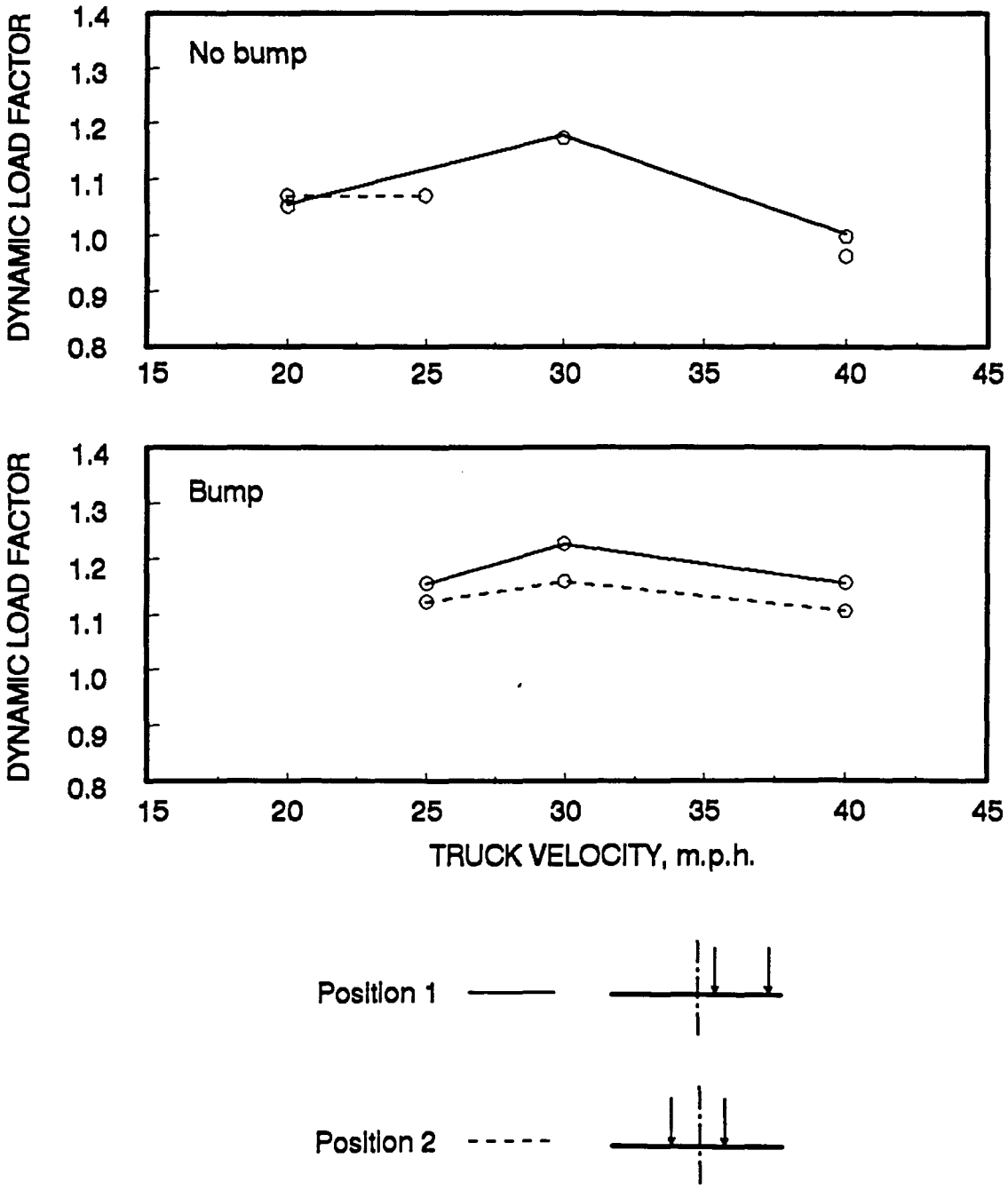

Fig. 17. Dynamic load factors bump and no bump

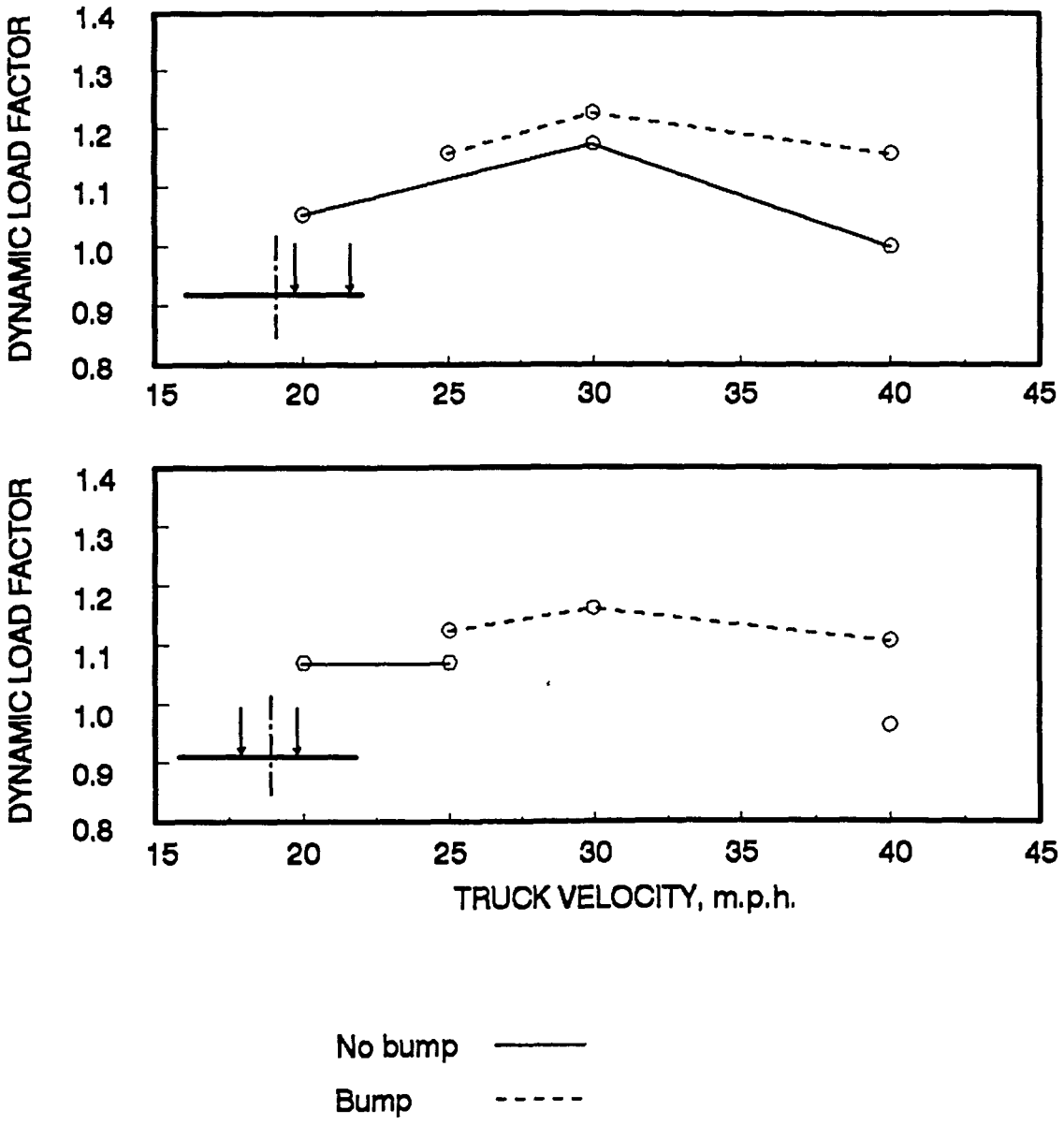

Fig. 18. Dynamic load factors for loading positions

vehicle positions. The DLF's were found to be consistently larger for the 2 ft right position for both the smooth and rough approach conditions. This agrees with the results found by Gupta were eccentric vehicle positions produced a larger dynamic response. Less resistance to deflections occur when the vehicle travels closer to a free edge as in the 2 ft right loading. Larger dynamic oscillations can result which then increase the maximum dynamic deflection and DLF.

Table 4. Dynamic load factors

Smooth Approach			
2' Right Loading		Centered Loading	
Velocity (mph)	DLF	Velocity (mph)	DLF
22	1.05	17	1.07
30	1.18	24	1.07
41	1.00	43	0.96
Rough Approach (bump)			
28	1.16	26	1.13
33	1.23	32	1.16
43	1.16	43	1.11

Figure 18 compares the DLF's for tests run with and without the artificial bump. As expected, the DLF's were always higher with the bump initiating vehicle oscillations. The increases were greatest at the highest velocity tested.

As the velocities increase, larger vehicle oscillations will occur as the truck impacts the bump. Therefore, the data suggests that larger initial vehicle oscillations result in larger increases in the dynamic response of the bridge.

2.3.3 Bridge Natural Period

The natural period of the unloaded bridge can be accurately determined from the free vibration resulting after the truck has exited the span. As previously discussed, the largest amplitudes of vibration occurred at the highest velocities. Thus, the free vibrations resulting from the 40 m.p.h. tests provide the best response on which the period of oscillation could be measured. In Fig. 19, the natural period of the bridge is determined by measuring the time between peaks in the free vibration for the first five periods of oscillation. The periods were then averaged for both vehicle positions. The resulting natural period of the bridge was determined to be approximately 0.13 seconds.

The natural period of a damped system is slightly smaller than that of an undamped system. However, the difference is negligible if the damping is less than about 10 percent of critical damping. In order to estimate the amount of damping present in the tested bridge, the free vibrations were used once again.

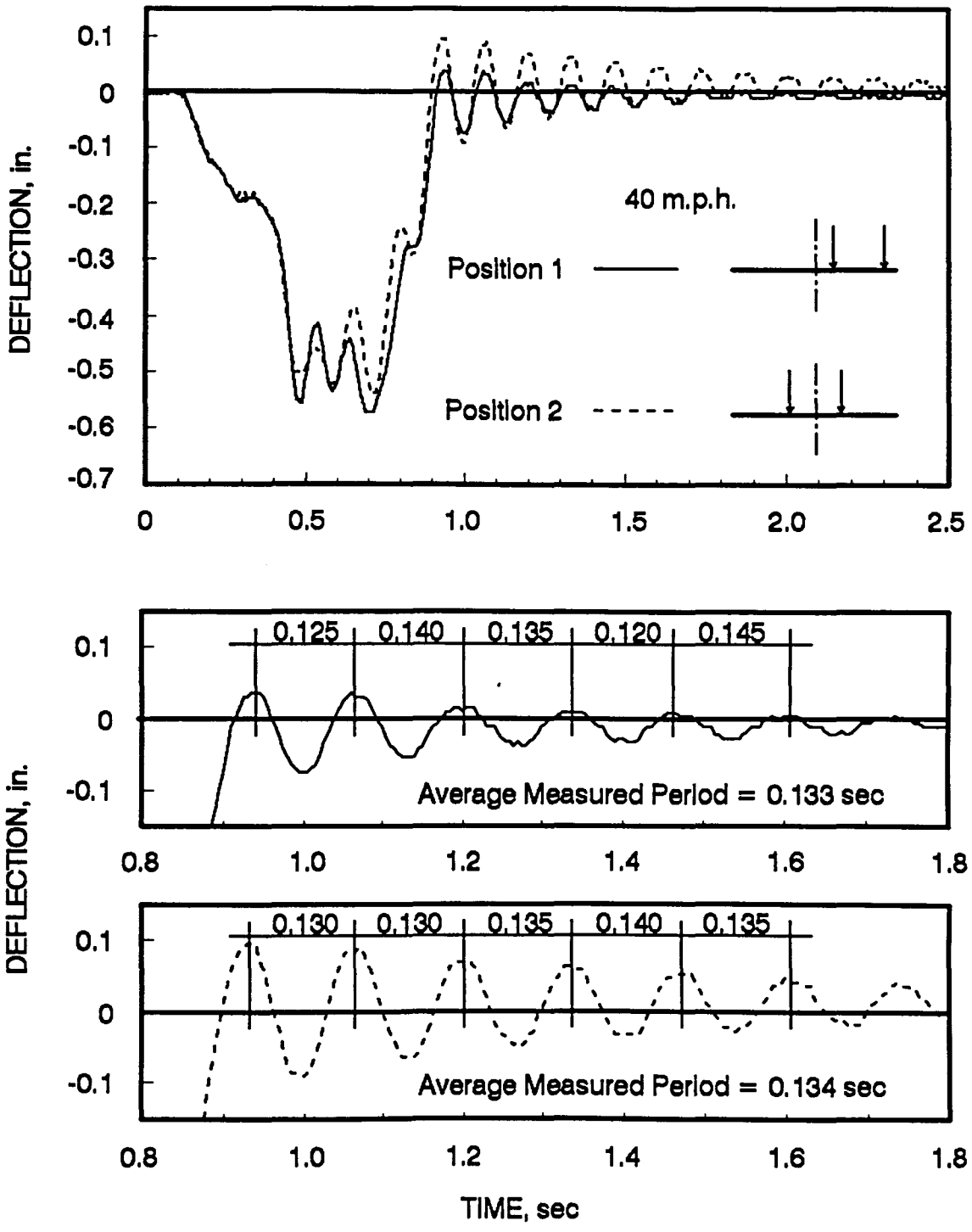

Fig. 19. Measurement of unloaded bridge period

2.3.4 Damping

The decay in amplitude of free vibration can be expressed as the logarithmic decrement, δ, and is defined as equation 2-3.

$$\delta = \ln \frac{y_1}{y_2} \tag{2-3}$$

In the above equation, y_1 is the peak amplitude of vibration at time one, and y_2 is the peak amplitude at a time $y_1 + nT_d$, where n is an integer and T_d is the damped period of vibration. A line drawn tangent to the oscillations of free vibration will have points of tangency very near the peaks of the vibration. The equation of that line may be written as equation 2-4.

$$y(t) = Ce^{-\xi\omega t} \tag{2-4}$$

C = Constant
ξ = Damping ratio
ω = Natural frequency
t = Time

The discrepancy between the points of tangency and the actual peaks of vibration is small and therefore they are considered to be the same point.

An average value of the damping was obtained using the first and sixth peak of free vibration. That is, y_2 is evaluated at $t_1 + 5T_d$. Evaluating the logarithmic decrement

where y_1 and y_2 are calculated from equation 2-4, results in the following.

$$\delta = 5\xi\omega T_d \tag{2-5}$$

The damped natural frequency can be written in terms of the undamped frequency by multiplying by the square root of $1-\xi^2$. The damped period can then be expressed as equation 2-6.

$$T_d = \frac{2\pi}{\omega_d} = \frac{2\pi}{\omega\sqrt{1-\xi^2}} \tag{2-6}$$

After substituting the equation of T_d into equation 2-5 and rearranging to solve for the damping ratio, ξ, equation 2-7 results and can be used to determine the damping ratio using the first and sixth peaks of free vibration.

$$\xi^2 = \frac{1}{\frac{100\pi^2}{\delta^2}+1} \tag{2-7}$$

Equation 2-7 was used to determine the damping ratio using several DCDT responses from the 40 m.p.h. tests. The values ranged from 0.022 to 0.034 with an average value of 0.027. Based on those calculations, the bridge damping is estimated to be approximately 3% of critical damping.

2.3.5 Other Observations

A couple of additional observations should be noted. First, because a couple of the tests resulted in actual average velocities being almost the same, a comparison between the bridge responses for the two seperate tests can be made. Figure 20 illustrates the results. Nearly the exact same response was obtained in two independent runs of the same velocity for each of the vehicle positions. This shows a consistency in the bridge response at a particular velocity. However, the position of the truck can significantly change the magnitude of the response.

Figure 21 shows how the vehicle position can change the magnitude of the bridge behavior. It is important that the truck crosses the bridge in the same location as in the crawl speed tests so that an accurate evaluation of the dynamic response can be made. In the first plot of Fig. 21, two bridge responses are compared both at 41 m.p.h., but one with the truck being 1 ft left of the correct position. The maximum dynamic response when the truck was off line is nearly 0.07 in. less than that with the vehicle in the correct position.

The second plot in Fig. 21 is the maximum transverse deflection profile during a test where the truck was 1 ft right of its correct position. The test was run for the centered vehicle loading, therefore, the deflection profile

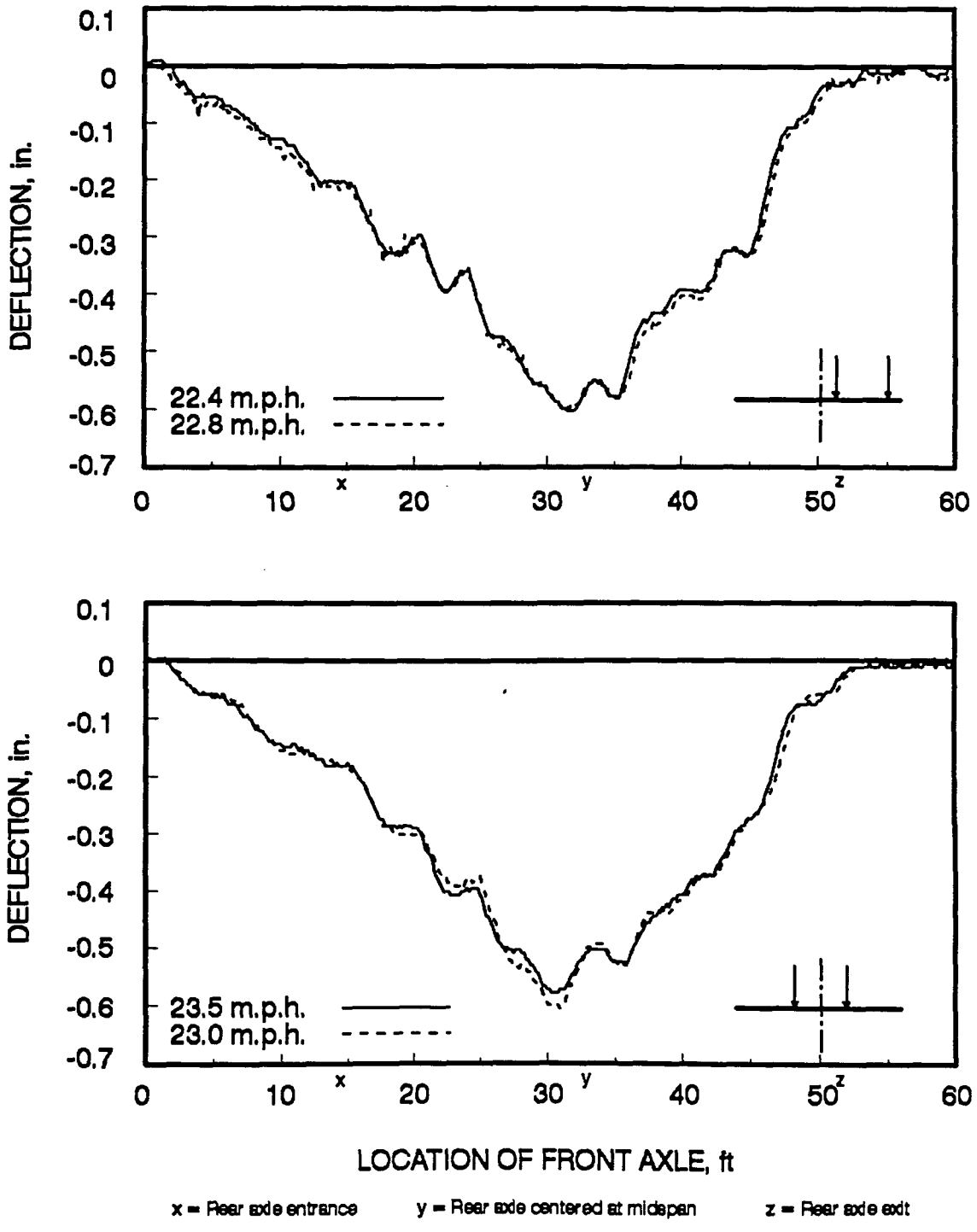

Fig. 20. Response of tests run at same velocities

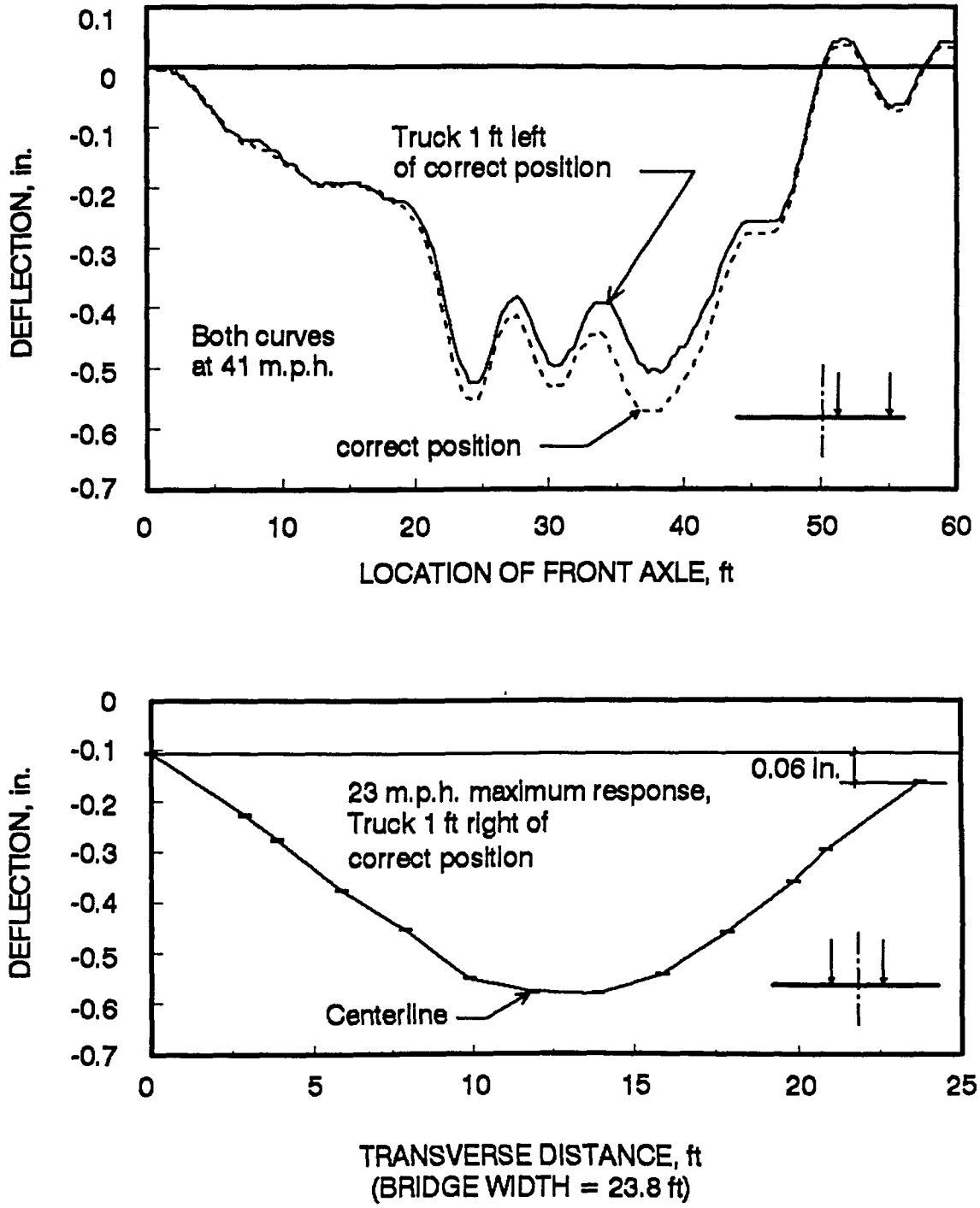

Fig. 21. Effect of vehicle misalignment

should be symmetric. With the truck off line, the deflection at the right edge of the bridge was 0.06 in. more than the left edge and the maximum deflection did not occur at the bridge centerline. In both the above mentioned situations, the DLF would be slightly smaller than it would be if the truck were in the correct position. Therefore, when using a crawl speed deflection in determining the DLF, it is important that the vehicle path during other tests be as close as possible to that of the crawl speed test. The truck position was closely monitored during the tests and any tests where the truck was significantly off line were rerun.

3. ANALYTICAL INVESTIGATION

3.1 General

An analytical model was developed to predict the dynamic behavior of stress laminated timber bridges. This chapter describes the analytical solution and presents the results. In addition, the analytical results are compared to the Teal river bridge experimental data as a means of verifying the model.

As previously mentioned in Section 1.3.2, stress laminated timber bridges behave as and are well represented by orthotropic plates. Therefore, a two dimensional finite element orthotropic plate model was used in the analytical study. The finite element program ANSYS was used to perform static, modal, and dynamic analyses of the bridge.

The loading model used in the dynamic analysis represented each wheel as a rolling mass. The forces applied to the finite element model were those of the wheel loads including gravity and mass acceleration effects. From the analysis, time-history curves of deflection were generated at nodes corresponding to field measurement locations. This allowed comparisons to be made between the experimental and analytical results.

The first step in developing the analytical model involved the selection of an element type and mesh size to accurately approximate the bridge behavior. This step is discussed in the next section.

3.2 Teal River Bridge Model

One of the key steps in using a finite element solution is the selection of an element type. The element must have degrees of freedom and stiffness that match the system being modeled in order to accurately represent the behavior.

A quadrilateral shell element was chosen for the analysis. The element has translational degrees of freedom in the x, y, and z directions as well as rotational degrees of freedom about all three axes. Both bending and membrane stiffnesses are available. However, because the bridge deflections are mainly influenced by plate bending, the bending stiffness only option was used.

The shell element allows the input of orthotropic plate properties. These properties have been experimentally determined for stress laminated timber bridges as discussed in Section 1.3.2 and defined as equations 1-1 and 1-2. Selecting the element coordinate system with the x-axis parallel to the longitudinal bridge direction and the y-axis running in the transverse direction, the following material

properties were input.

$$E_x=E'=1,780,000\ psi$$

$$E_y=0.013E'=23,140\ psi$$

$$G_{xy}=0.03E'=53,400\ psi$$

In addition, the thickness was input as 14.2 in. and the density as 0.000075 lb-sec^2/in.^{4}.

The size of the mesh used in the finite element model was mainly controlled by that required for load application. The mesh is smaller than needed to produce a converged solution, but was necessary to accommodate the dynamic loading. Transversely, nodes were placed at the same spacing as the midspan field measurement locations. This allowed direct comparisons to be made between field and analytical deflections. Longitudinally, the nodes were spaced such that the truck axle spacings would be an integer factor of the node spacing. This would allow vehicle forces to coincide with node locations as they moved across the bridge. That is, when the front axle forces are at a node location, the rear axle forces also line up over a node rather than being somewhere between. To do this, changes in the axle spacings and bridge length had to be made, but the differences were

small and considered negligible. Table 5 compares the actual and model dimensions.

The bridge deck was assumed to bear on the abutments at the midpoint of the bearing surface. Pinned end restraints were used at the support locations for the dynamic analyses, but a comparison using fixed ends was also made for the static load cases.

Table 5. Model Dimensions

Dimension	Actual	Model	Percent Diff.
Dist. between supports	372.0 in.	380.0 in.	2 %
Width	285.2 in.	285.2 in.	0 %
Thickness	14.2 in.	14.2 in.	0 %
Front axle spacing	175.2 in.	171.0 in.	2 %
Rear axle spacing	56.4 in.	57.0 in.	1 %

An initial verification of the model was done by performing the static analyses of the bridge. Using the finite element model, wheel loads equaling those of the test vehicle were applied statically to the bridge. The model vehicle was located to match the position producing the maximum crawl speed deflection for each lane position, i.e. with the rear axles centered about the bridge midspan. The results of the analysis are plotted in Fig. 22.

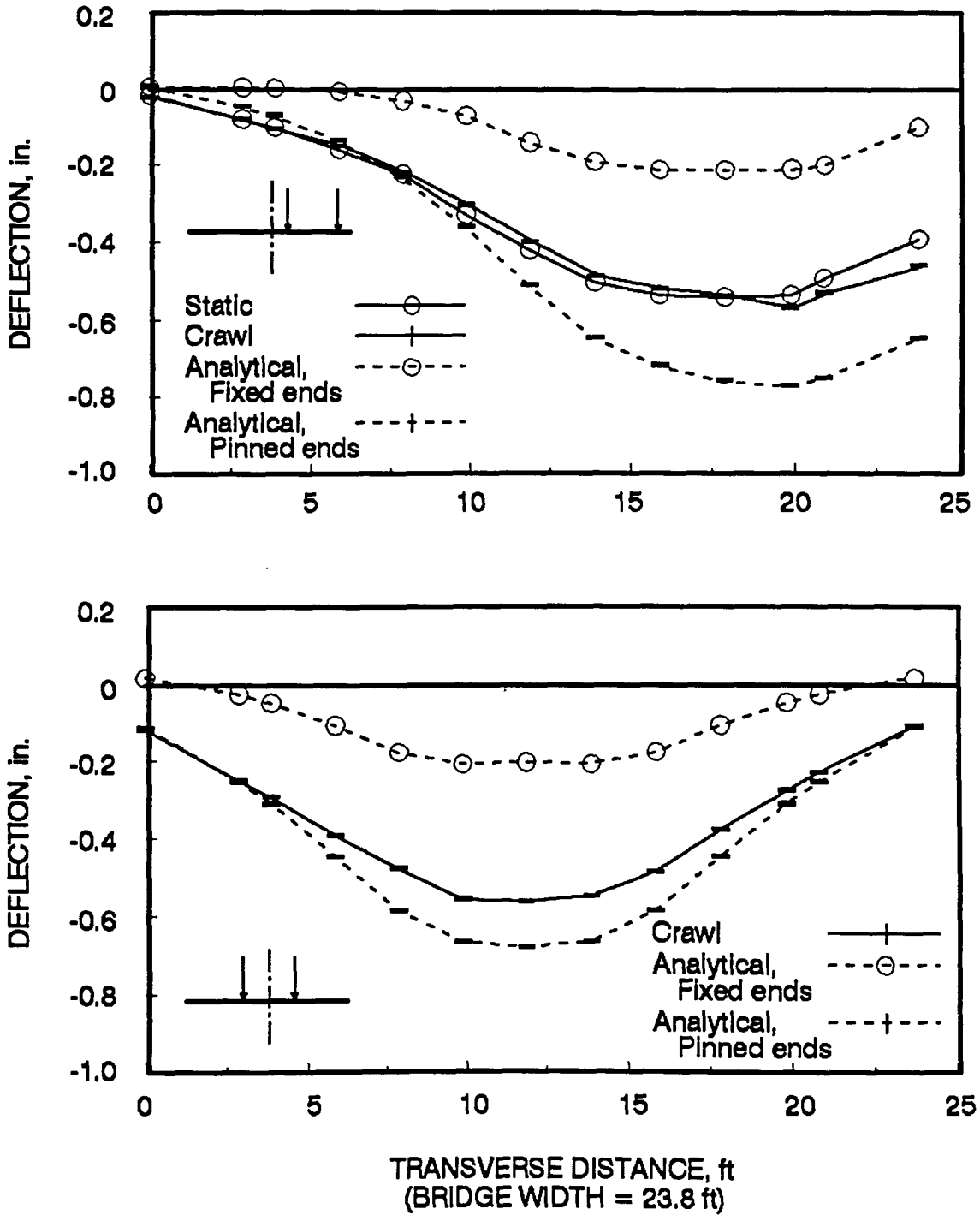

Fig. 22. Analytical static loading

For the 2 ft right loading, a comparison is made between the field static data, maximum transverse deflection profile from the crawl speed test, and the two analyses performed using the finite element model. As can be seen in Fig. 22, the pinned end model produced deflections larger than measured in the field, while the fixed end model underestimated the deflections. Similar results were found using the centered loading. Again, no static test was performed in the centered vehicle position, but the crawl speed data was found to accurately represent the static deflections.

Differences between the analytical and field data can clearly be justified in the end restraint assumptions. The assumed pinned and fixed conditions are idealizations. The actual field end restraints will be somewhere between the two conditions. From Fig. 22, the pinned end restraints better represented the bridge behavior and were therefore used in the modal and dynamic analyses.

3.3 Modal Analysis

Before the dynamic analyses of the bridge could be performed, a modal analysis was necessary. Information obtained from the modal analysis is needed to define parameters used in the dynamic study. This section explains

the ANSYS solution and presents the results.

3.3.1 Theory

The mode shapes and corresponding natural frequencies of vibration can be determined from a modal analysis. In the ANSYS solution, the mass and stiffness matrices are assumed to remain constant, that is, the structure remains linearly elastic. No damping is allowed in the solution, and only free vibrations are assumed (no external forces or displacements can be applied).

The analysis begins with the differential equation of motion as stated in equation 3-1.

$$[M]\{\ddot{u}\} + [C]\{\dot{u}\} + [K]\{u\} = \{F\} \qquad (3\text{-}1)$$

In the above equation, [M], [C], and [K] are the structure mass, damping, and stiffness matrices respectively. The vector {u} is the nodal displacement vector and its first and second derivative with respect to time are the nodal velocity and acceleration vectors. The time dependent force vector is represented by {F}. Neglecting the damping and setting the force vector equal to zero, results in the governing equation used in the modal analysis.

$$[M]\{\ddot{u}\} + [K]\{u\} = 0 \qquad (3\text{-}2)$$

The free vibration of a linear structure results in a harmonic motion defined by $\{u\} = \{u_0\}\cos\omega t$, where ω is the circular frequency of vibration, t is time, and $\{u_0\}$ is the amplitude of vibration. Substituting the value of $\{u\}$ and its second derivative into equation 3-2 leaves the eigenvalue equation 3-3.

$$([K]-\omega^2[M])\{u_0\}=\{0\} \qquad (3-3)$$

The only way a non-trivial solution would exist is if $([K]-\omega^2[M])$ cannot be inverted, i.e., its determinate must equal zero.

$$|[K]-\omega^2[M]|=0 \qquad (3-4)$$

Equation 3-4 has n solutions, where n is the dimension of the square matrices [M] and [K]. These roots, ω^2_1, $\omega^2_2,\ldots\omega^2_n$ are the squares of the natural frequencies. When substituted back into equation 3-3, the vector $\{u_0\}$ can be determined for each frequency. This vector is then the corresponding mode shape for the given natural frequency.

In order to save computation time, ANSYS performs its dynamic and modal analyses in terms of reduced matrices. The total degrees of freedom are divided into master and slave sets. The dynamic solution can then be done in terms of the master degrees of freedom (which are used to form the reduced

matrices), and the solutions later expanded to include all the degrees of freedom. This is possible because the number of degrees of freedom needed to adequately characterize the dynamic response is much less than the total degrees of freedom. For the Teal River Bridge, the master degrees of freedom were chosen as the vertical translation at every node.

3.3.2 Results

The first seven mode shapes were found for the bridge model. As discussed in Section 1.4, the first mode of vibration dominates dynamic bridge responses, therefore, its shape and frequency are the most important. The shape was that of a half sine wave and is typical of simply supported structures (see Fig. 23). A frequency of 6.86 Hz corresponding to a period of 0.146 sec was found for the first mode.

As a simple check, the first mode frequency for a simply supported beam of equivalent moment of inertia and modulus of elasticity was calculated using the following equation.

$$\omega_1 = \frac{\pi^2}{l^2}\sqrt{\frac{EI}{m}} \qquad (3\text{-}5)$$

In equation 3-5, ω_1 is the first mode frequency in rad/sec, l is the bridge length, I is the moment of inertia of the

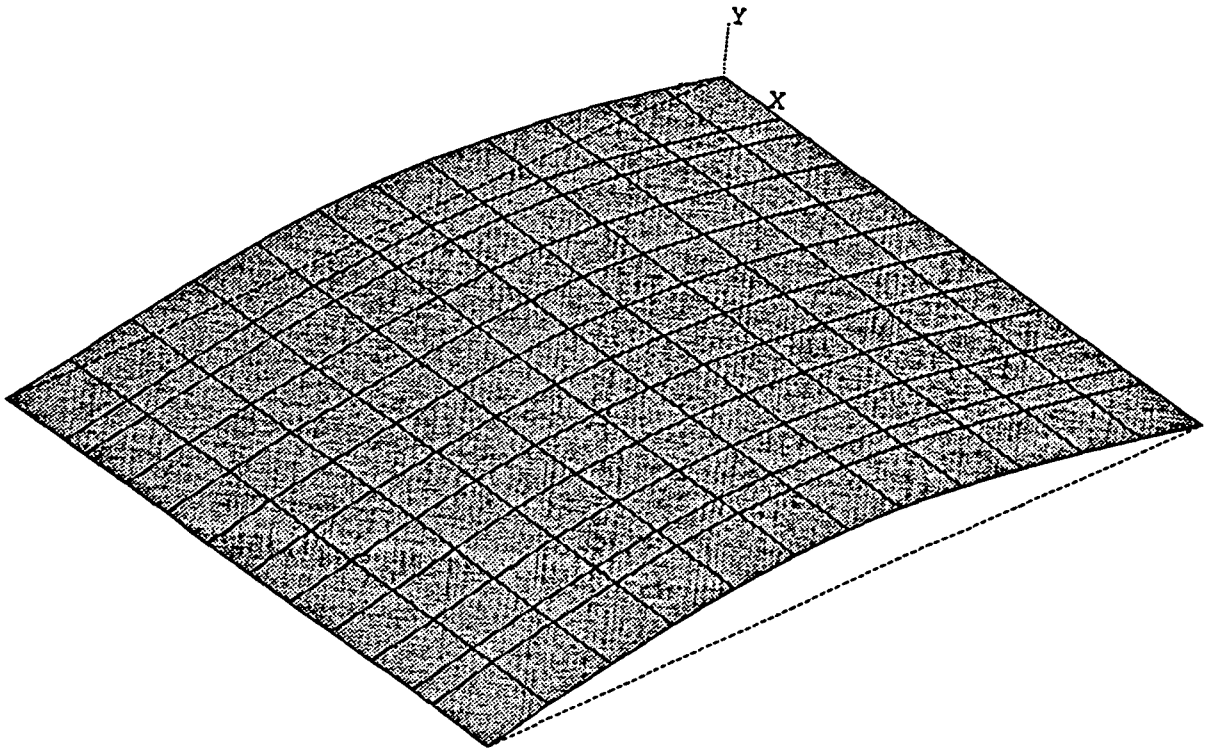

Fig. 23. First mode shape of Teal River bridge

bridge cross-section, and m is the mass per unit length. Using this equation, the first mode frequency was found to be 43.14 rad/sec or 6.87 Hz. This result very closely matches that of the ANSYS solution and shows that an equivalent simply supported beam can produce good results.

Mode shapes two through five were torsional mode shapes, mode six was the second bending mode, and seven was a combination of bending and torsion. The frequencies and corresponding periods are listed in Table 6. Plots of mode shapes two through seven can be found in Appendix B.

Table 6. Mode Frequencies

Mode	Frequency (Hz)	Period (sec)
1	6.86	0.146
2	7.62	0.131
3	10.29	0.097
4	15.70	0.064
5	24.38	0.041
6	27.34	0.037
7	28.04	0.036

From the field test data, the period of free vibration was measured to be 0.13 seconds. This compares fairly well with the first mode period determined from the analytical model. The difference, 8 percent, can again be attributed to

the end restraints. The field end conditions being somewhere between pinned and fixed would result in the bridge being stiffer than the model. Being stiffer, the actual bridge would have a quicker response as was realized in the above comparison.

3.4 Dynamic Response

3.4.1 ANSYS Solution

The dynamic behavior of stress laminated timber bridges was investigated using a linear transient dynamic analysis. The direct integration of the equation of motion (equation 3-1) was performed by ANSYS to determine the response at each node of the bridge model. Using a Newmark time integration scheme, ANSYS solves for the nodal displacements at user input time increments. As in the modal analysis, the dynamic response is determined in terms of the master degrees of freedom to save computer time.

Being a linear dynamic analysis, the mass, stiffness, and damping matrices are constant throughout the solution. The procedure allows loads to be applied at the nodes only, i.e., no pressure loadings can be used. In addition, a constant integration time step is used for the numerical integration.

The proper selection of the integration time step is

critical to obtaining accurate results. It must be small enough to characterize the forcing function as well as the dynamic response. It is recommended that at least seven iterations be performed along the shortest side of the forcing function. In addition, at least 20 iterations per period of vibration are recommended. Information obtained from the modal analysis aids in the selection of a proper time step.

3.4.2 Dynamic Loading

As mentioned in the literature review, representing the vehicle loading as a constant force crossing the bridge is not adequate in defining the bridge response. In order to better represent the actual loading, the effects of vehicle mass were included.

As a mass travels across a bridge and undergoes accelerations due to bridge oscillations, the force felt by the bridge will change depending on the direction of the mass accelerations. If the bridge is accelerating downward, the vehicle mass will resist a change in motion and decrease the force felt by the bridge. However, if the bridge acceleration is upward, the inertia effect will increase the force felt by the bridge. If the ratio of vehicle mass to bridge mass is small, this effect may not be significant in defining the bridge response, but when the ratio is large,

such as in short span timber bridges, the effect cannot be neglected.

A seperate study was performed to determine the forces felt by the bridge including the vehicle mass acceleration effects. These forces were then applied to the finite element model to obtain the final bridge response. The forces were obtained by considering the bridge as a simply supported beam, and the vehicle as three rolling masses, one for each axle. The differential equation of motion defining this system will now be derived.

The derivation begins by considering a simply supported beam subjected to an arbitrary loading p(x,t) with mass per unit length m, modulus of elasticity E, and moment of inertia I. A free body diagram of a beam section dx in length is shown in Fig. 24. Damping is neglected in the solution. Summing the forces in the y direction and equating to zero results in the following equation.

$$V-(V+\frac{\partial V}{\partial x}dx)+p(x,t)\,dx-m dx\frac{\partial^2 y}{\partial t^2}=0 \qquad (3\text{-}6)$$

After simplification and noting from simple beam theory that

$$V=\frac{\partial M}{\partial x}=EI\frac{\partial^3 y}{\partial x^3}$$

equation 3-6 becomes

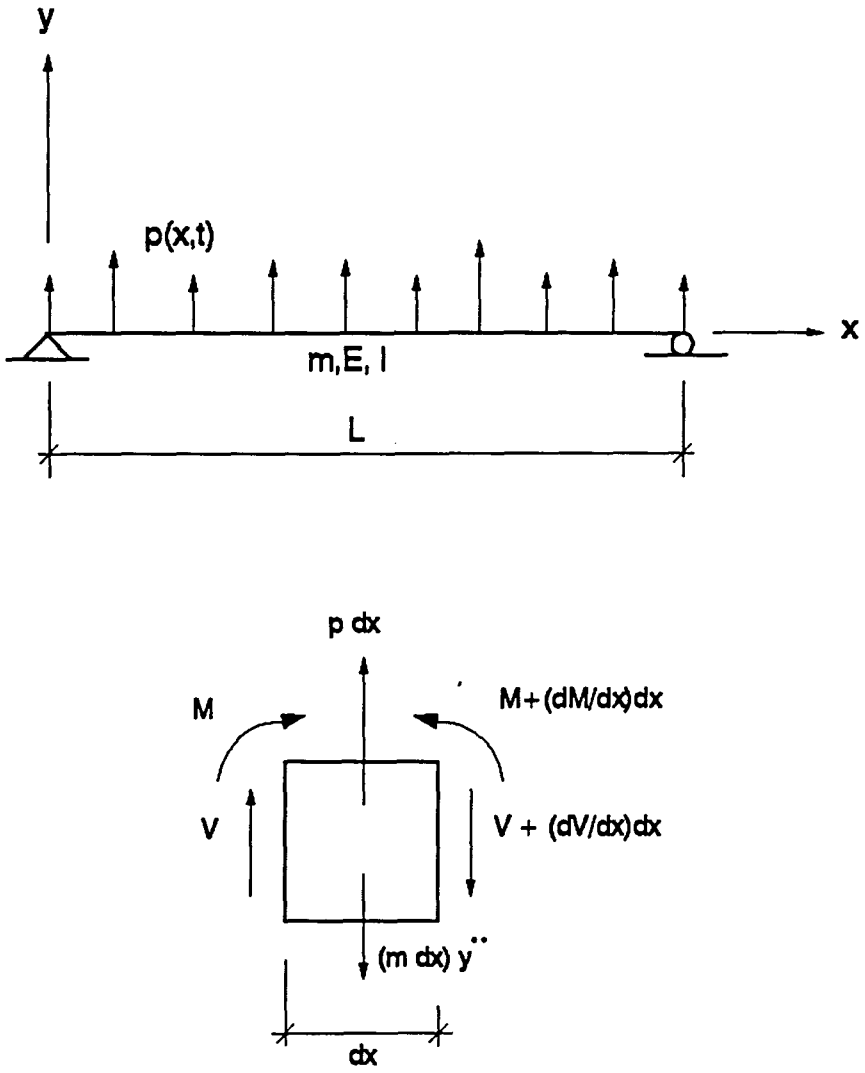

Fig. 24. Free body diagram of beam section

$$EI\frac{\partial^4 y}{\partial x^4}+m\frac{\partial^2 y}{\partial t^2}=p(x,t) \qquad (3\text{-}7)$$

First, consider free vibration, that is, let p(x,t)=0. It can be assumed that the solution to equation 3-7, y(x,t), can written as a function of position times a function of time.

$$y(x,t)=\Phi(x)f(t)$$

Substituting this results in equation 3-8

$$EIf(t)\frac{\partial^4\Phi(x)}{\partial x^4}+m\Phi(x)\frac{\partial^2 f(t)}{\partial t^2}=0 \qquad (3\text{-}8)$$

and upon rearranging, equation 3-9.

$$\frac{EI}{m}\frac{\Phi^{IV}(x)}{\Phi(x)}=\frac{-\ddot{f}(t)}{f(t)} \qquad (3\text{-}9)$$

Noticing in equation 3-9 that the left hand side is only a function of x and the right side only a function of t, the only way the equality can be true is if both sides are equal to a constant, say ω^2. That is,

$$\frac{EI}{m}\frac{\Phi^{IV}(x)}{\Phi(x)}=\omega^2 \quad or \quad \Phi^{IV}(x)-a^4\Phi(x)=0$$

where $a^4 = m\omega^2/EI$, and

$$\frac{-\ddot{f}(t)}{f(t)}=\omega^2 \quad or \quad \ddot{f}(t)+\omega^2 f(t)=0$$

The general solution to the first equation is

$$\Phi(x)=A\sin(ax)+B\cos(ax)+C\sinh(ax)+D\cosh(ax) \qquad (3\text{-}10)$$

Since the solution to equation 3-7 was assumed to be the function of x, $\Phi(x)$, times a function of time, the boundary conditions applying to the simply supported beam

$$y(0,t)=0 \quad y(L,t)=0 \quad M(0,t)=0 \quad M(L,t)=0$$

can also be applied to the shape function $\Phi(x)$, resulting in the following four boundary conditions that can be used to determine the constants A, B, C, and D of equation 3-10.

$$\Phi(0)=0 \quad \Phi(L)=0 \quad \Phi''(0)=0 \quad \Phi''(L)=0$$

After substitution of the boundary conditions, equation 3-10 reduces to

$$\Phi_n(x)=\sin\left(\frac{n\pi x}{L}\right) \qquad (3\text{-}11)$$

where n defines the mode number for the corresponding shape function. The dynamic response of bridges is primarily defined by first mode vibration, therefore, if only the first

mode is considered, the above equation becomes

$$\Phi(x) = \sin\left(\frac{\pi x}{L}\right) \tag{3-12}$$

Now consider the forced vibration of equation 3-7. The solution can be assumed to be the summation over the number of modes of a function of x (now defined as equation 3-11) and a different function of time, $z_n(t)$.

$$y(x,t) = \sum_{n=1}^{\infty} \Phi_n(x)\, z_n(t) \tag{3-13}$$

As found previously

$$EI\Phi_n{}^{IV}(x) = m\omega^2\Phi_n(x) \tag{3-14}$$

Combining equations 3-7, 3-13, and 3-14 leaves the following

$$\sum_{n=1}^{\infty} m\omega^2\Phi_n(x)\, z_n(t) = p(x,t) - m\sum_{n=1}^{\infty} \Phi_n(x)\, \ddot{z}_n(t) \tag{3-15}$$

Orthogonality between modes states that for two modes of different frequency, ω_n not equal to ω_m, the following must be true

$$\int_0^L \Phi_m(x)\,\Phi_n(x)\,m\,dx=0$$

Therefore, if both sides of equation 3-15 are multiplied by $\Phi_m(x)$ and it is integrated between 0 and L, only those terms with n equal to m will remain. That is, all terms with different frequencies (n not equal to m) will vanish due to the orthogonality condition. The following equation results.

$$M_n\ddot{z}_n(t)+\omega_n^2 M_n z_n(t)=F_n(t) \tag{3-16}$$

where

$$M_n=\int_0^L m\Phi_n^2(x)\,dx \tag{3-17}$$

is called the modal mass, and

$$F_n(t)=\int_0^L \Phi_n(x)\,p(x,t)\,dx \tag{3-18}$$

is called the modal force. In the rolling mass solution, the mass of the bridge was lumped at points corresponding to the longitudinal node locations of the finite element model. In addition, the loads were applied at discrete locations on the bridge rather than being distributed. This allowed the

integrals of equations 3-17 and 3-18 to be replaced with summations at the mass and force locations.

Using lumped masses, and considering only the first mode of vibration, the modal mass equation becomes

$$M_n=\sum_{i=1}^{m} m_i\Phi^2(x_i) \qquad (3\text{-}19)$$

where m is the number of lumped masses, and m_i is the mass at location x_i. As the vehicle crosses the bridge, the axle masses add to the bridge lumped masses changing the modal mass. This was accounted for in the solution by updating the modal mass as the vehicle crosses the bridge.

As the axle masses cross the bridge, they are assumed to remain in contact with the bridge surface. Therefore, the acceleration of the vehicle mass will be equal to the bridge acceleration at the same point. Knowing this, the forces felt by the bridge can be written in terms of the axle mass, bridge acceleration, and the acceleration of gravity. The force positions can be defined by the truck velocity and axle spacings.

$$F_1=M_1(g+\ddot{y}_1) \qquad at \qquad x_1=vt$$

$$F_2=M_2(g+\ddot{y}_2) \qquad at \qquad x_2=vt-d_1 \qquad (3\text{-}20)$$

$$F_3 = M_3(g+\ddot{y}_3) \qquad at \qquad x_3 = vt-d$$

In equations 3-20, v is the vehicle velocity, d_1 the distance between the front two axles, d the distance between the first and third axle, and g is the acceleration of gravity. The above conditions are illustrated in Fig. 25.

Knowing the forces and their discrete locations, the modal force of equation 3-18 can now be written as the summation of the forces times the shape function.

$$F_n(t) = -F_1\Phi(x_1) - F_2\Phi(x_2) - F_3\Phi(x_3) \qquad (3\text{-}21)$$

Referring back to equation 3-13, the bridge accelerations at any point can be calculated from the second derivative of the displacement, That is (considering only the first mode),

$$\ddot{y}(x,t) = \Phi(x)\ddot{z}(t) \qquad (3\text{-}22)$$

Because the vibration is assumed to be a half sine wave (shape function), the displacement or acceleration at any point can be defined by the midspan deflection. Therefore, the function of time, z(t), in equations 3-13 and 3-22 can be replaced by the midspan deflection, y_c, and acceleration.

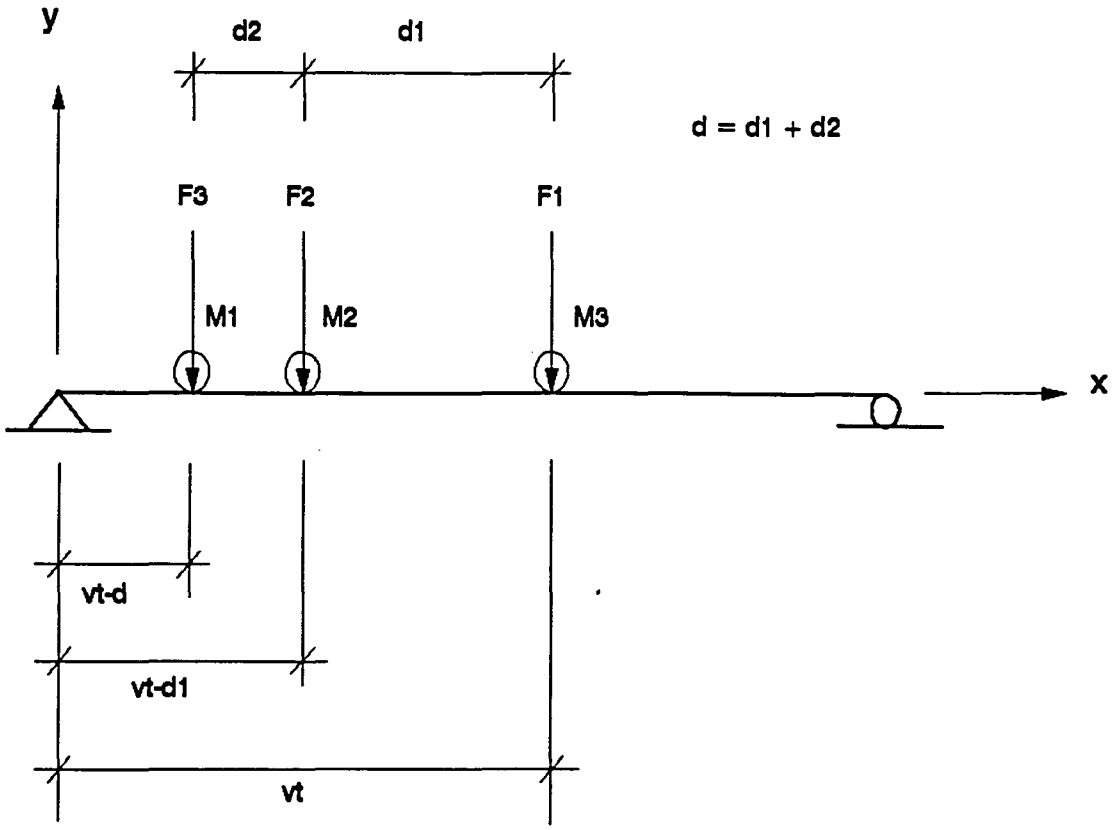

Fig. 25. Load positions

$$y(x,t) = y_c \Phi(x) \tag{3-23}$$

$$\ddot{y}(x,t) = \ddot{y}_c \Phi(x) \tag{3-24}$$

Substituting back into equation 3-16 the modal force, modal mass, and first mode shape function, and rearranging to form a differential equation in terms of the midspan deflection results in the following

$$\ddot{y}_c \left(M_n + M_1 \sin^2 \frac{\pi v t}{L} + M_2 \sin^2 \frac{\pi (vt - d_1)}{L} + M_3 \sin^2 \frac{\pi (vt - d)}{L}\right)$$

$$+ M_n \omega^2 y_c = -g \left(M_1 \sin \frac{\pi v t}{L} + M_2 \sin \frac{\pi (vt - d_1)}{L} + M_3 \sin \frac{\pi (vt - d)}{L}\right)$$

This is the differential equation that must be solved for the rolling mass solution. A fourth order Runge Kutta numerical integration scheme was used to solve for the midspan acceleration as a function of time. Once known, the bridge acceleration at any point can be determined using equation 3-24. The accelerations under the loads, which are therefore the accelerations of the axle masses, were used to determine the forces felt by the bridge according to equations 3-20.

As previously discussed, the loaded frequency of the bridge changes as the vehicle moves across. This is especially significant when the ratio of vehicle mass to

bridge mass is large. To account for this affect, the frequency in the rolling mass equation was updated as the truck moved along the bridge length. As a means of calculating the natural frequency for the different truck positions, Rayleigh's Method was used (Paz [12]). In this method, the Principle of Conservation of Energy is used by equating the maximum kinetic energy with the maximum potential energy.

The potential energy can be determined by summing the work done by each mass during application of the loads.

$$V_{max}=\sum_{i=1}^{m}\frac{1}{2}W_i y_i \qquad (3\text{-}25)$$

Again, m is the number of masses and includes the lumped bridge masses along with the axle masses, W_i is the weight of the masses, and y_i is the static vertical deflection at the mass location.

During vibration, the maximum kinetic energy will occur when the velocity is a maximum. The maximum velocities are ωy_i resulting in the kinetic energy being

$$T_{max}=\sum_{i=1}^{m}\frac{1}{2}\frac{W_i}{g}(\omega y_i)^2 \qquad (3\text{-}26)$$

Equating equations 3-25 and 3-26 and solving for the

frequency ,ω, provides an expression for the frequency which will change depending on the truck location.

$$\omega = \sqrt{\frac{g\sum_{i=1}^{m} W_i y_i}{\sum_{i=1}^{m} W_i y_i^2}} \qquad (3\text{-}27)$$

The frequency was updated whenever the axle locations corresponded to a longitudinal node location of the finite model. Figure 26 illustrates how the period changed during analytical load application of the Teal River Bridge. The initial and final period of 0.145 sec matched that calculated previously verifying the frequency calculation using Rayleigh's Method. The maximum period of 0.253 sec reveals how much the natural frequency slows down due to the heavy vehicle mass.

The fortran program used to implement the numerical solution of the rolling mass differential equation is printed in Appendix C. Output from the program listed the wheel load forces felt by the bridge considering the truck as three rolling masses. The forces were printed every time a wheel load was directly over a node in the corresponding finite element model. Because the truck axle spacings were an integer factor of the ANSYS model node spacing, all three axles were over a node at each time of printing. The

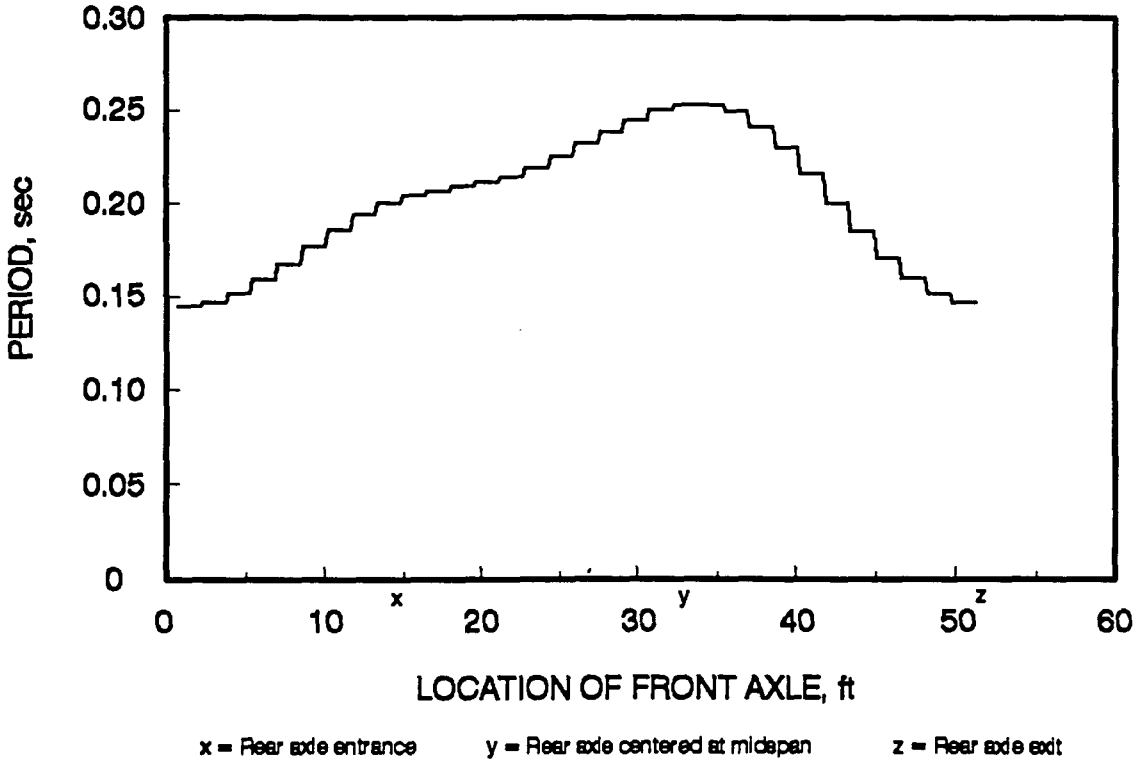

Fig. 26. Change in loaded bridge period

magnitudes and times of load application changes for each truck velocity, therefore, the fortran program was run for each velocity tested in the field. However, no differentiation could be made between the 2 ft right and centered loadings because only a one dimensional beam model was used in the rolling mass solution. The output for the various runs are included in the Appendix C.

The forces obtained from the rolling mass solution could then be applied to the finite element model. To do this, a series of triangular forcing functions as illustrated in Fig. 27 were used. As a force approaches a node, such as a front axle load, the force felt by the node increases until reaching a maximum when the force is directly over the node. It then decreases as the load moves away. In the finite element model, the force is applied linearly starting when the load is at the previous node location and reaching a maximum value equal to that obtained from the rolling mass solution when the load is directly over the node. It then decreases back to zero as the load reaches the next node. The length of time over which the forcing function is applied is equal to the time required for the load to move across two consecutive elements, i.e., the time to move from node n-1 to node n+1. A similar forcing function was applied for each wheel load at each node along the length of the bridge.

In order to verify the loading model, a comparison was

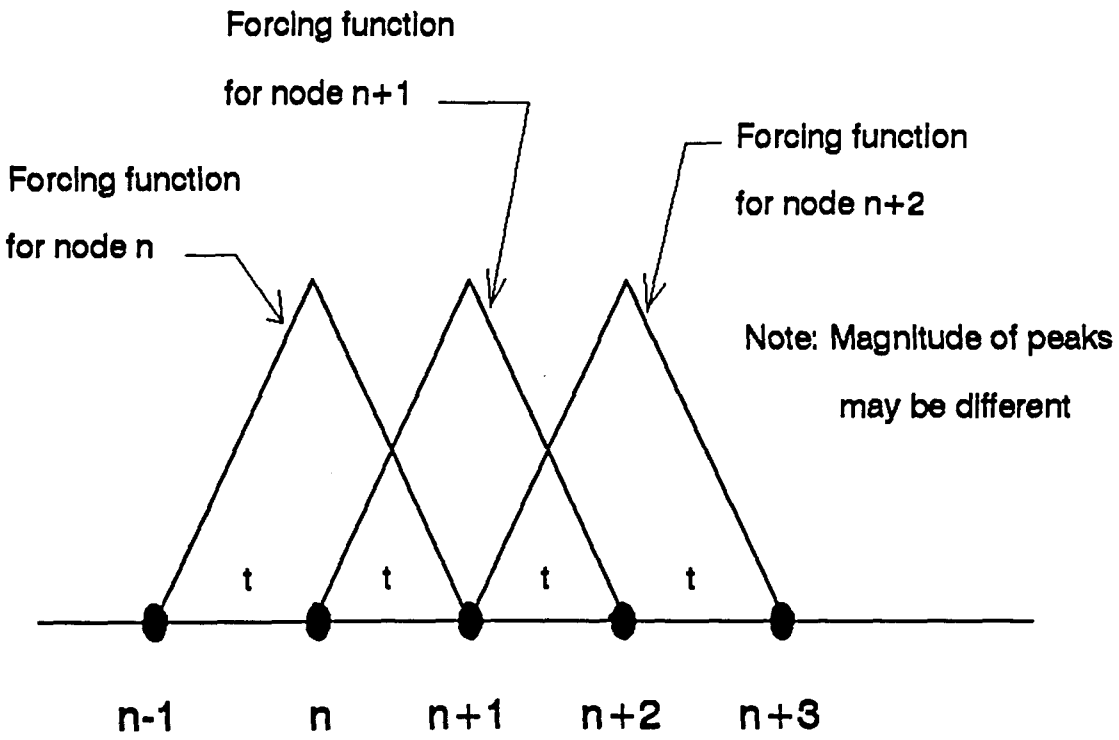

Total length of forcing function = 2t

t = time for load to move from one node to the next

Fig. 27. Load forcing function

made between this model and a rolling mass solution done by Looney [10]. In his study, Looney determined the deflection at midspan of a 30 ft bridge during passage of a two axle truck. The bridge was modeled as a simply supported beam, and the load as two rolling masses. The ratio of live load to dead load masses was 1.2.

A beam with the same properties was input into the Fortran program. The output forces were then input onto a finite element model of the bridge on ANSYS. No information on the modeled bridge dimensions were provided, therefore, the bridge was again model as a simply supported beam for the ANSYS solution. The deflections at midspan obtained from the current study and Looney's results are compared in Fig. 28. The results compared well, thus verifying the dynamic loading.

3.4.3 Analytical Results

Using the theory of rolling masses and the finite element model as previously described, analytical solutions to the tests run in the field were produced. Once again, plots were made of the reference point deflections versus front axle location for the different vehicle speeds and positions. The plots are reproduced in Fig. 29 through 34. Plots of the experimental results are provided with the analytical results for direct comparison.

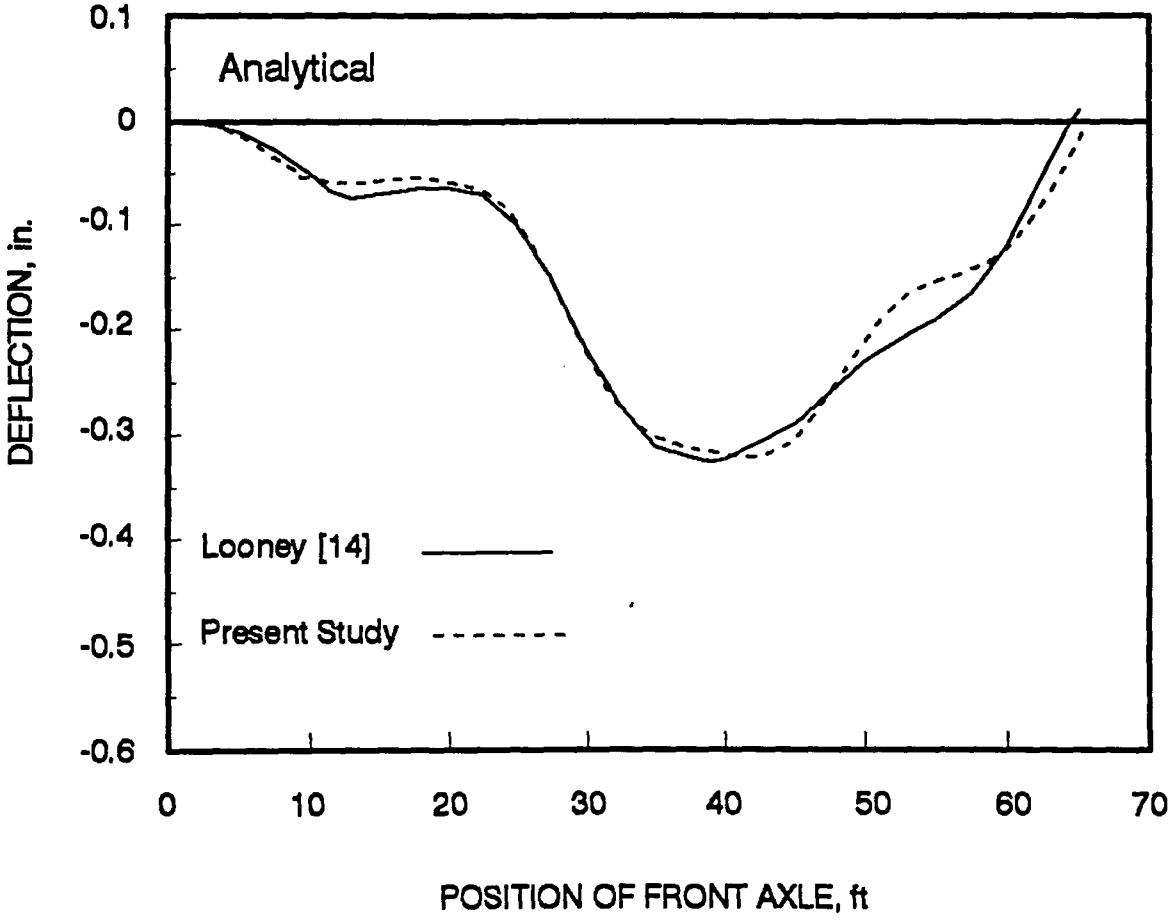

Fig. 28. Rolling mass verification

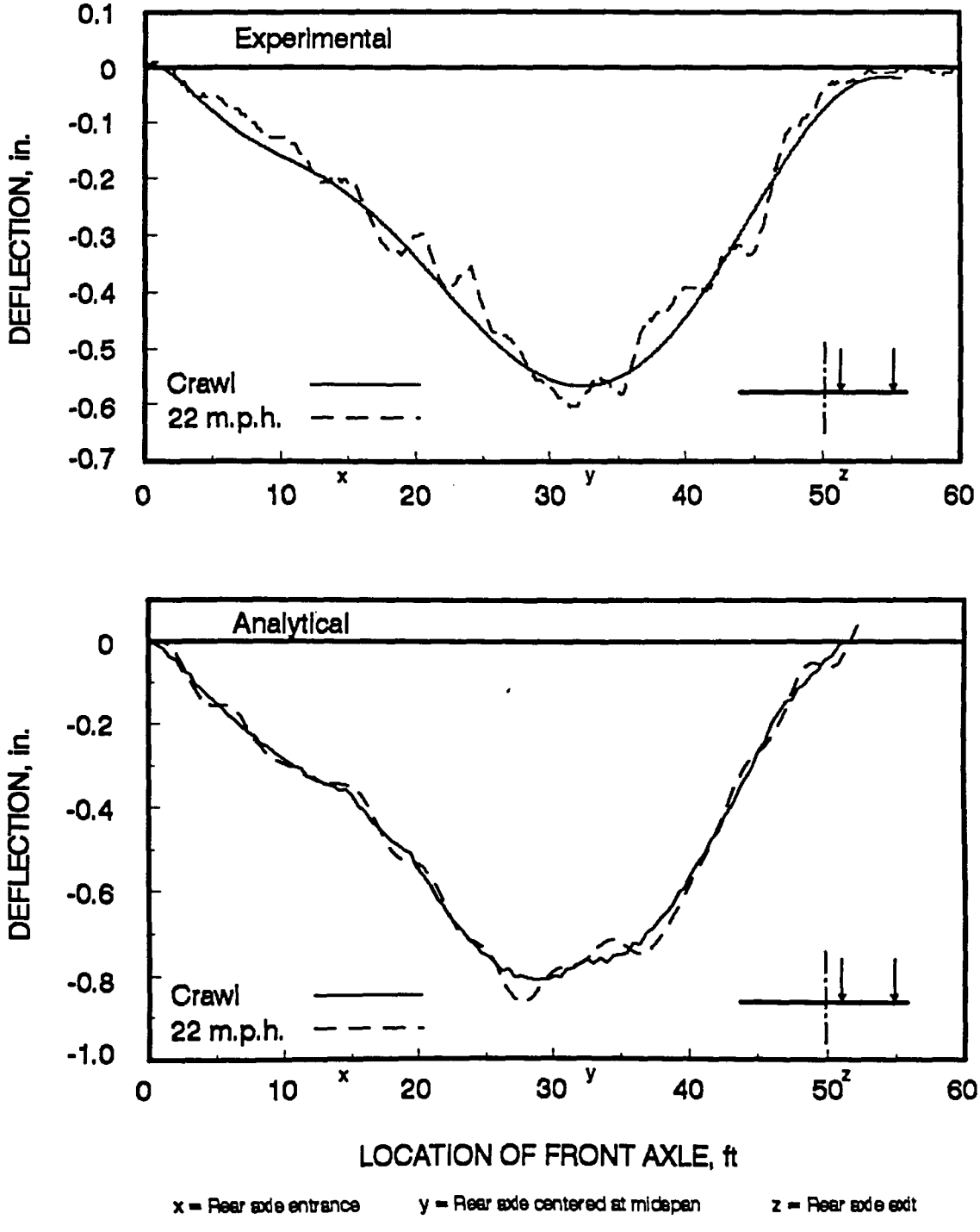

Fig. 29. Analytical bridge response 22 m.p.h.

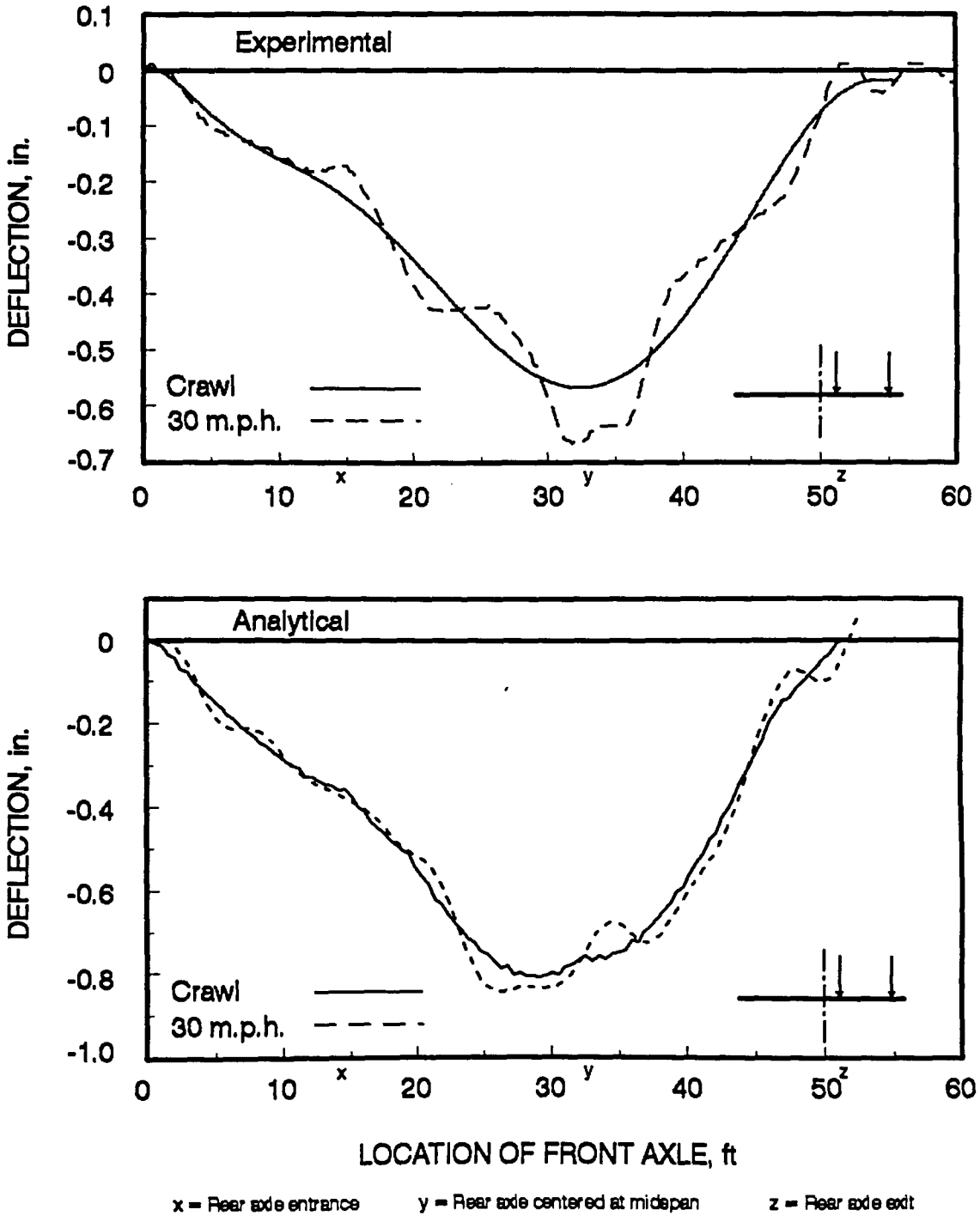

Fig. 30. Analytical bridge response 30 m.p.h.

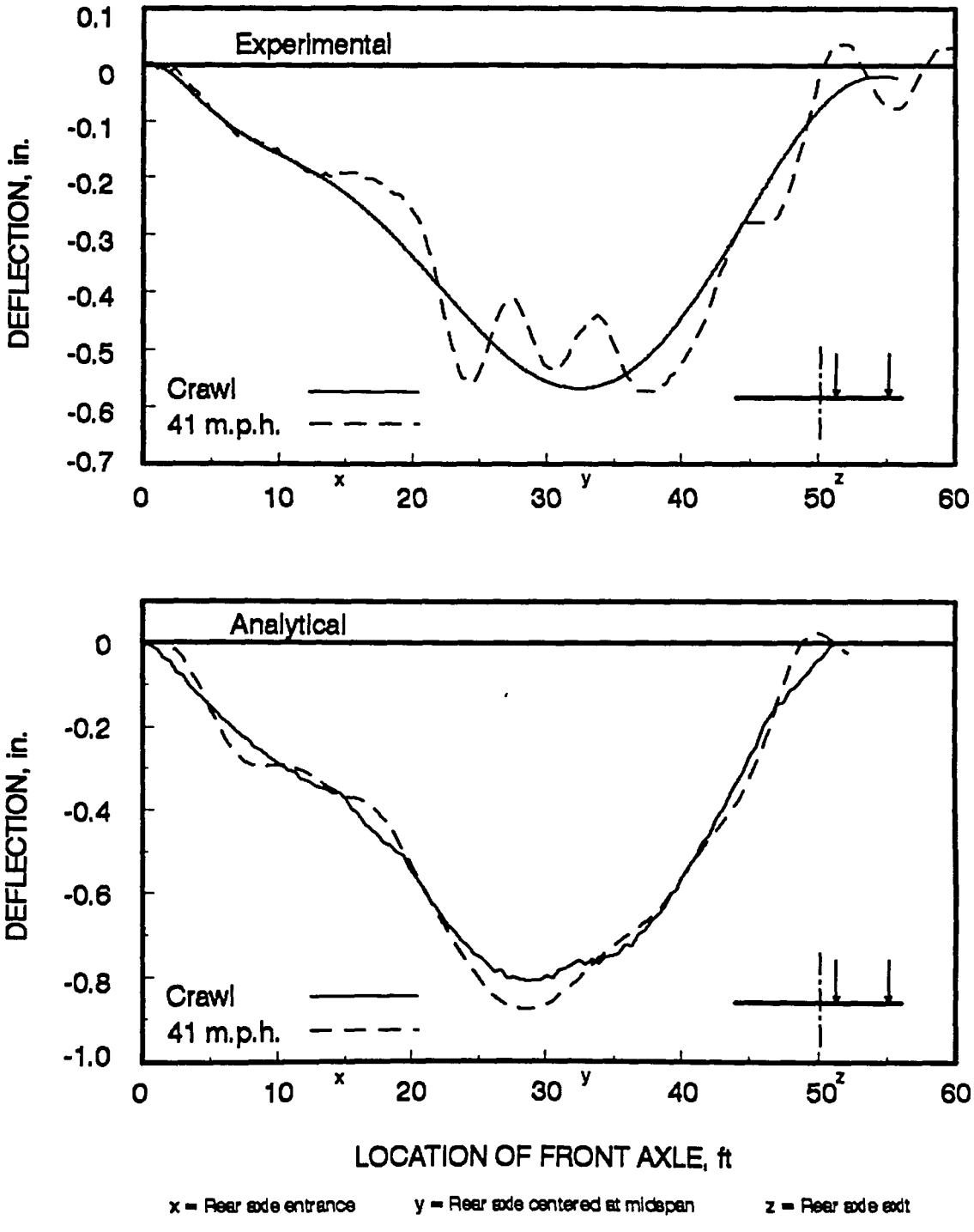

Fig. 31. Analytical bridge response 41 m.p.h.

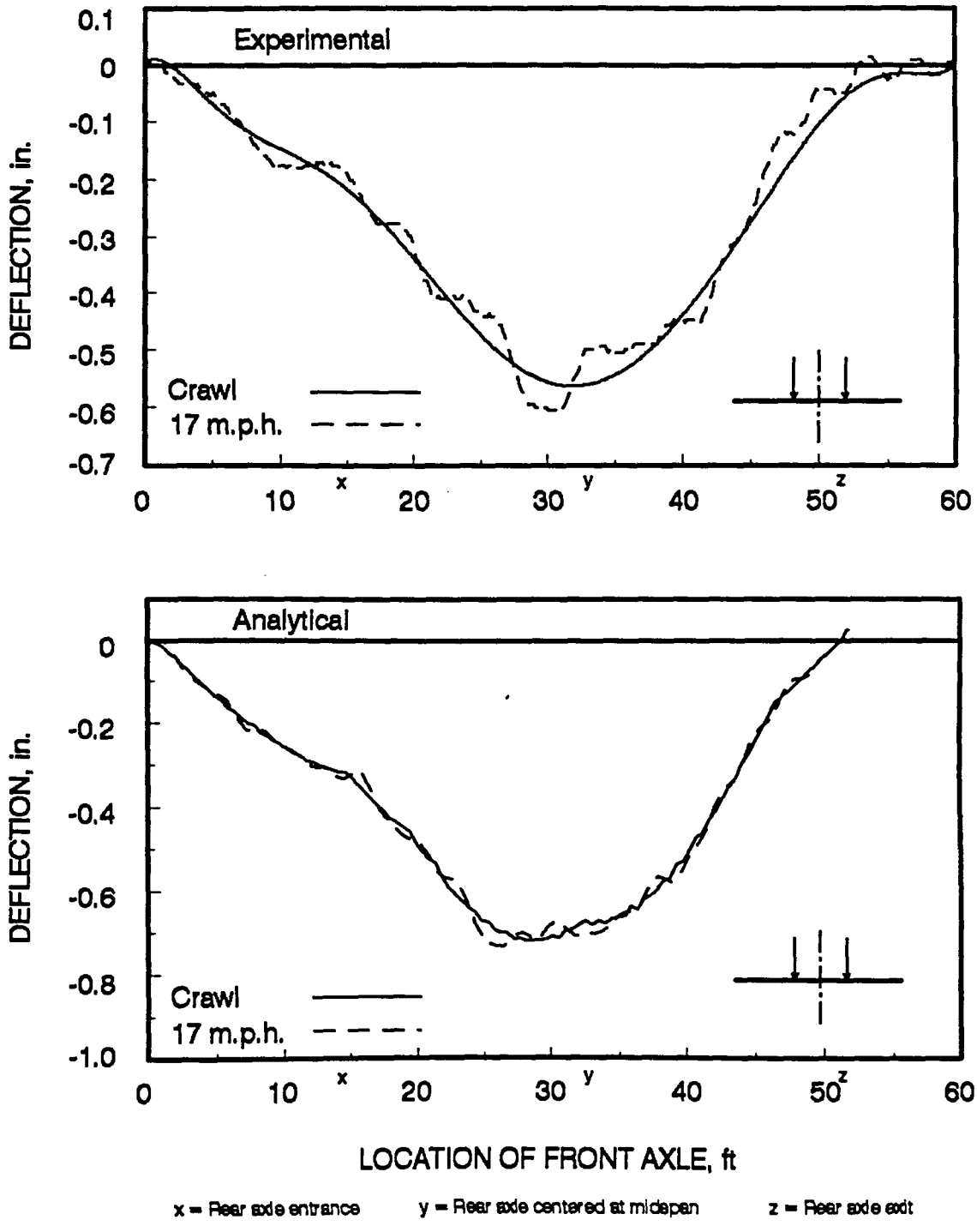

Fig. 32. Analytical bridge response 17 m.p.h.

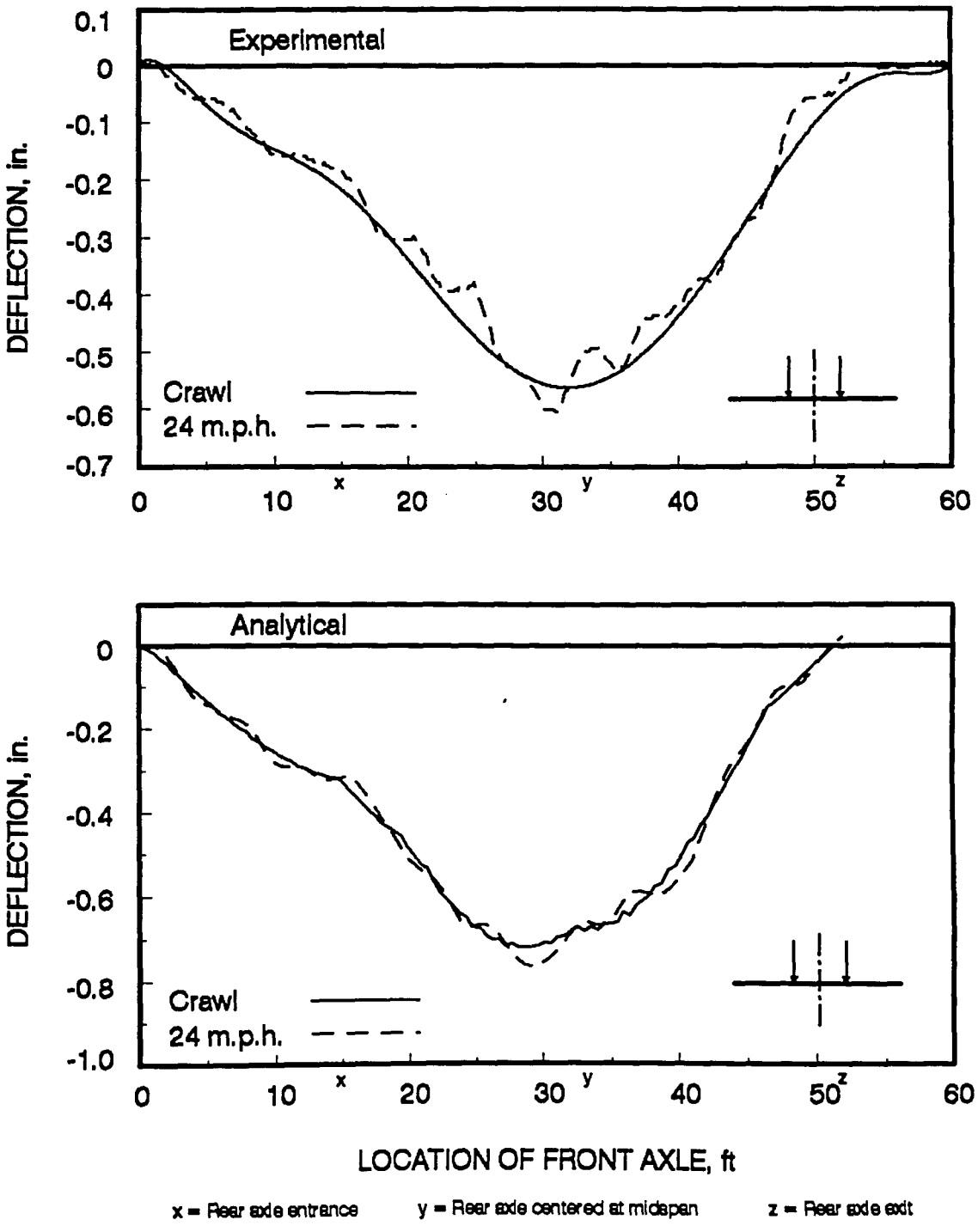

Fig. 33. Analytical bridge response 24 m.p.h.

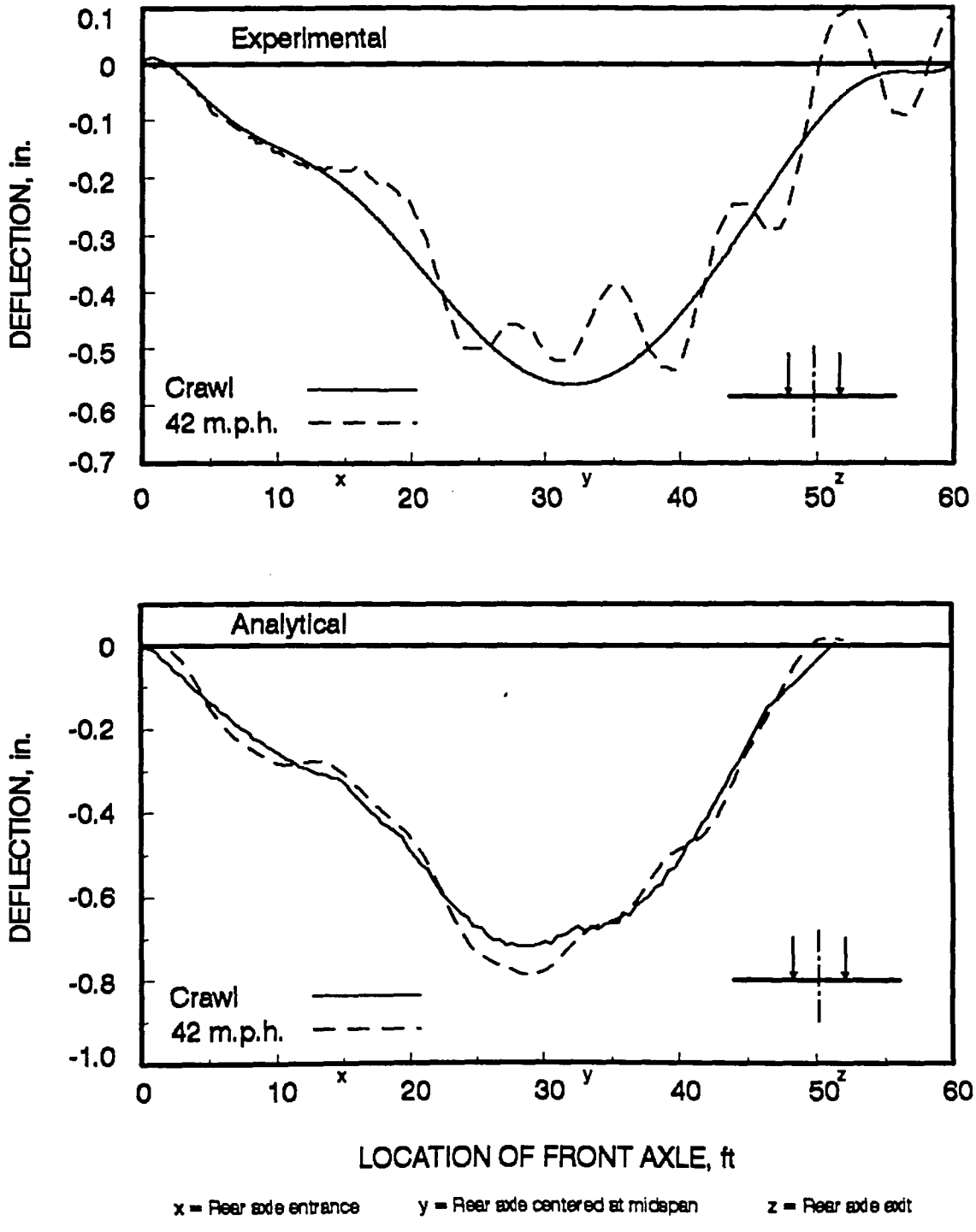

Fig. 34. Analytical bridge response 42 m.p.h.

First a comparison of the crawl speed responses should be made. Although the magnitudes of the responses do not match due to the end restraints, the general shapes match fairly well. However, it was noticed that the maximum responses were occurring in different locations. In the experimental response, the maximum deflection was occurring when the rear axles were approximately centered about midspan, but analytically, the maximum occurred when the center of gravity of the loads was at midspan.

Simple hand calculations were performed to determine the difference in deflection for the two vehicle positions. Considering the bridge as a simply supported beam, the loading with the truck centroid at midspan resulted in only a 0.01 in. larger deflection. Therefore, there is a difference, but it is small.

The end restraints could again be an explanation to the difference in maximum static deflection location. If there was more rotational restraint at one end of the bridge, the longitudinal location at which the maximum deflection would occur would shift toward the less restrained end. The corresponding vehicle location to produce that maximum deflection would also move toward the unrestrained end. For the Teal River bridge, if the entrance end of the bridge had more rotational restraint, the vehicle position to cause the maximum crawl speed deflection would shift further down the

bridge length as found experimentally. This shifting of the response was also noticed in the non-crawl speed runs.

One means of correcting the differences between the field and model end conditions would be to add rotational restraint to the bridge model. End restraint could be added until the transverse deflection profiles (Fig. 22) matched experimentally and analytically. The restrained bridge would be stiffer with different dynamic characteristics resulting in a response more accurately representing the actual bridge. Although this was not done in this investigation, it is reccommended for further study.

The current model also resulted in amplitudes of dynamic oscillation consistently smaller than obtained experimentally. This suggests that the rolling mass solution was not able to account for all factors influencing the response. Oscillations of the vehicle on its suspension system were not accounted for in the model and could explain the larger amplitudes of oscillations.

The number of oscillations also differed in some of the comparisons. This is especially noticeable at the higher velocities. In Fig. 31 and 34 (approximately 40 m.p.h. tests), the rolling mass solution showed only a single oscillation occurring about the maximum crawl defection. This was not the case experimentally where several oscillations occurred near the maximum crawl deflection.

This again suggests that the bridge response is being influenced by other factors. The interaction between the vehicle dynamics and the bridge response are believed to have caused the additional oscillations.

As was done with the experimental results, the bridge response was quantified using a DLF (see Fig. 35). The DLF's obtained from the analytical study did not show the trend of reaching a maximum value at approximately 30 m.p.h. as in the experimental results. Rather, the maximum DLF occurred at the highest velocity.

Additionally, the center span accelerations obtained from the rolling mass solution were plotted for comparison with the analytical deflections. Figures 36 through 41 illustrate the results. The figures clearly show the increase in accelerations as the rate of load application (velocity) increases. The larger accelerations at higher velocities result in larger amplitudes of dynamic oscillations.

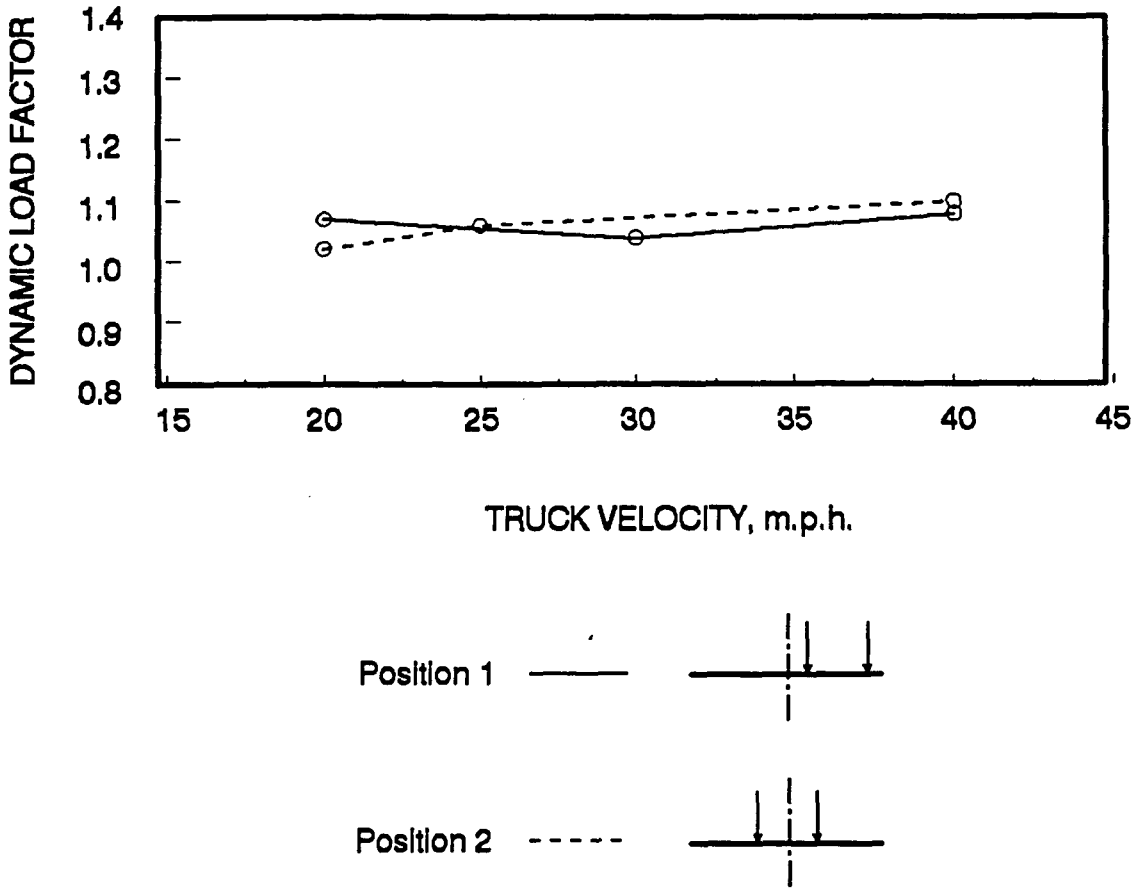

Fig. 35. Analytical dynamic load factors

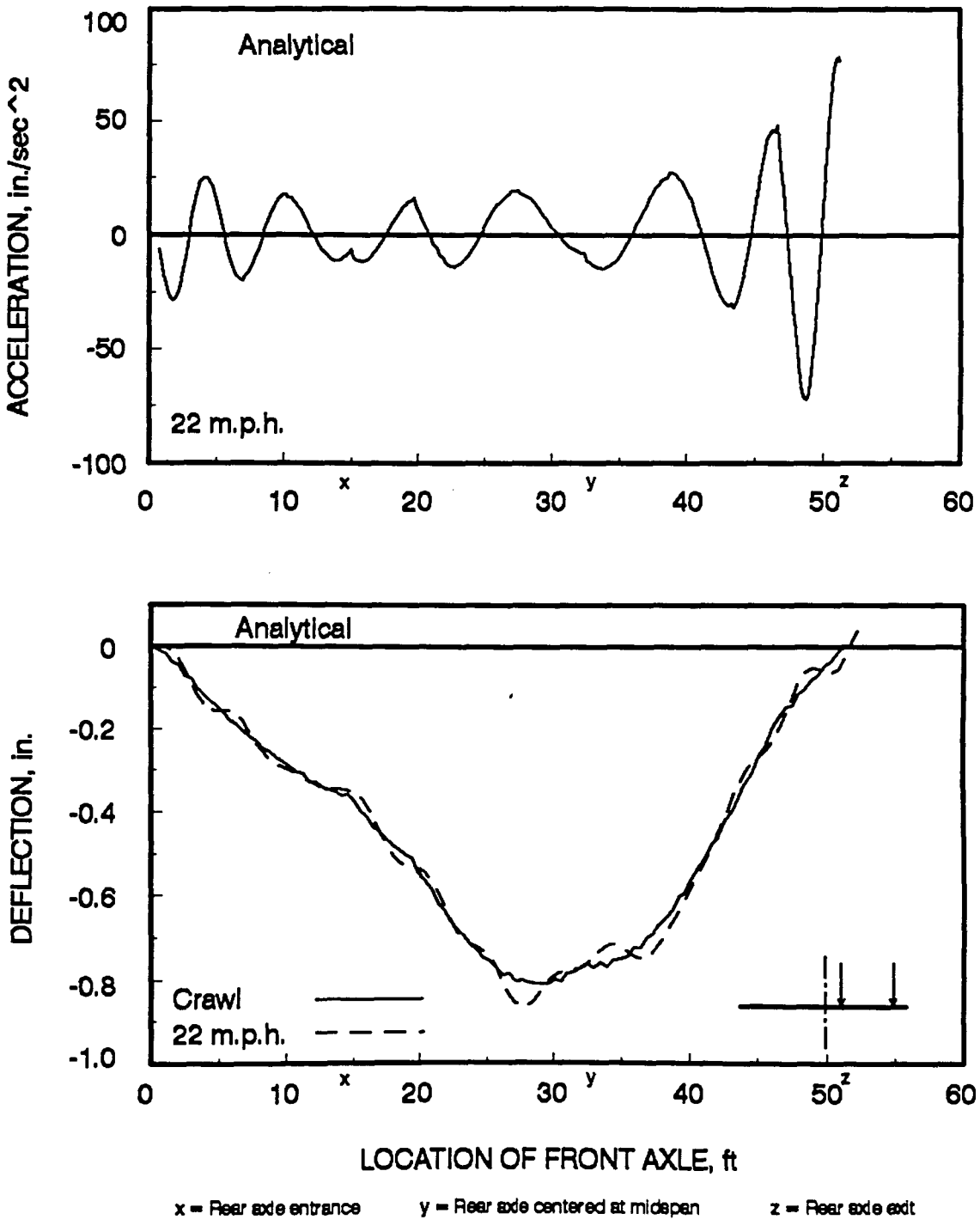

Fig. 36. Midspan accelerations 22 m.p.h.

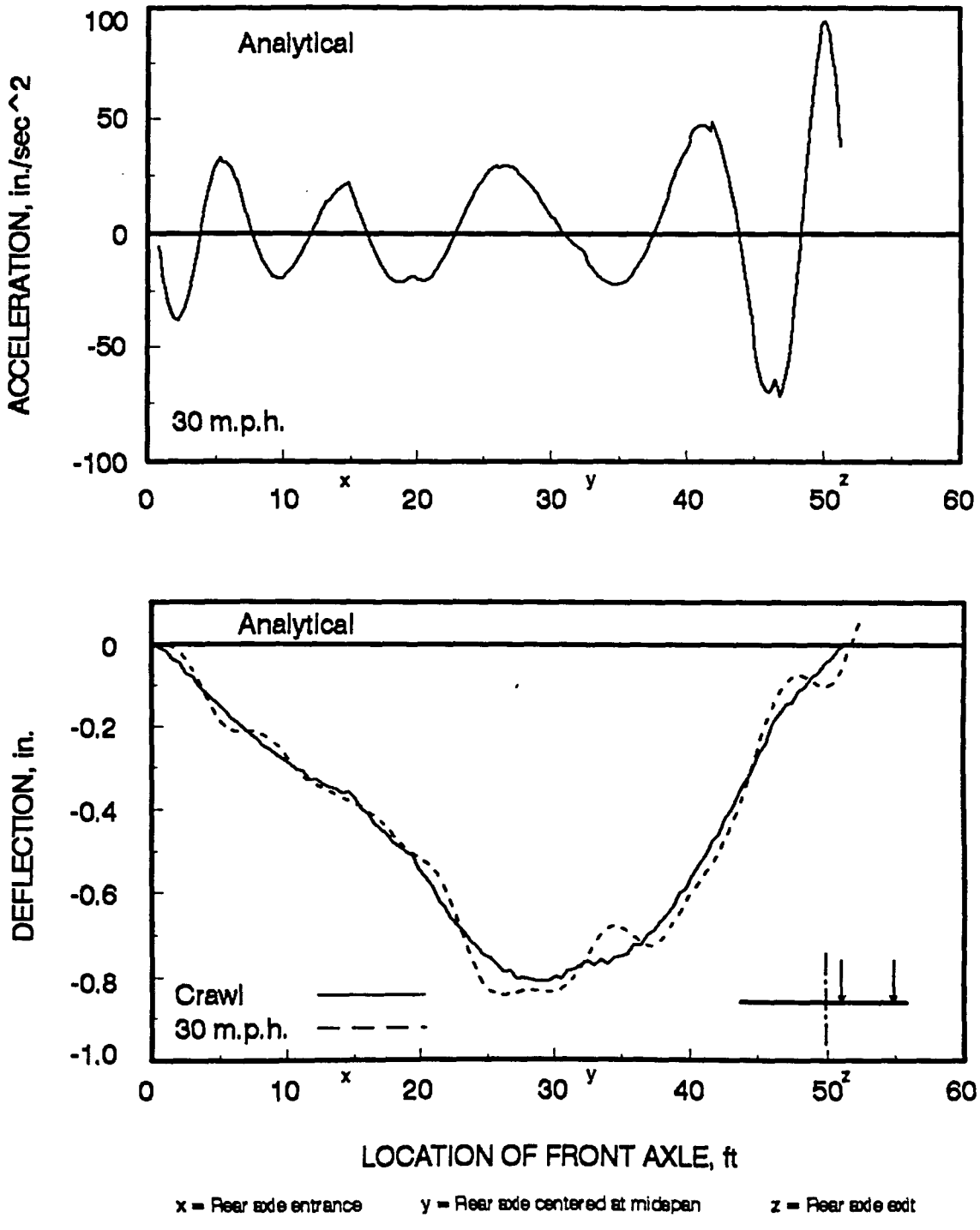

Fig. 37. Midspan accelerations 30 m.p.h.

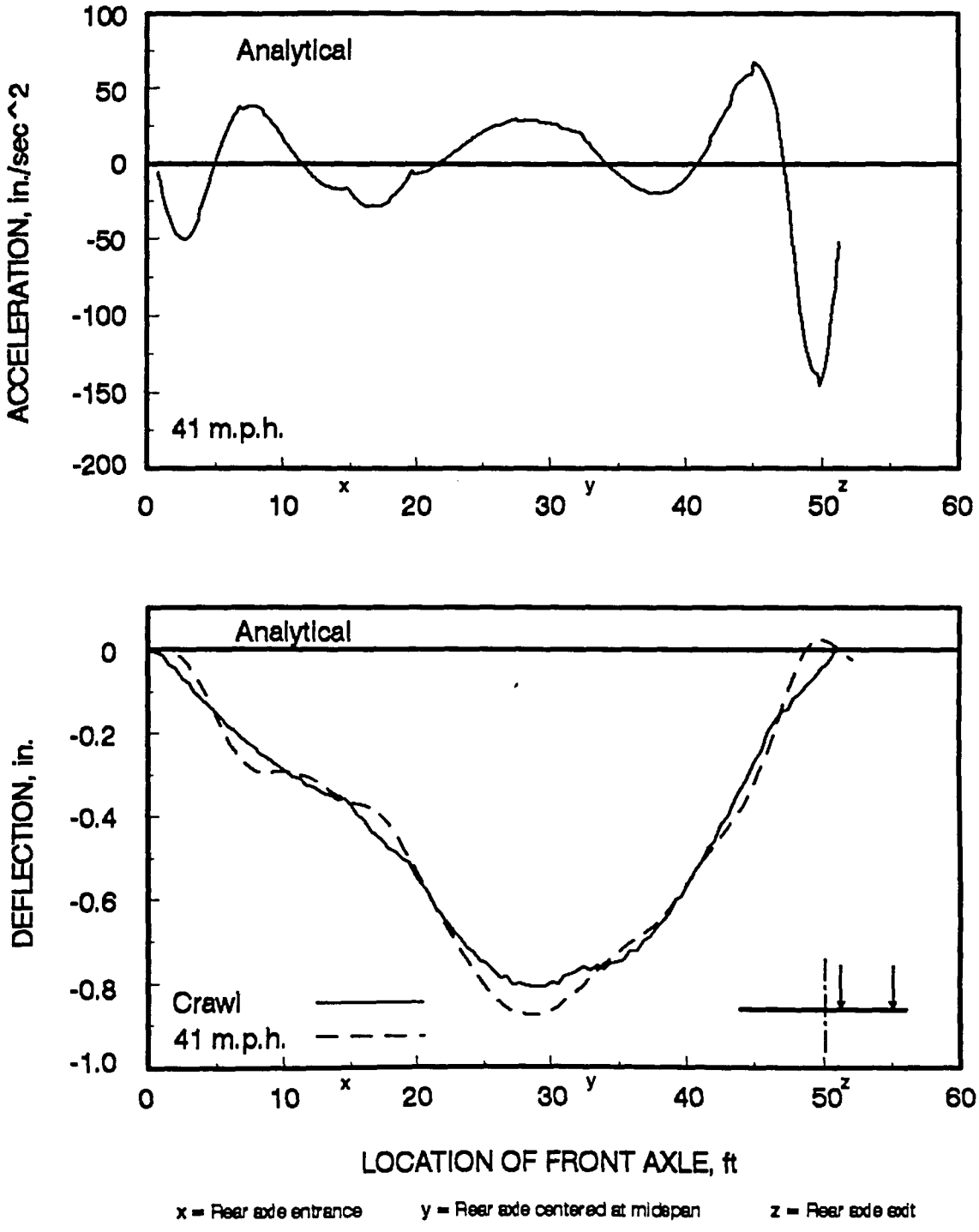

Fig. 38. Midspan accelerations 41 m.p.h.

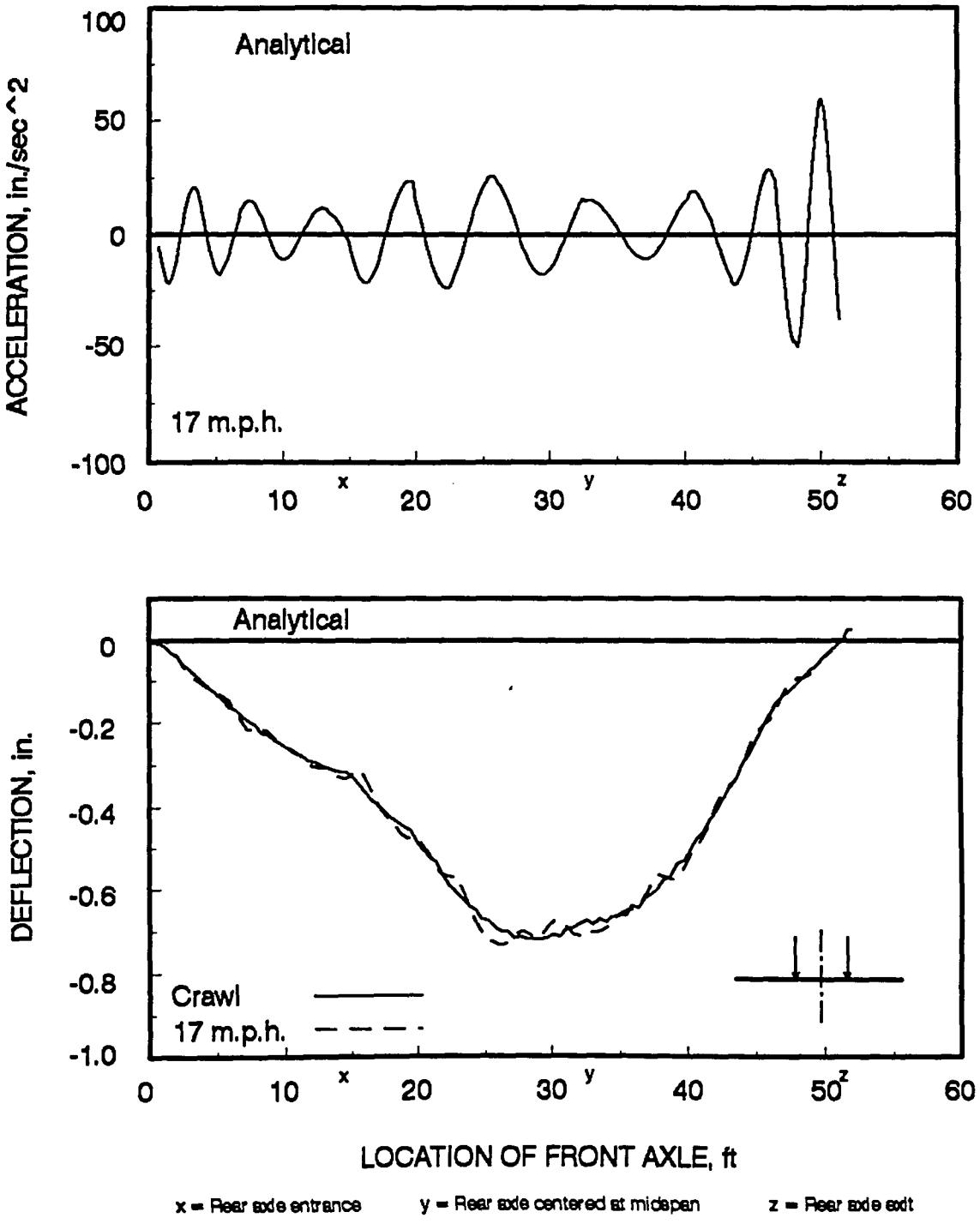

Fig. 39. Midspan accelerations 17 m.p.h.

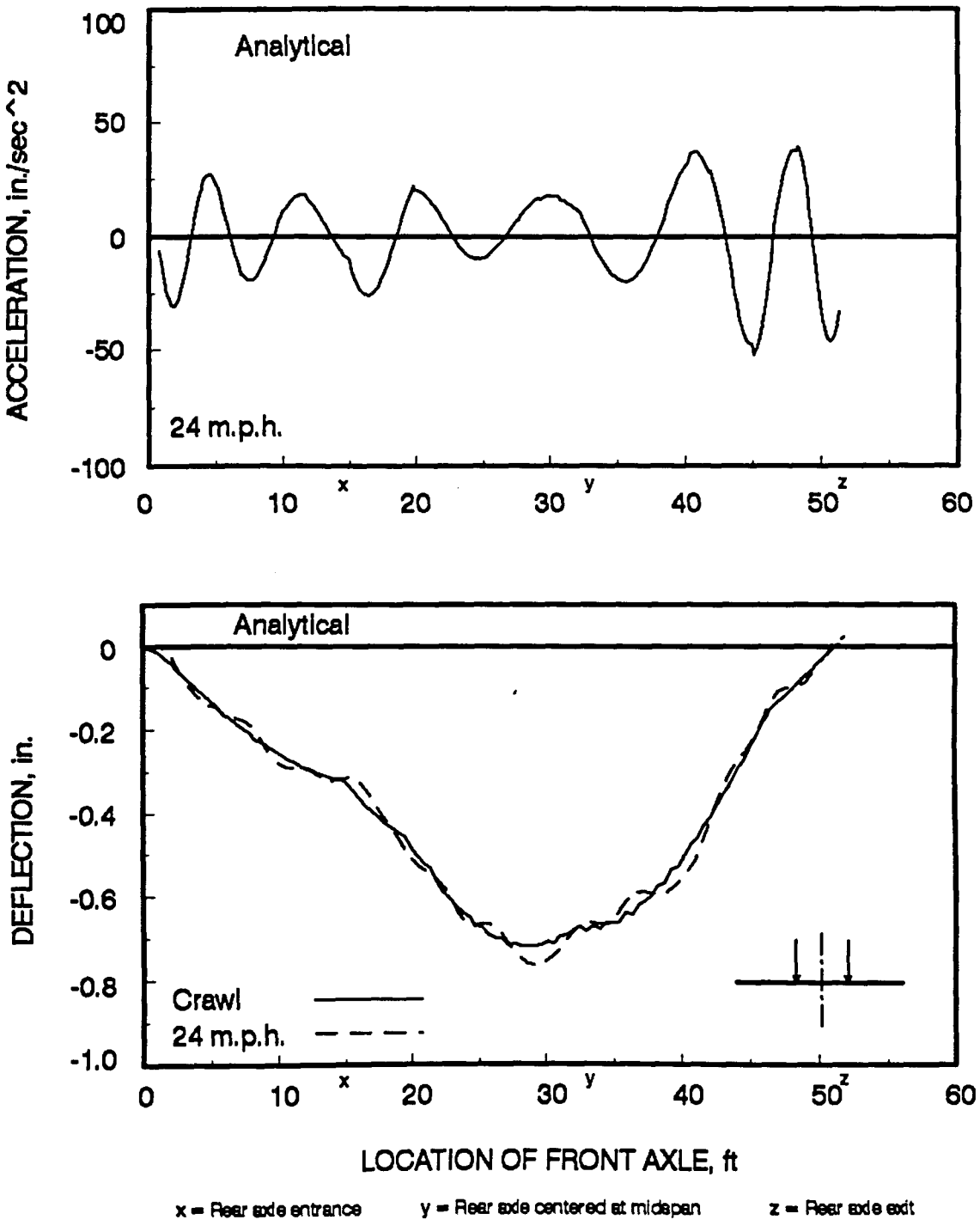

Fig. 40. Midspan accelerations 24 m.p.h.

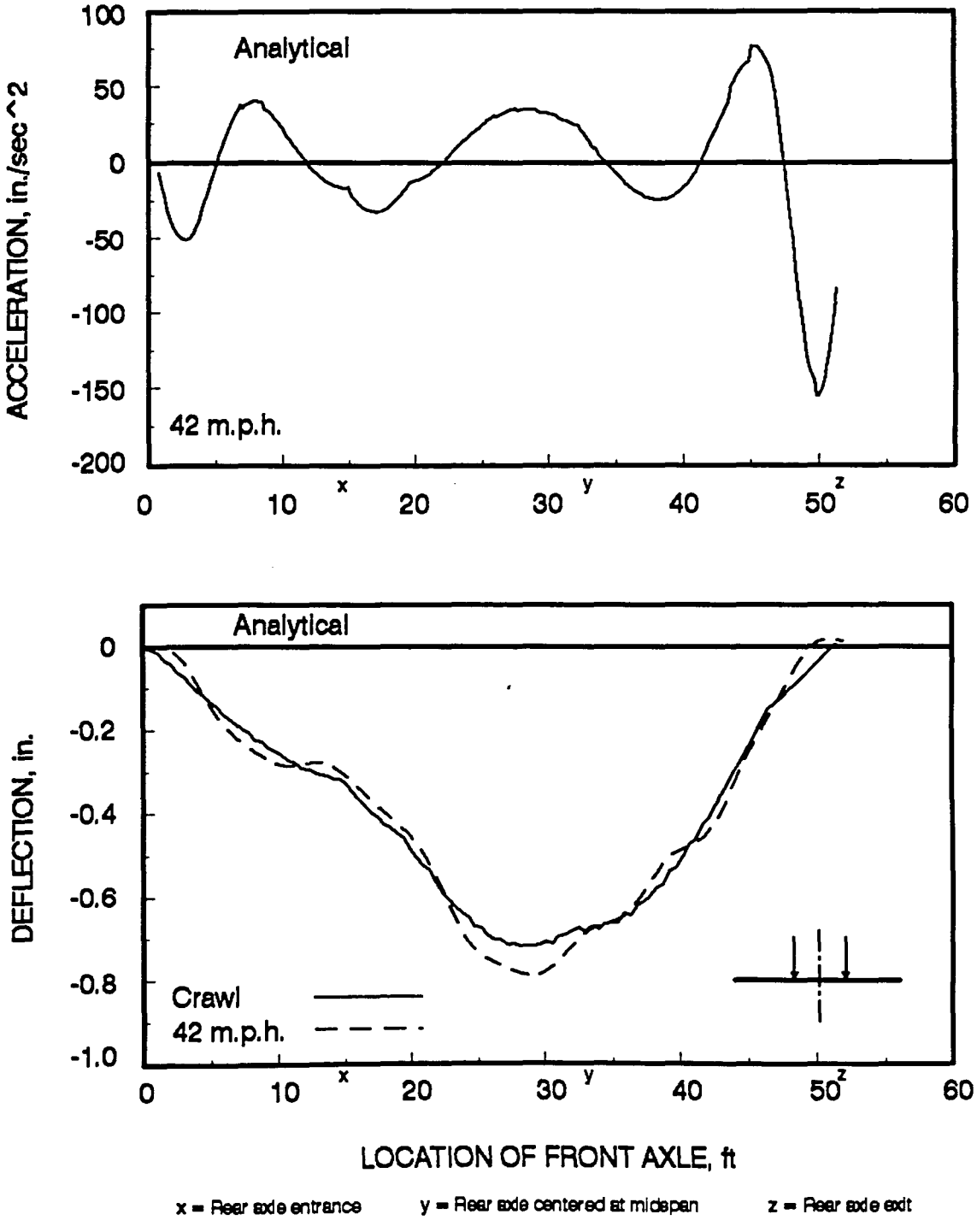

Fig. 41. Midspan accelerations 42 m.p.h.

4. CONCLUSIONS AND RECOMMENDATIONS

The dynamic behavior of stress laminated timber bridges has been investigated. The study included the dynamic field testing of a stress laminated bridge and the development of an analytical model to predict the bridge response. This chapter discusses the conclusions drawn from the study.

4.1 Experimental

The Teal River bridge located in northwestern Wisconsin was dynamically tested in the experimental investigation. The following conclusions were drawn from the study.

1. Loading the bridge at crawl speed (approximately 5 m.p.h.) accurately represented the static deflections.
2. The dynamic response due to the front axle alone is small. The closely spaced, heavy rear axles accounted for most of the response.
3. The amplitude of dynamic oscillation increased with increasing vehicle velocity, however, larger maximum dynamic deflections did not result.
4. A forced vibration occurred at points near the

load, while points away from the load exhibited a free vibration.

5. The placement of an artificial bump at the bridge entrance significantly increased the dynamic response. Both the amplitude of dynamic oscillation and the maximum dynamic response increased.
6. The dynamic load factors were greater for eccentric loading than for symmetric loading.
7. The general trend of the dynamic load factors was to increase with increasing velocity up to 30 miles per hour and then decrease at 40 miles per hour.
8. The natural period of the Teal River bridge as measured from the free vibration resulting after the truck had exited the span was 0.13 seconds.
9. Approximately 3% of critical damping was present in the bridge response.
10. A single upper bound value of the dynamic load factor for the bridge was determined to be 1.23. This value represents the DLF determined from only one test vehicle in two lane positions, and should be used with caution.

4.2 Analytical

The Teal River bridge was modeled as an orthotropic plate using the finite element program ANSYS. The dynamic loading was represented by rolling masses at each wheel position. The following conclusions were drawn from the study.

1. The bridge could be successfully modeled using a finite element orthotropic plate model. The static deflections as determined from the model agreed with field data if differences due to end restraints are considered.
2. The modal analysis performed with the bridge model provided good results. The first mode frequency closely matched the frequency measured in the field tests.
3. The loaded frequency of the bridge changes significantly from the unloaded frequency and must be accounted for in the analytical model. This is especially true for short span bridges, such as stress laminated timber bridges, where the live load mass to dead load mass ratios are large.
4. The rolling mass vehicle loading model was inadequate at reproducing the bridge response. The

rolling mass model resulted in smaller oscillations and smaller maximum dynamic deflections.

5. The dynamic characteristic of the vehicle on its suspension system are believed to greatly influence the bridges dynamic response.

4.3 Recommendations

The following recommendations are made based on the results obtained from this study.

1. More data should be collected from field test of stress laminated timber bridges. Different vehicles should be used to obtain a better single value of the dynamic load factor.
2. Data should also be collected on the dynamic response of the vehicle. A better understanding of how the bridge is behaving requires a better knowledge of the vehicle bridge interaction.
3. The vehicle model should be further developed to include effects of the suspension system.
4. The mass of the vehicle should be accounted for in the finite element bridge model to account for changes in the loaded frequency.
5. Rotational restraint should be added to the bridge

model to more accurately represent the actual field conditions. The added restraint would result in a stiffer bridge changing the dynamic characteristics and bridge respons.

REFERENCES

1. AASHTO, Guide Specifications for the Design of Stress Laminated Wood Decks, AASHTO, Washington, D.C., 1991, 1-12.

2. Bakht, B. and Pinjarkar, S. G. (1989). "Review of Dynamic Testing of Highway Bridges." Transportation Research Board, TRB 880532, 1-33.

3. Biggs, J. M. and Suer, H. S. (1956). "Vibration Measurements on Simple-Span Bridges." Highway Research Board, Bulletin 124, 1-15.

4. Biggs, J. M., Introduction to Structural Dynamics., McGraw-Hill Book Company, New York, 1964, 315-327.

5. Foster, B. M. and Oehler, L. T. (1956). "Vibration and Deflection of Rolled-Beam and Plate-Girder Bridges." Highway Research Board, Bulletin 124, 79-110.

6. Gupta, R. K. (1980). "Dynamic Loading of Highway Bridges." Journal of the Engineering Mechanics Division, ASCE, 106 (EM2), 377-394.

7. Humar, J. L. and Kashif, A. M. (1993). "Dynamic Response of Bridges Under Travelling Loads." Canadian Journal of Civil Engineering, 20 (2), 287-298.

8. Hwang, E. S. and Nowak, A. S. (1991). "Simulation of Dynamic Load for Bridges." Journal of Structural Engineering, ASCE, 117 (5), 1413-1434.

9. Inbanathan, M. J. and Wieland, M. (1987). "Bridge Vibrations due to Vehicle Moving Over Rough Surface." Journal of Structural Engineering, ASCE, 113 (9), 1994-2008.

10. Looney, C. T. G. (1958). "High-Speed Computer Applied to Bridge Impact." Journal of the Structural Division, ASCE, 84 (ST5), 1-41.

11. Oliva, M. G. and Dimakis, A. (1988). "Behavior of Stress Laminated Timber Highway Bridge." Journal of Structural Engineering, ASCE, 114 (8), 1850-1869.

12. Paz, M. Structural Dynamics: Theory and Computation, 3rd ed., Van Nostrand Reinhold, New York, N.Y., 1991, 129-136 and 438-460.

13. Ritter, M. A., Timber Bridges: Design, Construction, Inspection, and Maintenance., United States Department of Agriculture, Washington, D.C., 1990, 9-1 - 9-19.

14. Ritter, M. A., Geske, E. A., McCutcheon, W. J., Moody, R. C., Wacker, J. P., and Mason, L. E. (1991). "Methods for Assessing the Field Performance of Stress Laminated Timber Bridges." Proceedings of the 1991 International Timber Engineering Conference, TRADA, (3), 3.319-3.326.

15. Ritter, M. A. and Oliva, M. G. (1990). "Field Performance of U.S. Stress Laminated Wood Bridges." Proceedings of the 1990 International Timber Engineering Conference, Steering Committee of the International Timber Engineering Conference, (2), 564-569.

16. Seible, F., Priestley, M. J., Krishnan, K., Nagy, G., and Sharabi, N. (1990). "Simulation of Rolling Loads on the Gepford Overhead Bridge Section." Structural Systems Research Project, SSRP-90/05, 1-39.

17. Taylor, R. J., (1982). "Rehabilitation of Wood Highway Bridges in Ontario." Structural Research Report 82-SRR-2, MTC., Downsview, Ontario.

18. Taylor, R. J., Batchelor, B. D., and Van Dalen, K. (1982). "Prestressed Wood Bridges." Proceedings of the International Conference on Short and Medium Span Bridges, Toronto, Session 6, 203-218.

19. Wacker, J. P. and Ritter, M. A., Field Performance of Timber Bridges: 1. Teal River Stress Laminated Deck Bridge. Research Paper FPL-RP-515, USDA Forest Service, Washington, D.C.

20. Wang, T. L., Huang, D., and Shahawy, M. (1992). "Dynamic Response of Multigirder Bridges." Journal of Structural Engineering, ASCE, 118 (8), 2222-2238.

21. Wen, R. K., and Veletsos, A. S. (1962). "Dynamic Behavior of Simple-Span Highway Bridges." Highway Research Board, Bulletin 315, 1-26.

ACKNOWLEDGMENTS

I would like to thank Dr. Terry J. Wipf for his guidance and support throughout my graduate work and thesis preparation. I wish him continued success in the study of timber bridge dynamic behavior. I would also like to thank Dr. Fouad Fanous and Dr. Loren Zachary for serving on my committee.

In addition, I would like to thank Doug Wood, structures lab supervisor, for his help in preparing for the field test. His knowledge and assistance was greatly needed and appreciated.

Lastly, I would like to thank Joni Wright for her patience and understanding during the last few months. Finally it is done.

APPENDIX A. DAS PROGRAM LISTING

```
10    !
20    !!!!!!!!!!!!!!!!!!!!!!!!!!!!!!!!!!!!!!!!!!!!!!!!!!!
30    ! Program to measure dynamic response of bridges.  !
40    !   Measurements taken at rate specified by user.  !
50    !!!!!!!!!!!!!!!!!!!!!!!!!!!!!!!!!!!!!!!!!!!!!!!!!!!
60    !
70     COM /I_o/ @Dac,@Dac_off
80     DIM Test$[9]    ! Test$ will be limited to 8 characters
90     !                 to conform to DOS filesystem
91     DIM Bridge$[100], Speed$[90], Weight$[90], Run_time$[90],
             Read_rate$[90]
92     DIM Wt$[90]
100   REAL Total_rdgs,Init_volt(0:40),Rtime,Loop,Fact4 ! Array to
             hold original values
110    INTEGER Read_per,No_hi_level
120    ASSIGN @Dac TO 709
130    ASSIGN @Dac_off TO 709;FORMAT OFF,SWAP ON
131    OUTPUT @Dac;"RST"
150    CLEAR SCREEN
160    !
161    INPUT "Enter bridge description:",Bridge$
162    INPUT "Enter estimated vehicle speed:",Mph$
163    INPUT "Enter axle weight:",Wt$
164    Speed$="ESTIMATED VEHICLE SPEED = "&Mph$
165    Weight$="AXLE WEIGHT(S) = "&Wt$
166    D$=DATE$(TIMEDATE)
167    T$=TIME$(TIMEDATE)
170    INPUT "Enter the desired run time in seconds:",Rtime
171    Run_time$="DURATION OF TEST = "&VAL$(Rtime)&" SECONDS"
180    INPUT "Enter the number of DCDT's:",No_hi_level
190    INPUT "Enter the number of readings to be
            averaged:",Read_per
200   INPUT "Enter the delay between channel list scans:",Scdelay
201    Read_rate$="DATA INTERVAL = "&VAL$(Scdelay)&" SECONDS"
210    Loop=Rtime/Scdelay
220    Total_rdgs=Read_per*No_hi_level
230    !
240    Fact4=Total_rdgs/4.
250    IF FRACT(Fact4)=0. THEN
260      PRINT " Hey Bozo, you cannot have the number of DCDT's or"
270      PRINT " the number of readings to be averaged a factor of
              four;"
280       PRINT " hence, reinput the following:"
290       GOTO 180
300    END IF
310    !
320    CALL Create_files(Test$,@File_data,@File_exc,@File_temp)
321    OUTPUT @File_data;D$, T$, Bridge$, Speed$, Weight$,
```

```
            Run_time$, Read_rate$
322     OUTPUT @File_data USING "5/"
340     CALL Init_dac(Total_rdgs,Read_per,No_hi_level)
350     CALL Read_init (Total_rdgs, Init_volt(*), Read_per,
                        No_hi_level, @File_exc)
380     CALL Meas_lp (Totalrdgs$, Total_rdgs, Init_volt(*), Loop,
                      Scdelay, Rtime, Read_per, No_hi_level,
                      @File_data, @File_temp)
390     !
400     !
410     PRINT "          DONE"
420     END
430     !
440     !!!!!!!!!!!!!!!!!!!!!!!!!!!!!!!!!!!!!!!!
450     ! Subroutine to read initial voltages !
460     !!!!!!!!!!!!!!!!!!!!!!!!!!!!!!!!!!!!!!!!
470     !
480   SUB Read_init(REAL Total_rdgs,Init_volt(*),INTEGER Read_per,
                    No_hi_level, @File_exc)
490       COM /I_o/ @Dac,@Dac_off
500       INTEGER Rdg_indx,In
510      ALLOCATE INTEGER Packed(0:Total_rdgs-1) ! Temporary array
520     ALLOCATE REAL Temp_v(0:Total_rdgs-1),Init(0:No_hi_level-1)
530       OUTPUT @Dac;"PTRIG SGL"
540       OUTPUT @Dac;"SCTRIG HOLD"
550       ENTER @Dac_off;Packed(*)
560       !
570       CALL Unpk13(Packed(*),Total_rdgs,Temp_v(*))
580       !
590       FOR Rdg_indx=0 TO No_hi_level-1
600         FOR Avg=0 TO Read_per-1
610           Init_volt(Rdg_indx) = Temp_v (Rdg_indx*Read_per+Avg)
                    + Init_volt(Rdg_indx)
620         NEXT Avg
630         Init_volt(Rdg_indx)=Init_volt(Rdg_indx)/(Read_per)
640       NEXT Rdg_indx
650       DEALLOCATE Packed(*)
660       DEALLOCATE Temp_v(*)
661     FOR In=0 TO No_hi_level-1
662        Init(In)=Init_volt(In)
663     NEXT In
664     OUTPUT @File_exc;Init(*)
665     ASSIGN @File_exc TO *
670     SUBEND
680     !
690     !!!!!!!!!!!!!!!!!!!!!!!!!!!!!!!!!!!!!!!!
700     ! Subroutine to initialize the DAS !
710     !!!!!!!!!!!!!!!!!!!!!!!!!!!!!!!!!!!!!!!!
720     !
730     SUB Init_dac(REAL Total_rdgs,INTEGER Read_per,No_hi_level)
740       COM /I_o/ @Dac,@Dac_off
750       INTEGER Slot,Chan,It
```

```
760       DIM Total_rdgs$[4]
770       Total_rdgs$=VAL$(Total_rdgs-1)
780       CLEAR @Dac
790       OUTPUT @Dac;"RESET"
800       WAIT .3
810       OUTPUT @Dac;"OUTBUF ON; INBUF ON"
820       OUTPUT @Dac;"DISABLE LABELS; DISP OFF"
830     !
840     ! WE WILL SET UP A 3852A ARRAY TO HOLD ALL CHANNEL VALUES
850     ! AND A SECOND TO HOLD THE RANGE FOR EACH CHANNEL
860     ! THE D_PACK ARRAY IS A 3852A ARRAY FOR DATA FROM 16 BIT
870     ! VOLTMETER.  IT IS USED TO TEMPORARILY HOLD DATA
880     !
890       OUTPUT @Dac;"INTEGER CHAN(";Total_rdgs$;")"
900       OUTPUT @Dac;"PACKED D_PACK(";2*Total_rdgs-1;")"
910       PRINT "Setting the 3852A channel list with
                  Read_per*No_hi-level ch."
920       Chan_cntr=0
930       IF No_hi_level<=24 THEN
940         Slot=4
950       FOR Chan=0 TO No_hi_level-1
960         FOR Avg=1 TO Read_per
970           OUTPUT @Dac;"CHAN(";VAL$(Chan_cntr);") =
                              ";VAL$(Slot*100+Chan)
980           Chan_cntr=Chan_cntr+1
990         NEXT Avg
1000      NEXT Chan
1010      ELSE
1020        Slot=4
1030      FOR Chan=0 TO 23
1040        FOR Avg=1 TO Read_per
1050          OUTPUT @Dac;"CHAN(";VAL$(Chan_cntr);") =
                              ";VAL$(Slot*100+Chan)
1060          Chan_cntr=Chan_cntr+1
1070        NEXT Avg
1080      NEXT Chan
1100        Slot=5
1110        It=No_hi_level-24
1120      FOR Chan=0 TO It-1
1130        FOR Avg=1 TO Read_per
1140          OUTPUT @Dac;"CHAN(";VAL$(Chan_cntr);") =
                              ";VAL$(Slot*100+Chan)
1150          Chan_cntr=Chan_cntr+1
1160        NEXT Avg
1170      NEXT Chan
1180      END IF
1190    !
1200  Setup_pacer:OUTPUT @Dac;"PTRIG HOLD"
1210      OUTPUT @Dac;"PACER .001,1"
1220      !
1230      !!!!!!!!!!!!!!!!!
1240      !  SUB TRAN_INT  !
```

```
1250     !!!!!!!!!!!!!!!!!!
1260     !
1270 Setup_intr1:OUTPUT @Dac;"SUB TRAN_INT"
1280     OUTPUT @Dac;" XRDGS 600,";Total_rdgs;" INTO D_PACK"
                  !Transfers data from VM buffer to mainframe
1290     OUTPUT @Dac;" VREAD D_PACK,PACK"
                  !Moves Data from M/F to HPIB
1300     OUTPUT @Dac;" ENABLE INTR USE 600"
                  ! Enbles VM to interrupt M/F
1310     OUTPUT @Dac;"SUBEND"
1320     !
1330     PRINT " Setting up High Speed Voltmeter"
1340     !
1350     !
1360   Setup_vm: !
1370     OUTPUT @Dac;"USE 600"
1380     OUTPUT @Dac;"STA?"
1390     OUTPUT @Dac;"CLROUT"
1400     OUTPUT @Dac;"SCANMODE ON"
1410     OUTPUT @Dac;"SCTRIG HOLD"
420      OUTPUT @Dac;"FUNC DCV"
1430     OUTPUT @Dac;"DISABLE INTR SYS"
1440     OUTPUT @Dac;"RANGE 10"
1450     OUTPUT @Dac;"ARMODE BEFORE"
1460     OUTPUT @Dac;"TERM RIBBON"
1470     OUTPUT @Dac;"RDGS SYS"
1490     OUTPUT @Dac;"RDGSMODE END"
1510     OUTPUT @Dac;"NRDGS 1"
1520     OUTPUT @Dac;"AZERO ONCE"
1530     OUTPUT @Dac;"TRIGOUT ON"
1540     OUTPUT @Dac;"TRIG INT"
1550     OUTPUT @Dac;"SPER 10E-6"
1560     OUTPUT @Dac;"SCDELAY 0,.01"
1570     OUTPUT @Dac;"ENABLE INTR SYS"
1580     OUTPUT @Dac;"ENABLE INTR USE 600"
1590     OUTPUT @Dac;"PRESCAN 1"
1600     OUTPUT @Dac;"POSTSCAN 0"
1610     OUTPUT @Dac;"ASCAN OFF"
1620     OUTPUT @Dac;"CLWRITE SENSE CHAN"
1630     !
1640     OUTPUT @Dac;"STSLOPE LH"
1650     OUTPUT @Dac;"STTRIG INT"
1660     OUTPUT @Dac;"SCTRIG EXT1"
1670     OUTPUT @Dac;"ON INTR USE 600 CALL TRAN_INT"
1690   SUBEND
1700   !
1710  !!!!!!!!!!!!!!!!!!!!!!!!!!!!!!!!!!!!!!!!!!!!!!!!!!!!!!!!!!!!!!!!!!!!!!!
1720   ! Subroutine to unpack packed arrays for initial readings !
1730  !!!!!!!!!!!!!!!!!!!!!!!!!!!!!!!!!!!!!!!!!!!!!!!!!!!!!!!!!!!!!!!!!!!!!!!
1740   !
1750   SUB Unpk13(INTEGER Pack(*),REAL Number,Volt(*))
1760     INTEGER I
```

```
1770      REAL R(0:3)
1780      DATA 256.,32.,4.,1.
1790      READ R(*)
1800      FOR I=0 TO Number-1
1810        M=BINAND(Pack(I),4095)
1820        IF Pack(I)>0 OR M=4095 THEN
1830          Volt(I)=1.E+38
1840        ELSE
1850          Volt(I)=M*.0025/R(BINAND(SHIFT(Pack(I),13),3))
1860          IF BIT(Pack(I),12) THEN Volt(I)=-Volt(I)
1870        END IF
1880      NEXT I
1890    SUBEND
1900    !
1910    !!!!!!!!!!!!!!!!!!!!!!!!!!!!!!!!!!!!!!!!!!!!!!!!!!!!!!!!!!!!!!!!!!!!!!!
1920    ! Subroutine to read required voltages and perform post
           processing !
1930    !!!!!!!!!!!!!!!!!!!!!!!!!!!!!!!!!!!!!!!!!!!!!!!!!!!!!!!!!!!!!!!!!!!!!!!
1940    !
1950    SUB Meas_lp(Total_rdgs$,REAL Total_rdgs, Init_volt(*),
                    Loop,Scdelay,Rtime,INTEGER Read_per,
                    No_hi_level, @File_data, @File_temp)
1960      COM /I_o/ @Dac,@Dac_off
1970      DIM Mark$[8]
1980      ALLOCATE REAL Factor(0:No_hi_level-1)
1990      ALLOCATE REAL Disp(0:No_hi_level-1)
2000    INTEGER Rdg_indx,I,Gnrt,Acnt,Bcnt,Ccnt,Begin,End,Post,Aooa
2010      ALLOCATE REAL Meas_v(Loop,0:No_hi_level-1)
2020      ALLOCATE INTEGER Packed(0:Total_rdgs-1)
2030      ALLOCATE REAL Temp_v(0:Total_rdgs-1),
                        Atemp_v(Loop,0:Total_rdgs-1)
2040      REAL Bemp_v
2050      Total_rdgs$=VAL$(Total_rdgs-1)
2060      CLEAR @Dac
2070      OUTPUT @Dac;"RESET"
2080      WAIT 1
2090    ! PRINT " "
2100    !PRINT "        DON'T HIT THE ROAD RUNNER !!!!!!"
2110    !PRINT "        ------------------------------"
2120    !WAIT 2
2130    !PRINT "  "
2140    !OUTPUT @Dac;"BEEP ONCE"
2150    !OUTPUT @Dac;"WAIT 0.125"
2160    !OUTPUT @Dac;"BEEP ONCE"
2170    !PRINT "        ZIP BANG !!"
2180    !WAIT 2
2190    !PRINT " "
2200      OUTPUT @Dac;"INTEGER CHAN(";Total_rdgs$;")"
2210      OUTPUT @Dac;"PACKED E_PACK(";8.*Loop*Total_rdgs;")"
2220       Chan_cntr=0
2230       IF No_hi_level<=24 THEN
2240         Slot=4
```

```
2250      FOR Chan=0 TO No_hi_level-1
2260        FOR Avg=1 TO Read_per
2270          OUTPUT @Dac;"CHAN(";VAL$(Chan_cntr);")=
                         ";VAL$(Slot*100+Chan)
2280          Chan_cntr=Chan_cntr+1
2290        NEXT Avg
2300      NEXT Chan
2310      ELSE
2320        Slot=4
2330      FOR Chan=0 TO 23
2340        FOR Avg=1 TO Read_per
2350          OUTPUT @Dac;"CHAN(";VAL$(Chan_cntr);") =
                         ";VAL$(Slot*100+Chan)
2360          Chan_cntr=Chan_cntr+1
2370        NEXT Avg
2380      NEXT Chan
2400        Slot=5
2410        It=No_hi_level-24
2420      FOR Chan=0 TO It-1
2430        FOR Avg=1 TO Read_per
2440          OUTPUT @Dac;"CHAN(";VAL$(Chan_cntr);") =
                         ";VAL$(Slot*100+Chan)
2450          Chan_cntr=Chan_cntr+1
2460        NEXT Avg
2470      NEXT Chan
2480      END IF
2490      !
2500     OUTPUT @Dac;"OUTBUF ON; INBUF ON"
2510     OUTPUT @Dac;"DISABLE LABELS; DISP OFF"
2520     OUTPUT @Dac;"USE 600"
2530     OUTPUT @Dac;"STA?"
2540     OUTPUT @Dac;"CLROUT"
2550     OUTPUT @Dac;"SCANMODE ON"
2560     OUTPUT @Dac;"SCTRIG HOLD"
2570     OUTPUT @Dac;"FUNC DCV"
2580     OUTPUT @Dac;"DISABLE INTR SYS"
2590     OUTPUT @Dac;"RANGE 10"
2600     OUTPUT @Dac;"ARMODE BEFORE"
2610     OUTPUT @Dac;"TERM RIBBON"
2620     OUTPUT @Dac;"RDGSMODE DAV"
2630     OUTPUT @Dac;"NRDGS 1"
2640     OUTPUT @Dac;"SPER 10E-6"
2650     OUTPUT @Dac;"SCDELAY 0";Scdelay
2660     OUTPUT @Dac;"ASCAN OFF"
2670     OUTPUT @Dac;"CLWRITE SENSE CHAN"
2680     OUTPUT @Dac;"PRESCAN 0"
2690     OUTPUT @Dac;"POSTSCAN";Loop
2700     OUTPUT @Dac;"STTRIG HOLD"
2710     !
2720     PRINT "   INTERRUPT SETUP"
2730     !
2750     !!!!!!!!!!!!!!!!!
```

```
2760      !  SUB TRANSFER  !
2770      !!!!!!!!!!!!!!!!!
2780      !
2790 Setup_intr:OUTPUT @Dac;"SUB TRANSFER"
2800      OUTPUT @Dac;" ENABLE INTR USE 600"
2810      OUTPUT @Dac;" XRDGS 600,";Total_rdgs;"INTO E_PACK"
2820      OUTPUT @Dac;"SUBEND"
2840      OUTPUT @Dac;"ON INTR USE 600 CALL TRANSFER"
2850      OUTPUT @Dac;"ENABLE INTR SYS"
2860      OUTPUT @Dac;"ENABLE INTR USE 600"
2870     PRINT "         INITAIL READINGS HAVE BEEN TAKEN."
2880     PRINT "         PROGRAM IS CURRENTLY PAUSED."
2890     PRINT "         CONTINUE AS TRUCK IS APPROACHING"
2900     PRINT "   "
2910      PAUSE
2920      !
2930      PRINT "   WAITING FOR TRUCK TRIGGER (WITHIN 10 SECONDS)"
2940      OUTPUT @Dac;"WAIT FOR EVENT"
2950      OUTPUT @Dac;"SCTRIG INT USE 600"
2960      Rtime=Rtime+10.
2970      WAIT Rtime
2980       OUTPUT @Dac;" VREAD E_PACK,RL64"    ! Transfer readings
2990      !
3000      !!!!!!!!!!!!!!!!!!!!!!!!!!!!!!!!!!!!!!!!!!!!!!!!
3010      ! Transfer data into two dimensional array !
3020      !!!!!!!!!!!!!!!!!!!!!!!!!!!!!!!!!!!!!!!!!!!!!!!!
3030      !
3040      PRINT "    TRANSFER DATA INTO TWO DIMENSIONAL ARRAY"
3050      !
3060      Begin=0
3070      End=Total_rdgs-1
3080      FOR Aooa=1 TO Loop
3090      DISP Aooa
3100        FOR Post=Begin TO End
3110          ENTER @Dac_off;Bemp_v
3120          Atemp_v(Aooa,Post)=Bemp_v
3130        NEXT Post
3140      NEXT Aooa
3150      !
3160      PRINT "     POST PROCESSING"
3161      !
3163      CLEAR @Dac
3164      OUTPUT @Dac;"RESET"
3180      WAIT 1
3190      !
3200      !!!!!!!!!!!!!!!!!!!
3210      ! Post Processing !
3220      !!!!!!!!!!!!!!!!!!!
3230      !
3240      FOR Gnrt=1 TO Loop
3250        FOR Rdg_indx=0 TO No_hi_level-1
3260          FOR Avg=0 TO Read_per-1
```

```
3270            Meas_v(Gnrt,Rdg_indx) =
                 Atemp_v(Gnrt,Rdg_indx*Read_per+Avg)
                  +Meas_v(Gnrt,Rdg_indx)
3280          NEXT Avg
3290          Meas_v(Gnrt,Rdg_indx)=Meas_v(Gnrt,Rdg_indx)/Read_per
3300          IF (ABS(Meas_v(Gnrt,Rdg_indx)>10.24)) THEN
                        Meas_v(Gnrt,Rdg_indx)=99.99
3310        NEXT Rdg_indx
3320      NEXT Gnrt
3330      DATA 1,1,1,1,1,1,1,1,1,1,1,1,1,1,1,1,1,1,1,1,1,1,1,
             1,1,1,1,1,1,1,1
3340      READ Factor(*)
3350      PRINT "       CALCULATING DISPLACEMENTS"
3360      WAIT 1.
3370      FOR Acnt=1 TO Loop
3380        FOR Bcnt=0 TO No_hi_level-1
3390          Disp(Bcnt)=(Meas_v(Acnt,Bcnt)-Init_volt(Bcnt))
                        *Factor(Bcnt)
3400        NEXT Bcnt
3410        OUTPUT @File_data;Disp(*)
3420      NEXT Acnt
3430      DEALLOCATE Packed(*)
3440      DEALLOCATE Temp_v(*)
3450      SUBEXIT
3460    SUBEND
3470    !
3480    !!!!!!!!!!!!!!!!!!!!!!!!!!!!!!!!!!!!
3490    ! Subroutine to create needed files !
3500    !!!!!!!!!!!!!!!!!!!!!!!!!!!!!!!!!!!!
3510    !
3520    SUB Create_files(Test$,@File_data,@File_exc,@File_temp)
3530      DIM Msg$[180],File1$[50],File2$[50]
3540 Input_file:Msg$="Please type in the name of the test"&CHR$(10)
3550      Msg$=Msg$&"This name will be used to store the
                    data"&CHR$(10)
3560      Msg$=Msg$&"in the appropriate file.  It is limited to 8
                    chars"
3570      DIALOG "STRING",Msg$,Button;SET("TITLE":"FILE NAME
                    INPUT","COLUMNS":8),RETURN("VALUE":Test$)
3580      IF Button=1 THEN GOTO Input_file
3590      File1$="C:\IBASIC\THEW\"&Test$&".PRN"
3600      File2$="C:\IBASIC\THEW\"&Test$&".EXC"
3610      ON ERROR GOTO Create_err
3620      CREATE File1$,1
3630      ASSIGN @File_data TO File1$;FORMAT ON
3640      CREATE File2$,1
3650      ASSIGN @File_exc TO File2$;FORMAT ON
3660      OFF ERROR
3670      SUBEXIT
3680 Create_err:IF ERRN=54 THEN
3690        Msg$="File Already Exists."&CHR$(10)
3700        Msg$=Msg$&"   Would you like to Overwrite?"
```

```
3710        DIALOG "QUESTION",Msg$,Btn;
                  SET("TITLE":"Overwrite","DEFAULT BUTTON":1)
3720        IF Btn=0 THEN
3730          PURGE File1$
3740          PURGE File2$
3750          CREATE File1$,1
3760          ASSIGN @File_data TO File1$;FORMAT ON
3770          CREATE File2$,1
3780          ASSIGN @File_exc TO File2$;FORMAT ON
3790        ELSE
3800          BEEP
3810          DIALOG "INFORMATION","Please specify a new file to
                       create";SET("TIMEOUT":3000)
3820          IF Btn=1 THEN GOTO Input_file
3830        END IF
3840      ELSE
3850        PRINT "Unexpected error occurred."
3860        PRINT "error number : ";ERRN
3870        PRINT "Occured on line number : ";ERRLN
3880        PRINT "With the following message: ";ERRM$
3890        PRINT "The program is paused, try to correct in alpha
                   window"
3900        PAUSE
3910      END IF
3920    SUBEND
```

APPENDIX B. ANSYS MODE SHAPES

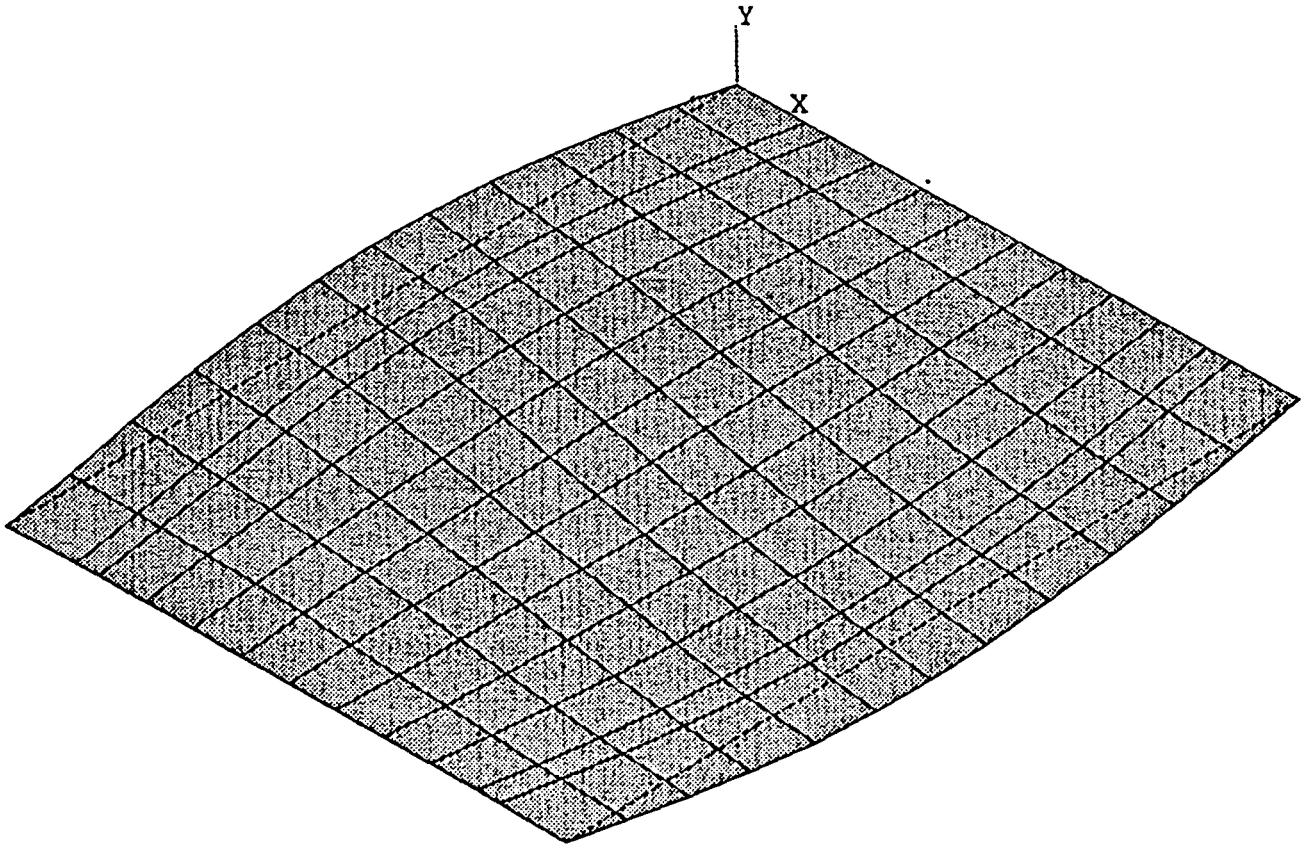

TEAL RIVER BRIDGE, MODE 2 FREQ = 7.62 Hz

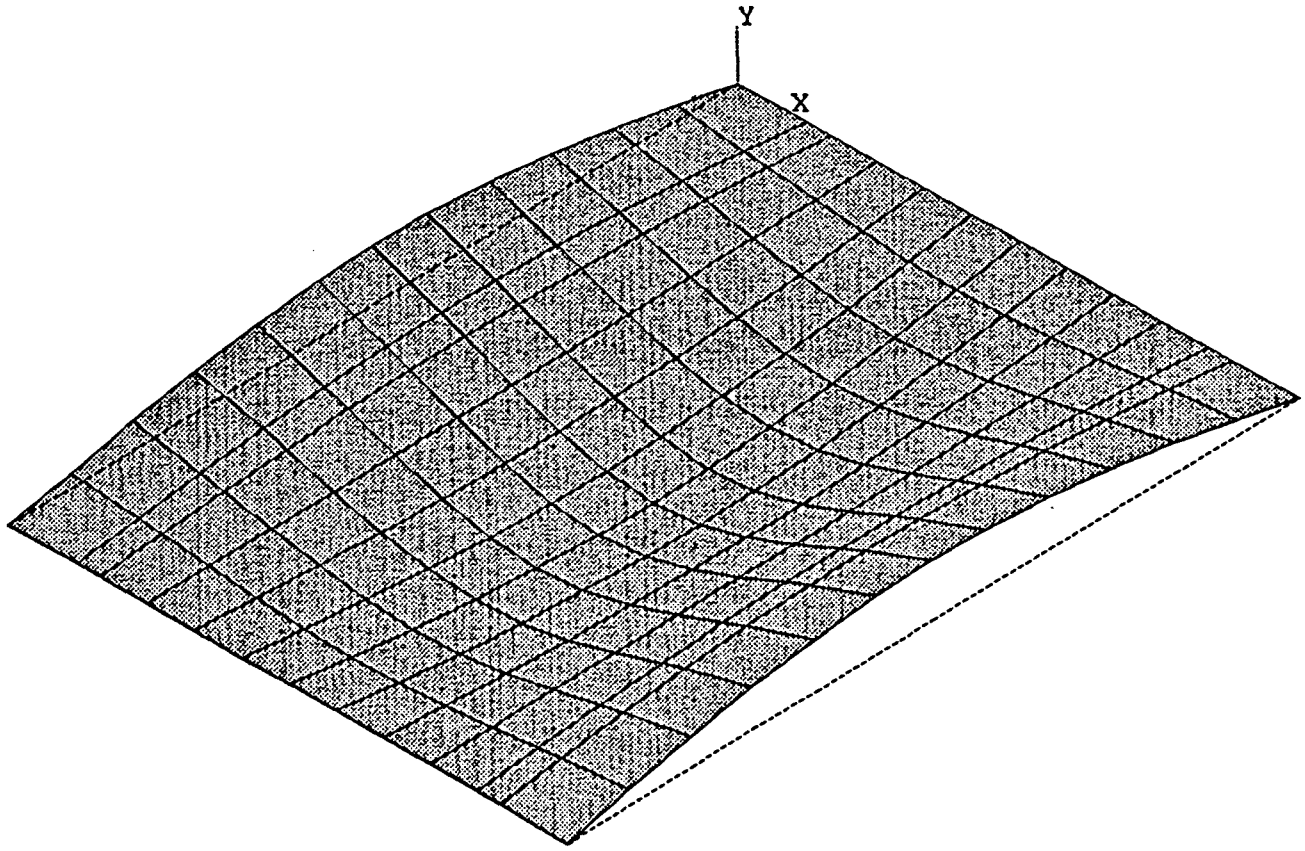

TEAL RIVER BRIDGE, MODE 3 FREQ = 10.29 Hz

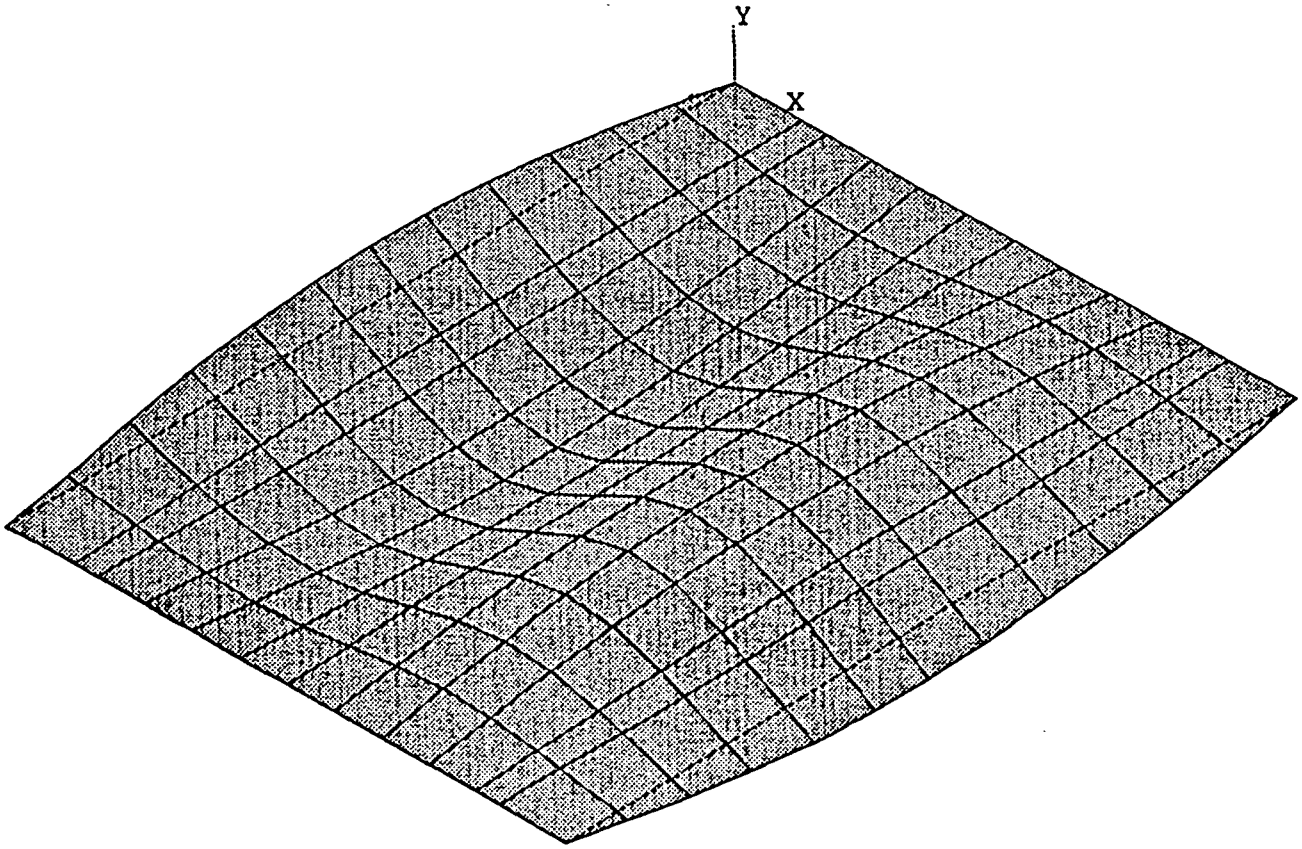

TEAL RIVER BRIDGE, MODE 4 FREQ = 15.70 Hz

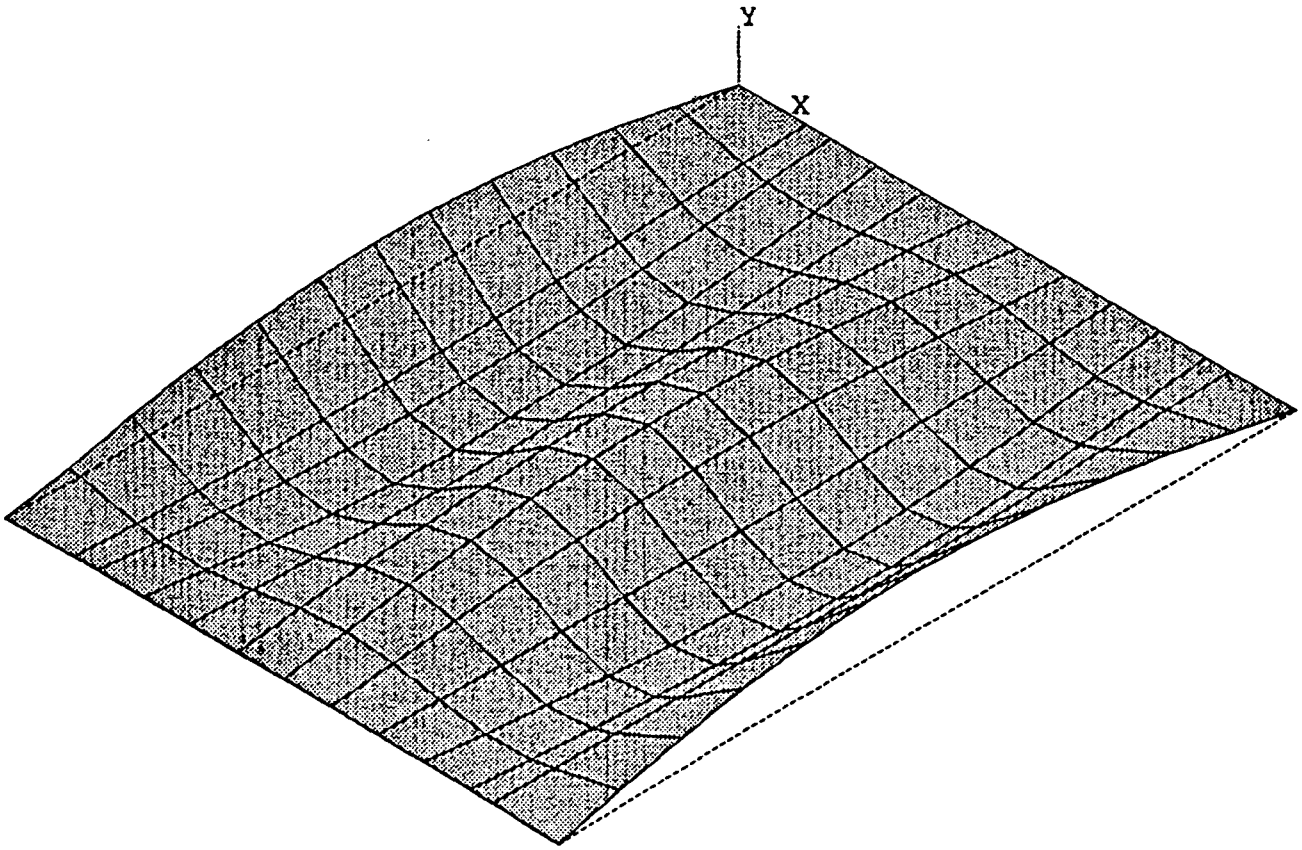

TEAL RIVER BRIDGE, MODE 5 FREQ = 24.38 Hz

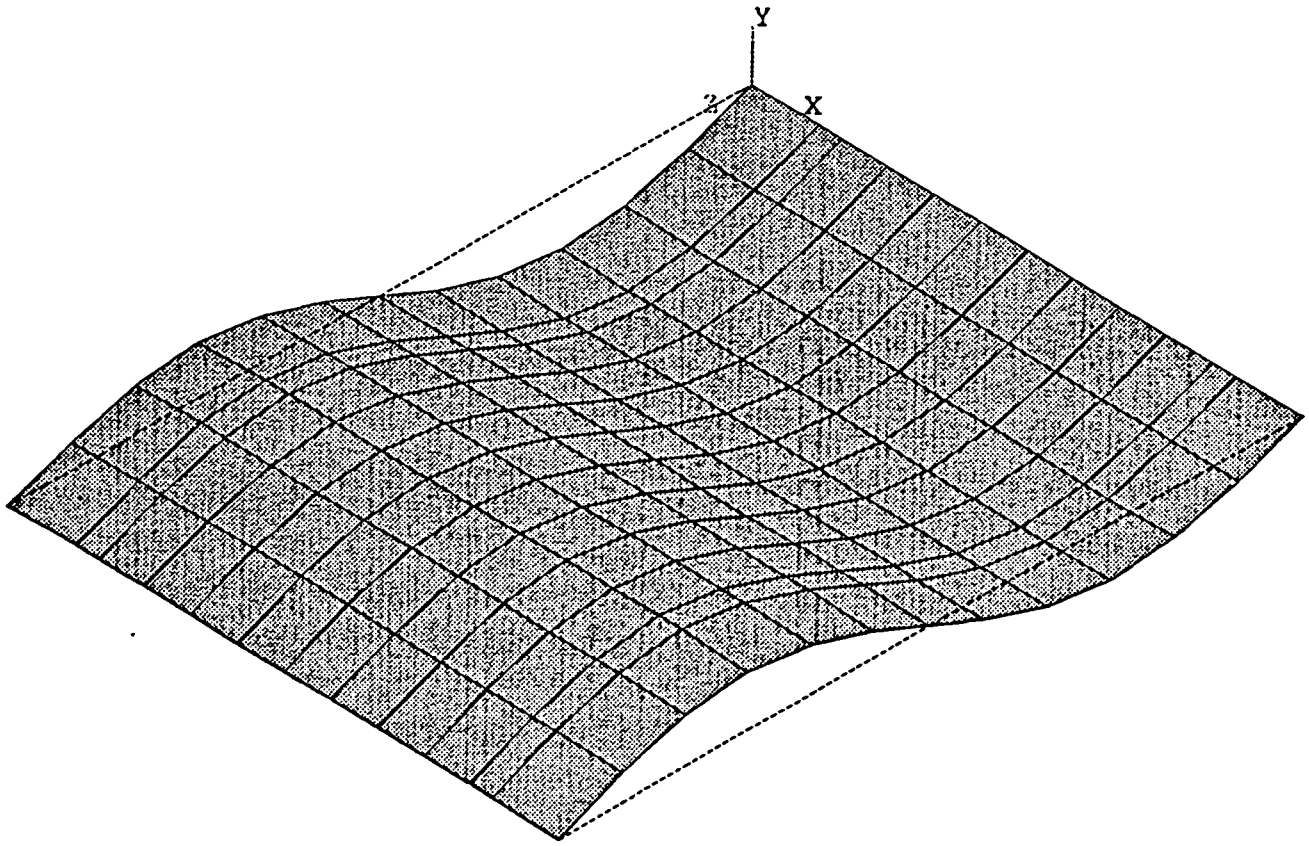

TEAL RIVER BRIDGE, MODE 6 FREQ = 27.34 Hz

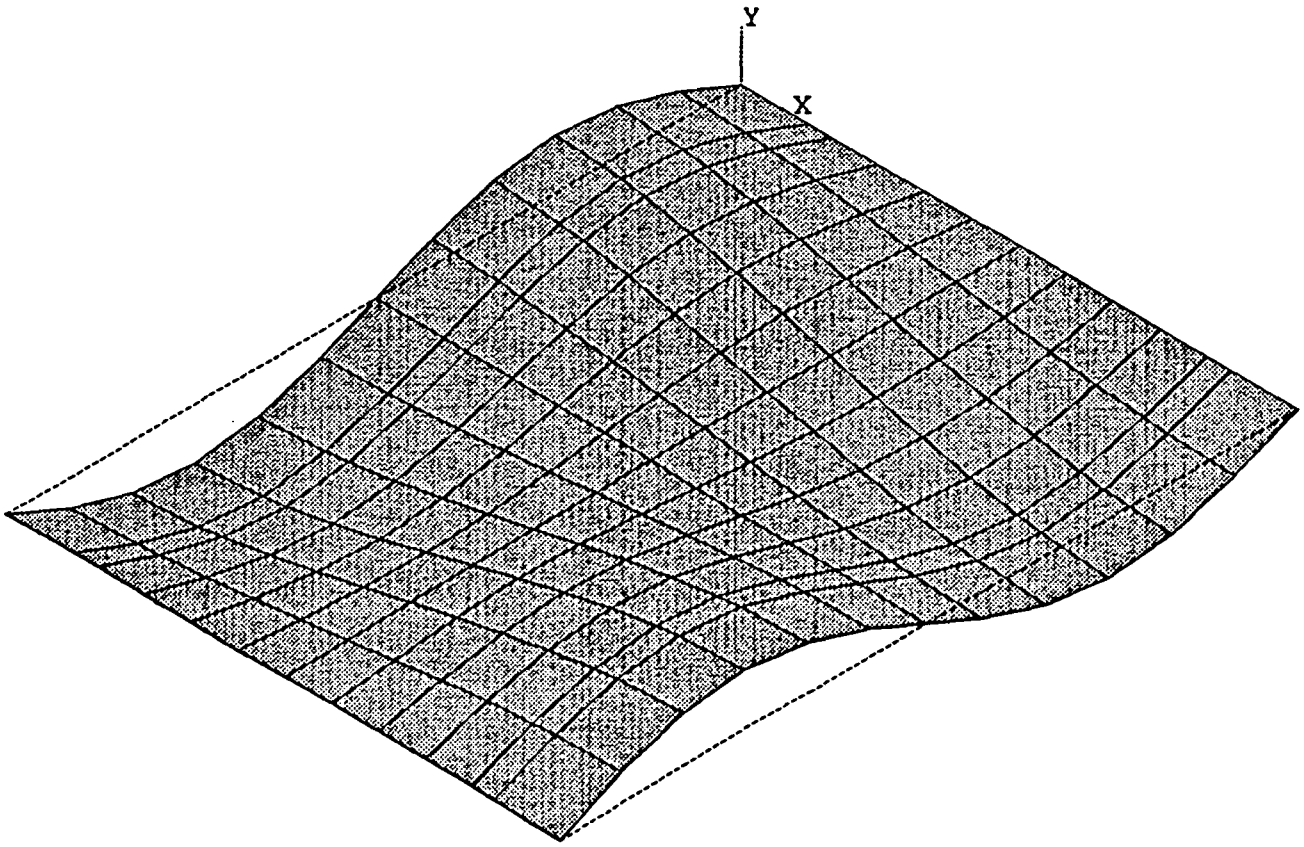

TEAL RIVER BRIDGE, MODE 7 FREQ = 28.04 Hz

APPENDIX C. FORTRAN PROGRAM LISTING AND OUTPUT

```
      PROGRAM ROLLMASS


      REAL*8 Y1,V1,T1,MPH,LEN,MBAR,G,MA1,MA2,D,H,M1,M2,PI,T,OMEGA
      REAL*8Y,VEL,K1,K2,K3,K4,YM1,YM2,F1,F2,TM2ON,TM1OFF,NTIMES,I
      REAL*8 MA3,D2,D1,M3,TM3ON,TM2OFF,YM3,F3,E,MSTAR
*     REAL*8 A1

      INTEGER*4 NUMIT,NODES,PRT,CNT,N1,N2,L1,L2,L3,K

      CHARACTER*60 TITLE


FUNCT(M1,M2,M3,Y,T,OMEGA,MSTAR)=(-1.*(M1*G*SIN(PI*VEL*T/LEN)+M2*G*

&SIN(PI*(VEL*T-D1)/LEN)+M3*G*SIN(PI*(VEL*T-D)/LEN))-OMEGA**2.*MSTAR

&*Y)/(MSTAR+M1*(SIN(PI*VEL*T/LEN))**2.+M2*(SIN(PI*(VEL*T-D1)/LEN))*
     &*2.+M3*(SIN(PI*(VEL*T-D)/LEN))**2.)


OPEN(UNIT=10,FILE='E:FORCES.OUT',ACCESS='SEQUENTIAL',STATUS='NEW')

      WRITE(6,*)' ENTER TITLE'
      READ(5,4) TITLE
4     FORMAT(A)
      WRITE(6,*)' ENTER THE NUMBER OF ITERATIONS BETWEEN NODES'
      READ(5,*) NUMIT
      WRITE(6,*)' ENTER THE VEHICLE VELOCITY IN M.P.H.'
      READ(5,*) MPH
      WRITE(6,*)' ENTER NUMBER OF EQUALLY SPACED NODES ALONG LENGTH
OF B
     +RIDGE'
      READ(5,*) NODES
      WRITE(6,*)' ENTER TOTAL LENGTH OF BRIDGE IN INCHES'
      READ(5,*) LEN
      WRITE(6,*)' ENTER MASS PER LENGTH OF BRIDGE IN LB*SEC^2/IN^2'
      READ(5,*) MBAR
      WRITE(6,*)' ENTER MASS OF FIRST AXLE IN LB*SEC^2/IN'
      READ(5,*) MA1
      WRITE(6,*)' ENTER MASS OF SECOND AXLE IN LB*SEC^2/IN'
      READ(5,*) MA2
      WRITE(6,*)' ENTER MASS OF THIRD AXLE IN LB*SEC^2/IN'
      READ(5,*) MA3
      WRITE(6,*)' ENTER NUMBER OF EQUAL SPACES BETWEEN FIRST TWO
AXLES'
      READ(5,*) N1
      WRITE(6,*)' ENTER NUMBER OF EQUAL SPACES BETWEEN SECOND TWO
```

```
AXLES'
      READ(5,*) N2
      WRITE(6,*)' ENTER MODULUS OF ELASTICITY OF THE BRIDGE IN PSI'
      READ(5,*) E
      WRITE(6,*)' ENTER MOMENT OF INERTIA OF THE BRIDGE IN IN^4'
      READ(5,*) I

      PI=3.141593
      G=386.4
      PRT=NUMIT
      T1=0.0
      V1=0.0
      Y1=0.0
      VEL=MPH*17.6
      L1=0
      L2=0-N1
      L3=0-(N1+N2)
      D1=N1*(LEN/(NODES-1))
      D2=N2*(LEN/(NODES-1))
      D=D1+D2
      NTIMES=((NODES-1)+D/(LEN/(NODES-1)))*NUMIT
      H=((LEN/(NODES-1))/(MPH*17.6))/NUMIT

                                                C      A      L      L
FREQ(E,I,LEN,NODES,MBAR,OMEGA,MA1,MA2,MA3,L1,L2,L3,MSTAR)

      CNT=0
      TM2ON=D1/VEL
      TM3ON=D/VEL
      TM1OFF=LEN/VEL
      TM2OFF=(LEN+D1)/VEL
      M1=MA1
      M2=0.0
      M3=0.0

      WRITE(10,2) ' '
2     FORMAT(A,////)
      WRITE(10,*) '                ',TITLE
      WRITE(10,*) ' '
      WRITE(10,*) ' '
      WRITE(10,30)' VEHICLE VELOCITY =',MPH
      WRITE(10,31)' LENGTH OF BRIDGE = ',LEN
30    FORMAT(15X,A,F5.1)
31    FORMAT(15X,A,F7.2)
      WRITE(10,*) ' '
      WRITE(10,40)' MASS OF FIRST AXLE =',MA1
      WRITE(10,40)' MASS OF SECOND AXLE =',MA2
      WRITE(10,40)' MASS OF THIRD AXLE =',MA3
40    FORMAT(15X,A,F6.2)
      WRITE(10,60)' MASS PER LENGTH OF BRIDGE =',MBAR
60    FORMAT(15X,A,F7.5)
      WRITE(10,61)' DISTANCE BETWEEN FIRST TWO AXLES =',D1
```

```
      WRITE(10,61)' DISTANCE BETWEEN SECOND TWO AXLES =',D2
61    FORMAT(15X,A,F6.1)
      WRITE(10,*) ' '
      WRITE(10,50)' MODULUS OF ELASTICIY =',E
      WRITE(10,51)' MOMENT OF INTERTIA =',I
50    FORMAT(15X,A,F10.1)
51    FORMAT(15X,A,F9.2)
      WRITE(10,*) ' '
      WRITE(10,20)' NUMBER OF ITERATIONS PER NODE = ',NUMIT
      WRITE(10,21)' NUMBER OF EQUALLY SPACED NODES = ',NODES
20    FORMAT(15X,A,I5)
21    FORMAT(15X,A,I3)
       WRITE(10,*)' '
      WRITE(10,*)' '
      WRITE(10,*)'                    TIME            FORCE 1
FORCE 2
     +            FORCE 3'
      WRITE(10,*)' '

      DO 100 K=1,NTIMES

        K1=H*FUNCT(M1,M2,M3,Y1,T1,OMEGA,MSTAR)
        K2=H*FUNCT(M1,M2,M3,Y1+H/2.*V1,T1+H/2.,OMEGA,MSTAR)
        K3=H*FUNCT(M1,M2,M3,Y1+H/2.*V1+H/4.*K1,T1+H/2.,OMEGA,MSTAR)
        K4=H*FUNCT(M1,M2,M3,Y1+H*V1+H/2.*K2,T1+H,OMEGA,MSTAR)

        Y1=Y1+H*V1+H/6.*(K1+K2+K3)
        V1=V1+1./6.*(K1+2.*K2+2.*K3+K4)
        T1=T1+H
        CNT=CNT+1

*       A1=FUNCT(M1,M2,M3,Y1,T1,OMEGA,MSTAR)
*       WRITE(10,16) OMEGA,(T1*80*1.5),Y1,V1,A1
*16     FORMAT(F5.2,3X,F6.2,3X,F6.3,3X,F9.4,3X,F10.4)

        IF(CNT.EQ.PRT)THEN
            PRT=PRT+NUMIT
            A=FUNCT(M1,M2,M3,Y1,T1,OMEGA,MSTAR)
            YM1=A*SIN(PI*VEL*T1/LEN)
            YM2=A*SIN(PI*(VEL*T1-D1)/LEN)
            YM3=A*SIN(PI*(VEL*T1-D)/LEN)

                                                  C     A     L     L
FREQ(E,I,LEN,NODES,MBAR,OMEGA,MA1,MA2,MA3,L1,L2,L3,
     &                 MSTAR)

            F1=M1*(G+YM1)
            F2=M2*(G+YM2)
            F3=M3*(G+YM3)
            WRITE(10,10) T1,F1/2.,F2/2.,F3/2.
10          FORMAT(14X,F7.5,8X,F8.2,8X,F9.2,8X,F9.2)
        ENDIF
```

```
      IF(T1.LT.TM2ON)THEN
          M1=MA1
          M2=0.0
          M3=0.0
      ELSEIF((T1.GE.TM2ON).AND.(T1.LT.TM3ON))THEN
          IF(T1.LE.TM1OFF)THEN
           M1=MA1
           M2=MA2
           M3=0.0
          ELSEIF(T1.GT.TM1OFF)THEN
           M1=0.0
           M2=MA2
           M3=0.0
          ENDIF
      ELSEIF(T1.GE.TM3ON)THEN
          IF(T1.LE.TM1OFF)THEN
           M1=MA1
           M2=MA2
           M3=MA3
          ELSEIF((T1.GT.TM1OFF).AND.(T1.LE.TM2OFF))THEN
           M1=0.0
           M2=MA2
           M3=MA3
          ELSEIF((T1.GT.TM1OFF).AND.(T1.GT.TM2OFF))THEN
           M1=0.0
           M2=0.0
           M3=MA3
          ENDIF
      ENDIF

100   CONTINUE

      CLOSE(10)
      END

*****************************************************************
******

      SUBROUTINE FREQ(E,IN,L,NODES,MBAR,OMEGA,MA1,MA2,MA3,L1,L2,L3,
     &                MSTAR)


      REAL*8 Y(150,150),YI(150),E,IN,L,OMEGA,G
      REAL*8 W(150),X,PLOC,A,B,MBAR,MA1,MA2,MA3,W1,W2,W3
      REAL*8 TOP,BOTTOM,AA,BB,XX,PIE,MSTAR

      INTEGER*4 I,J,NODES,LOOP,L1,L2,L3,M

      G=386.4
      PIE=3.141593
      LOOP=NODES-2
```

```
      DO 100 I=1,LOOP
       DO 200 J=1,LOOP
           Y(I,J)=0.0
200    CONTINUE
100   CONTINUE

      DO 300 I=1,LOOP
       YI(I)=0.0
300   CONTINUE

      DO 150 I=1,LOOP
       W(I)=0.0
150   CONTINUE

      DO 400 I=1,LOOP
       W(I)=MBAR*L*G/(NODES-1)
400   CONTINUE

      W1=MA1*G
      W2=MA2*G
      W3=MA3*G

      IF((L1.GT.0).AND.(L1.LT.(LOOP+1))) THEN
       W(L1)=W(L1)+W1
      ENDIF

      IF((L2.GT.0).AND.(L2.LT.(LOOP+1))) THEN
       W(L2)=W(L2)+W2
      ENDIF

      IF((L3.GT.0).AND.(L3.LT.(LOOP+1))) THEN
       W(L3)=W(L3)+W3
      ENDIF

      L1=L1+1
      L2=L2+1
      L3=L3+1

      PLOC=L/(NODES-1)
      J=(NODES-1)/2
      X=L/2.0

      DO 600 I=1,LOOP
         B=L-PLOC
         A=PLOC
           IF ((X.LT.(PLOC+0.001)).AND.(X.GT.(PLOC-0.001))) THEN
           Y(I,J)=W(I)*(A**2)*(B**2)/(3.*E*IN*L)
           ELSEIF (X.LT.PLOC) THEN
           Y(I,J)=W(I)*B*X*(L**2-B**2-X**2)/(6.*E*IN*L)
           ELSEIF (X.GT.PLOC) THEN
           AA=B
           BB=A
```

```
            XX=L-X
            Y(I,J)=W(I)*BB*XX*(L**2-BB**2-XX**2)/(6.*E*IN*L)
            ENDIF
      PLOC=PLOC+(L/(NODES-1))
600    CONTINUE

       DO 1100 I=1,LOOP
          X=L/(NODES-1)
          DO 1200 M=1,LOOP
             Y(I,M)=Y(I,J)*SIN(PIE*X/L)
             X=X+(L/(NODES-1))
1200      CONTINUE
1100   CONTINUE

       DO 700 I=1,LOOP
        DO 800 J=1,LOOP
            YI(I)=YI(I)+Y(J,I)
800     CONTINUE
700    CONTINUE

       TOP=0.0
       BOTTOM=0.0

       DO 900 I=1,LOOP
        TOP=TOP+W(I)*YI(I)
900    CONTINUE

       DO 1000 I=1,LOOP
        BOTTOM=BOTTOM+W(I)*(YI(I)**2)
1000   CONTINUE

       TOP=TOP*G
       OMEGA=SQRT(TOP/BOTTOM)
       X=L/(NODES-1)
       MSTAR=0.0
       DO 1300 I=1,LOOP
          MSTAR=MSTAR+W(I)/G*(SIN(PIE*X/L))**2.
          X=X+(L/(NODES-1))
1300   CONTINUE
       WRITE(5,1330) OMEGA,MSTAR
1330   FORMAT(F7.3,5X,F7.3)

       RETURN
       END
```

Teal River Bridge

VEHICLE VELOCITY = 5.0
LENGTH OF BRIDGE = 380.00

MASS OF FIRST AXLE = 57.40
MASS OF SECOND AXLE = 61.90
MASS OF THIRD AXLE = 61.90
MASS PER LENGTH OF BRIDGE = .30400
DISTANCE BETWEEN FIRST TWO AXLES = 171.0
DISTANCE BETWEEN SECOND TWO AXLES = 57.0

MODULUS OF ELASTICIY = 1780000.0
MOMENT OF INTERTIA = 68051.00

NUMBER OF ITERATIONS PER NODE = 50
NUMBER OF EQUALLY SPACED NODES = 21

TIME	FORCE 1	FORCE 2	FORCE 3
.21591	11086.09	.00	.00
.43182	11116.87	.00	.00
.64773	11019.01	.00	.00
.86364	11078.69	.00	.00
1.07955	11139.00	.00	.00
1.29545	11149.07	.00	.00
1.51136	11125.81	.00	.00
1.72727	11075.15	.00	.00
1.94318	11022.62	.00	.00
2.15909	11108.22	11962.21	.00
2.37500	11194.28	11994.37	.00
2.59091	11183.64	12007.45	.00
2.80682	11165.39	12012.94	11973.41
3.02273	11061.94	11932.93	11947.65
3.23864	11012.36	11863.68	11905.55
3.45455	11094.88	11967.58	11964.69
3.67045	11139.59	12071.84	12042.92
3.88636	11081.82	11932.00	11936.90
4.10227	11083.65	11917.52	11922.05
4.31818	11089.68	12067.19	12063.18
4.53409	.00	12006.91	12008.75
4.75000	.00	11843.79	11829.69
4.96591	.00	12037.38	12054.68
5.18182	.00	12021.37	12042.86
5.39773	.00	11875.77	11832.79
5.61364	.00	11879.27	11816.85
5.82955	.00	11925.26	11881.68
6.04545	.00	11936.15	11872.93
6.26136	.00	11959.08	11825.34
6.47727	.00	.00	11912.72
6.69318	.00	.00	12023.77
6.90909	.00	.00	11959.08

Teal River Bridge

VEHICLE VELOCITY = 17.0
LENGTH OF BRIDGE = 380.00

MASS OF FIRST AXLE = 57.40
MASS OF SECOND AXLE = 61.90
MASS OF THIRD AXLE = 61.90
MASS PER LENGTH OF BRIDGE = .30400
DISTANCE BETWEEN FIRST TWO AXLES = 171.0
DISTANCE BETWEEN SECOND TWO AXLES = 57.0

MODULUS OF ELASTICIY = 1780000.0
MOMENT OF INTERTIA = 68051.00

NUMBER OF ITERATIONS PER NODE = 50
NUMBER OF EQUALLY SPACED NODES = 21

TIME	FORCE 1	FORCE 2	FORCE 3
.06350	11052.24	.00	.00
.12701	11233.14	.00	.00
.19051	10859.07	.00	.00
.25401	11275.29	.00	.00
.31751	11211.37	.00	.00
.38102	10827.07	.00	.00
.44452	11176.79	.00	.00
.50802	11401.11	.00	.00
.57152	11033.43	.00	.00
.63503	10485.93	11857.23	.00
.69853	11240.49	12009.96	.00
.76203	11726.72	12287.02	.00
.82553	10756.44	11722.01	11895.99
.88904	10620.77	11517.10	11765.93
.95254	11322.16	12245.91	12120.04
1.01604	11516.02	12656.02	12418.84
1.07955	11135.34	12062.23	12035.77
1.14305	10941.64	11448.80	11541.11
1.20655	11053.03	11706.41	11733.95
1.27005	11089.68	12401.89	12385.46
1.33356	.00	12319.34	12333.21
1.39706	.00	11905.46	11898.91
1.46056	.00	11691.30	11632.16
1.52406	.00	11940.11	11933.56
1.58757	.00	12247.37	12396.10
1.65107	.00	12078.55	12171.98
1.71457	.00	11783.19	11556.60
1.77807	.00	11961.40	11967.79
1.84158	.00	11959.08	12315.11
1.90508	.00	.00	11509.90
1.96858	.00	.00	12195.45
2.03209	.00	.00	11959.08

Teal River Bridge

VEHICLE VELOCITY = 22.0
LENGTH OF BRIDGE = 380.00

MASS OF FIRST AXLE = 57.40
MASS OF SECOND AXLE = 61.90
MASS OF THIRD AXLE = 61.90
MASS PER LENGTH OF BRIDGE = .30400
DISTANCE BETWEEN FIRST TWO AXLES = 171.0
DISTANCE BETWEEN SECOND TWO AXLES = 57.0

MODULUS OF ELASTICIY = 1780000.0
MOMENT OF INTERTIA = 68051.00

NUMBER OF ITERATIONS PER NODE = 50
NUMBER OF EQUALLY SPACED NODES = 21

TIME	FORCE 1	FORCE 2	FORCE 3
.04907	10983.44	.00	.00
.09814	11294.07	.00	.00
.14721	11166.41	.00	.00
.19628	10757.64	.00	.00
.24535	11120.54	.00	.00
.29442	11508.63	.00	.00
.34349	11249.75	.00	.00
.39256	10834.30	.00	.00
.44163	10876.68	.00	.00
.49070	10808.38	11911.62	.00
.53977	11202.86	11997.26	.00
.58884	11515.65	12178.36	.00
.63791	10982.62	11882.92	11938.81
.68698	10770.33	11658.07	11827.54
.73605	11022.75	11876.50	11912.74
.78512	11317.37	12331.29	12204.62
.83419	11344.78	12535.39	12387.56
.88326	11193.32	12316.30	12251.68
.93233	11085.01	11926.88	11930.39
.98140	11089.68	11723.87	11732.59
1.03048	.00	11543.68	11527.68
1.07955	.00	11820.35	11803.39
1.12862	.00	12282.19	12353.55
1.17769	.00	12510.67	12700.97
1.22676	.00	12261.31	12417.22
1.27583	.00	11782.61	11644.62
1.32490	.00	11678.72	11317.55
1.37397	.00	11995.86	12097.27
1.42304	.00	11959.08	12593.33
1.47211	.00	.00	11480.74
1.52118	.00	.00	11867.30
1.57025	.00	.00	11959.08

Teal River Bridge

VEHICLE VELOCITY = 24.0
LENGTH OF BRIDGE = 380.00

MASS OF FIRST AXLE = 57.40
MASS OF SECOND AXLE = 61.90
MASS OF THIRD AXLE = 61.90
MASS PER LENGTH OF BRIDGE = .30400
DISTANCE BETWEEN FIRST TWO AXLES = 171.0
DISTANCE BETWEEN SECOND TWO AXLES = 57.0

MODULUS OF ELASTICIY = 1780000.0
MOMENT OF INTERTIA = 68051.00

NUMBER OF ITERATIONS PER NODE = 50
NUMBER OF EQUALLY SPACED NODES = 21

TIME	FORCE 1	FORCE 2	FORCE 3
.04498	10963.19	.00	.00
.08996	11255.61	.00	.00
.13494	11325.01	.00	.00
.17992	10814.04	.00	.00
.22491	10839.12	.00	.00
.26989	11362.59	.00	.00
.31487	11550.35	.00	.00
.35985	11209.05	.00	.00
.40483	10824.79	.00	.00
.44981	10348.48	11834.04	.00
.49479	10815.52	11866.58	.00
.53977	11621.13	12232.66	.00
.58475	11459.00	12221.82	12029.01
.62973	11076.33	11946.50	11953.58
.67472	10894.68	11718.48	11824.06
.71970	11005.92	11822.16	11868.75
.76468	11186.47	12177.73	12121.64
.80966	11240.18	12477.83	12383.99
.85464	11168.45	12502.08	12442.90
.89962	11089.68	12268.80	12257.32
.94460	.00	11658.58	11647.01
.98958	.00	11423.03	11357.45
1.03456	.00	11675.47	11612.83
1.07955	.00	12202.62	12286.64
1.12453	.00	12549.43	12853.98
1.16951	.00	12356.50	12667.29
1.21449	.00	11839.34	11685.09
1.25947	.00	11733.07	11109.86
1.30445	.00	11959.08	12019.04
1.34943	.00	.00	12320.66
1.39441	.00	.00	11875.64
1.43939	.00	.00	11959.08

Teal River Bridge

VEHICLE VELOCITY = 30.0
LENGTH OF BRIDGE = 380.00

MASS OF FIRST AXLE = 57.40
MASS OF SECOND AXLE = 61.90
MASS OF THIRD AXLE = 61.90
MASS PER LENGTH OF BRIDGE = .30400
DISTANCE BETWEEN FIRST TWO AXLES = 171.0
DISTANCE BETWEEN SECOND TWO AXLES = 57.0

MODULUS OF ELASTICIY = 1780000.0
MOMENT OF INTERTIA = 68051.00

NUMBER OF ITERATIONS PER NODE = 50
NUMBER OF EQUALLY SPACED NODES = 21

TIME	FORCE 1	FORCE 2	FORCE 3
.03598	10920.10	.00	.00
.07197	11073.33	.00	.00
.10795	11521.40	.00	.00
.14394	11371.55	.00	.00
.17992	10839.09	.00	.00
.21591	10650.44	.00	.00
.25189	10975.94	.00	.00
.28788	11465.52	.00	.00
.32386	11716.83	.00	.00
.35985	11029.37	11948.91	.00
.39583	10540.90	11773.92	.00
.43182	10591.47	11702.61	.00
.46780	10627.04	11629.95	11871.49
.50379	11056.80	11928.09	11945.54
.53977	11471.05	12429.63	12223.13
.57576	11595.25	12785.54	12504.28
.61174	11453.92	12781.93	12570.87
.64773	11236.47	12465.04	12373.51
.68371	11102.65	12048.50	12038.76
.71970	11089.68	11754.22	11761.81
.75568	.00	11375.35	11352.87
.79167	.00	11404.30	11336.44
.82765	.00	11781.96	11742.84
.86364	.00	12306.08	12425.80
.89962	.00	12668.04	13033.77
.93561	.00	12595.67	13093.49
.97159	.00	12118.61	12324.11
1.00758	.00	11758.39	11205.02
1.04356	.00	11959.08	11054.34
1.07955	.00	.00	11779.48
1.11553	.00	.00	12352.63
1.15152	.00	.00	11959.08

Teal River Bridge

VEHICLE VELOCITY = 41.0
LENGTH OF BRIDGE = 380.00

MASS OF FIRST AXLE = 57.40
MASS OF SECOND AXLE = 61.90
MASS OF THIRD AXLE = 61.90
MASS PER LENGTH OF BRIDGE = .30400
DISTANCE BETWEEN FIRST TWO AXLES = 171.0
DISTANCE BETWEEN SECOND TWO AXLES = 57.0

MODULUS OF ELASTICIY = 1780000.0
MOMENT OF INTERTIA = 68051.00

NUMBER OF ITERATIONS PER NODE = 50
NUMBER OF EQUALLY SPACED NODES = 21

TIME	FORCE 1	FORCE 2	FORCE 3
.02633	10879.46	.00	.00
.05266	10765.58	.00	.00
.07899	11207.75	.00	.00
.10532	11737.04	.00	.00
.13165	11836.92	.00	.00
.15798	11503.84	.00	.00
.18431	11028.45	.00	.00
.21064	10690.89	.00	.00
.23697	10633.67	.00	.00
.26330	10281.83	11822.80	.00
.28963	10396.53	11725.21	.00
.31596	10883.84	11853.12	.00
.34229	11011.85	11903.71	11944.34
.36863	11250.55	12110.71	12025.35
.39496	11452.41	12406.63	12210.23
.42129	11530.30	12679.37	12434.24
.44762	11480.00	12840.86	12614.68
.47395	11351.38	12861.11	12697.94
.50028	11206.10	12761.62	12674.15
.52661	11089.68	12591.25	12567.80
.55294	.00	12067.22	12071.38
.57927	.00	11688.63	11655.55
.60560	.00	11512.97	11414.44
.63193	.00	11564.41	11428.25
.65826	.00	11809.77	11732.75
.68459	.00	12137.01	12276.16
.71092	.00	12347.64	12848.20
.73725	.00	12250.02	13052.26
.76358	.00	11959.08	12549.90
.78991	.00	.00	11316.36
.81624	.00	.00	11295.14
.84257	.00	.00	11959.08

Teal River Bridge

VEHICLE VELOCITY = 42.0
LENGTH OF BRIDGE = 380.00

MASS OF FIRST AXLE = 57.40
MASS OF SECOND AXLE = 61.90
MASS OF THIRD AXLE = 61.90
MASS PER LENGTH OF BRIDGE = .30400
DISTANCE BETWEEN FIRST TWO AXLES = 171.0
DISTANCE BETWEEN SECOND TWO AXLES = 57.0

MODULUS OF ELASTICIY = 1780000.0
MOMENT OF INTERTIA = 68051.00

NUMBER OF ITERATIONS PER NODE = 50
NUMBER OF EQUALLY SPACED NODES = 21

TIME	FORCE 1	FORCE 2	FORCE 3
.02570	10877.11	.00	.00
.05141	10743.60	.00	.00
.07711	11166.02	.00	.00
.10281	11719.72	.00	.00
.12852	11883.15	.00	.00
.15422	11605.94	.00	.00
.17992	11140.36	.00	.00
.20563	10759.30	.00	.00
.23133	10624.62	.00	.00
.25703	10192.68	11807.76	.00
.28274	10253.55	11676.97	.00
.30844	10735.54	11776.78	.00
.33415	10909.41	11830.84	11924.95
.35985	11220.70	12082.58	12013.05
.38555	11487.20	12449.54	12234.31
.41126	11599.04	12791.74	12508.37
.43696	11549.39	12997.62	12731.23
.46266	11399.41	13026.65	12833.53
.48837	11226.50	12902.29	12799.49
.51407	11089.68	12683.58	12656.71
.53977	.00	12100.81	12106.27
.56548	.00	11662.93	11626.70
.59118	.00	11435.94	11320.41
.61688	.00	11454.29	11280.14
.64259	.00	11696.37	11560.85
.66829	.00	12058.00	12135.36
.69399	.00	12331.82	12812.00
.71970	.00	12282.30	13173.53
.74540	.00	11959.08	12776.53
.77110	.00	.00	11463.75
.79681	.00	.00	11264.81
.82251	.00	.00	11959.08